An assessment of the effects of the storms on the morphological changes in the Luebeck Bay: a numerical-model-based study

Dissertation

zur Erlangung des Doktorgrades

der Mathematisch-Naturwissenschaftlichen Fakultät

der Christian-Albrechts-Universität zu Kiel

vorgelegt von

Néstor Jaime Jiménez Echeverri

Kiel

Januar 2012

Referent:	Prof. Dr. Roberto Mayerle
Koreferent:	Prof. Dr. Horst Sterr
Tag der Disputation:	06.07.2011
Zum Druck genehmigt:	Kiel, 13.01.2012
Der Dekan:	Prof. Dr. Lutz Kipp

Acknowledgements

The author would like to thank CORELAB-FTZ institute at the University of Kiel for providing all the computing resources and the data used in this thesis work. Acknowledgments are due to Prof. Dr. Roberto Mayerle, for being the mentor and permanent support during this investigation, assisting with his expertise and advice.

During this investigation a number of projects have contributed not only with financial support, but also with the experience provided through several cases of practical engineering application. For its relevance and the participation of a great number of multidisciplinary institutions in Germany, the project MUSTOK-SEBOK-A, sponsored by The Federal Ministry of Education and Research of Germany, has been the leading project during the PhD program.

The author also gives recognition to all the people committed in the academic support of the institute-FTZ-CORELAB. Special acknowledgments are due to Prof. Dr. Narayanan, who diligently assisted with his corrections on the thesis taking pains to improve a text written by a non-native English-speaker. This thesis could not haven been possible without the support of the data provided to setup, calibrate and validate the numerical models. Data of waves and flows in the Luebeck Bay were provided and prepared by Dr. Klaus Ricklefs at CORELAB-FTZ, in Buesum. The bathymetry and sediment characteristics have been provided by the Institute of Sedimentology and Geology of Coasts and Continental Shelves at the University of Kiel, under the direction of Dr. Klaus Schwarzer.

Last, but not least, the author is grateful to all students and personal at CORELAB; they were also a support in this work, being not only colleagues but friends as well.

Notation

t	Computational time step
Δx	The length of the grid cells in x -direction
Δy	The length of the grid cells in y-direction
Δz	The length of the grid cells in z-direction
u	Current velocity component in x-direction
v	Current velocity component in y-direction
w	Current velocity component in z-direction
f	Coriolis parameter
g	Gravitational acceleration
ρ	Density of water
S_{xx}	Radiation stress tensor in x-direction
S_{xy}	Radiation stress tensor in y-direction
ν	Horizontal eddy viscosity
ν_t	Vertical eddy viscosity
p_a	Atmospheric pressure
ρ_o	Reference density of water
F_u	Gradient-stress relation
S	Source term in the energy balance equation
S_{in}	Source of wind-energy wave generation
S_{ln}	Source of nonlinear wave-energy transfer
S_{ds}	Sink of wave-energy dissipation
S_{bot}	Sink of wave-energy dissipation on the bottom
S_{surf}	Sink of depth-induced wave-breaking
d50	Mean grain size of sediment
q_t	Total sediment transport
q_b	Bed load transport
q_s	Load of transport in suspension
τ	Shear stress
c	Instantaneous sediment concentration
w	Fall velocity of sediment
Φ_b	Dimensionless bed load
Θ_c	Critical Shields parameter
n	Bed porosity
z	Bed level
Sx	Total transport in the x-direction
Sy	Total transport in the x-direction
ΔS	Sediment sink or source
C_1,C_2,C_3	First, second and third cost functions
W_n, W_e	Variables of short term in the cost functions
$W_{n\text{-}lt}$, $W_{e\text{-}lt}$	Variables of long term in the cost functions

σ	Standard deviation
SMF	Speedup Morphodynamic Factor
EOF	Empirical Orthogonal Functions
λ	Eigenvalues in the EOFs system
R	Covariance Matrix in the EOFs System
C	Matrix of eingenvectors
Λ	Vector of eigenvalues
F	Matrix of variables
EC	Expansion coefficients

Abstract

Nowadays a consensus on the effects of storms on the medium and long term geomorphologic evolution of the coastal zones has not yet been reached (Anderson et al., 2010). Some authors argue that the effects of extreme events are only temporarily and that during fairly weather conditions the shore-face recovers completely (Zhang et al., 2002). In other studies it has been found that the cumulative effects of the storms are permanent (Costas et al., 2005). To improve the understanding of the relevance of the storms in the morphological evolution of coastal areas extensive analyses of measured beach profiles and bathymetries, as well as, physical and numerical model studies, have been published (Frazer et al., 2009; Houser et al., 2007).

In the present investigation, a method to do morphodynamic simulations for medium-term durations is setup combining normal conditions and the effects of the storms. The method consists of an ensemble of storms and calm conditions that are sequentially executed.

Two numerical models are setup. Simulations of the hydrodynamic conditions of the Baltic Sea region are carried out by means of the Baltic Sea Regional model (BSRmod). The morphodynamics in the inner Luebeck Bay (study area) are computed using the Luebeck Bay Local model (LBLmod). The local model is integrated into the model covering the Baltic Sea region. In this regard the hydrodynamics that are generated in the deep areas, outside the Luebeck Bay, are taken into account in the generation of boundary conditions of the LBLmod.

The effects that the storms have on the morphological evolution of the study area are investigated based on numerical simulations of extreme scenarios. A group of physically consistent storm scenarios is used to compute the principal changes that are produced during storms. The method of empirical orthogonal functions (EOF) is used to analyze the results of the numerical simulations.

A preliminary map of bathymetrical changes in the Luebeck Bay is presented for the first and second mode of the EOFs. The principal components of the EOFs are localized within the first two modes. The bathymetrical changes were consistent with the tendencies observed in the area.

The above mentioned methodology of medium-term morphodynamic simulations is applied over a period of one year. Initially, the storm period is simulated assuming the conditions of one storm as representative. Subsequently, the morphological simulations for a period of calm conditions are carried applying the

morphological factors (morfac) technique. A period of one month in year 2007 is selected as representative of calm conditions using the cost function method.

Three sectors along the coast line of the Luebeck Bay are defined for the analysis of the bathymetrical changes. The profiles of the bathymetrical changes produced by storms and thereafter, at the end of the total period of simulations, are compared. Different tendencies in the evolution of the coast associated with each sector along the coast have been identified. The western sector (Timmendorf) showed a progradating tendency close to the beach, while the central (Niendorf) and the eastern (Brodten) sectors were stable along the coastline. Offshore Brodten (in the eastern domain) the submerged platform in front of the cliff-coast showed a tendency of erosion in the medium-term period.

Zusammenfassung

Bis heute ist noch keine Einigung über die Wirkung von Stürmen auf die mittel- und längerfristige geomorphologischer Entwicklung von Küstenregionen erzielt worden. (Anderson et al. 2010). Manche Autoren behaupten, dass die Wirkungen von extremen Ereignissen nur kurzzeitig andauern und dass während gemässigter Wetterbedingungen sich die Küsten vollständig erholen. (Zhang et al 2002). In anderen Studien hat man herausgefunden, dass die kumulativen Effekte der Stürme dauerhaft sind. (Coast et al 2005). Um das Verständnis der Bedeutung der Stürme in der morphologischen Entwicklung der Küstenregionen zu verbessern, wurden umfangreiche Untersuchungen über gemessene Strandprofile und Bathymetrien wie auch Studien an physikalischen und numerischen Modelle veröffentlicht. (Frazer et al 2009; Houser et al 2007).

In der gegenwärtigen Untersuchung wird eine Methode aufgebaut, mit der man morphodynamische Simulationen für einen mittelfristigen Zeitraum anwendet, die normale Bedingungen und die Wirkungen von Stürmen kombiniert. Die Methode besteht aus einem Zusammenwirken von Stürmen und ruhigen Bedingungen die im Folgenden aufgeführt werden.

Zwei numerische Modelle sind aufgebaut. Simulationen von den hydrodynamischen Bedingungen der Ostsee sind mit Hilfe des Modells der Ostsee-Region (BSRmod) berechnet worden. Die Morphodynamik der inneren Lübecker Bucht (Forschungsgebiet) wird mit dem Lübecker Bucht Modell berechnet(LBLmod). Dieses lokale Modell ist in das Ostsee-Modell integriert. Daher sind die Hydrodynamiken die in den tiefen Regionen ausserhalb der Lübecker Bucht gebildet werden für die Berechnungen der Bildung von Randbedingungen der LBL-Modelle berücksichtigt worden.

Die Wirkungen die Stürme auf die morphologische Entwicklung des untersuchten Gebietes haben, sind mit Hilfe numerischer Simulation von extremen Bedingungen erforscht worden. Mehrere physikalisch mögliche Sturmszenarien sind angewendet worden um die hauptsächlichen Veränderungen zu berechnen, die sich während eines Sturmes entwickeln. Die Methode der empirischen orthogonalen Funktionen (EOF) wird angewendet um die Ergebnisse der numerischen Simulationen zu analysieren.

Eine vorläufige Karte von bathymetrischen Veränderungen in der Lübecker Bucht wird für das erste und zweite Verfahren der EOF präsentiert. Die Hauptbestandteile der EOFs befinden sich der ersten beiden Eigenvalues. Die bathymetrischen Veränderungen stimmten mit den in dem Gebiet beobachteten Tendenzen überein.

Die oben erwähnte Methode über mittelfristige morphodynamische Simulationen wurde über einen Zeitraum von einem Jahr angewendet. Zunächst wurde die Strumperiode simuliert unter der Annahme dass die Bedingungen von einem einzigen Sturm repräsentativ sind. Anschliessend wurden die morphologischen Simulationen für einen Zeitraum von ruhigen Bedingungen mit Hilfe der Methode der morphologischen Faktoren (morfac) ausgeführt. Ein Zeitraum von einem Monat im Jahre 2007 wurde mit Hilfe der „cost function“ –Methode als repräsentativ für ruhige Bedingungen ausgewählt.

Drei Gebiete entlang der Küstenlinie der Lübecker Bucht wurden für die Berechnung der bathymetrischen Veränderungen definiert. Die Profile der bathymetischen Veränderungen die durch Stürme hervorgerufen wurden werden am Ende des gesamten Zeitraumes der Simulation mit den Gesamtveränderungen der Küste verglichen. Es wurden verschiedene Tendenzen in der Entwicklung von Küsten die mit jedem Gebiet entlang Küste verbunden sind eruiert. Das westliche Gebiet (Timmendorf) zeigte eine zunehmende Tendenz nahe am Strand zu sedimentiern, während der zentrale Bereich (Niendorf) und der östliche Bereich (Bordten) entlang der Küste stabil waren. Vor der Küste zeigte Bordten (im östlichen Gebiet) eine Ebene unter Wasser gegenüber der Klippen mit der Tendenz zur Erosion in einem mittelfristigen Zeitaum.

Contents

List of Figures

List of Tables

Chapter 1

Introduction

1.1 Description of the project and objectives

In most places of the world, people live near coasts for livelihood, habitation, recreation and commerce. During the last decades the threats of erosion and flooding have affected the coastal areas where a growing demand of human activities has been taking place, i.e. fishery, hotels, housing, etc. For that reason, in present times the number of structures of coastal protection has been increasing in order to guarantee the long-term safety of the habitants and their belongings. Hydrodynamic and morphological studies in the coastal areas have been necessary to establish a balance between cost and level of protection in order to avoid excessive financial-burdens of construction while preventing from ecologic disasters, destruction of the infrastructure and/or life-threatening situations. In this work the numerical model is used to study the morphological changes along the coast of the Luebeck Bay, in the south-western German Baltic Sea. This investigation combines the results of numerical simulations during normal and storm conditions to assess the effects of the short-term events on the medium-term evolution of the bathymetry.

During the last decades numerical models have been increasingly applied in the study and design of engineering projects in the coastal regions. Nowadays, with the evolution of modern computers, coastal engineers have the capability to obtain in relatively short periods of time information about water levels, currents, waves and sediment transport. Notwithstanding, it should be born in mind that because of the tendency to develop more rigorous and complex numerical models, the required computing capacity is rapidly becoming inadequate. For medium-term periods of simulation it has been proposed the use of morphologic acceleration factors (Roelvink, 2006). The morphologic acceleration factors can make complex models efficient and accurate, combining the hydrodynamic and morphodynamic processes online during one representative period of normal conditions. At CORELAB-FTZ institute, University of Kiel, in Germany, Wilkens (2004) and Etri (2007) have contributed with several investigations analyzing different implementations of those acceleration methods.

The different spatial and temporal time scales that can be distinguished in the studies of morphodynamics, has been always a matter of discussion when deciding about the kind of model that has to be used. Accordingly, the spatial and temporal scales are selected depending on the objectives of the investigation and the phenomena that are studied. Figure 1-1 schematizes the relationship between the type of phenomenon that is investigated and the range of the spatial and temporal scales. As shown in Figure 1-1, in the range of scales in morphodynamics, the maximum detail of the analysis can be reached within the instantaneous scale, comprising phenomena like 'toe scour' and 'sediment entrainment'. For larger-scale phenomena that happen within the event scale, like 'storm response' and 'inter-storm recovery', in the study of the morphodynamics, the average of multiple instantaneous processes are supposed to be a realistic representation during the event itself. In most of the engineering (scale) applications in morphodynamics the main interest of the investigations are focused on those phenomena which can be observed within periods of duration longer than seasons. According to that, for those kinds of applications periods of months and up to tenths of years can be considered sufficiently accurate. The range of spatial scales, on the other hand, can be between 500 m and 100 km (Terwindt and Battjes, 1991; De Vriend, 1992). Never before, the long-term phenomena, including the sea level rise and the resulting coastal evolution, have been as relevant as a topic of investigation in the study of the morphodynamics in the coastal areas. In that case, the geological (scale) phenomena are primarily descriptive reconstructed on the basis of paleoenvironmental evidence.

In this investigation, morphodynamic numerical simulations within the so-called engineering scale have been carried out. Both normal and storm conditions are taken into account in this study. The numerical results of the hydrodynamic and morphological simulations are presented in the last chapters of this thesis. This thesis is the first study based on morphodynamic numerical models to assess the medium term evolution of the Luebeck Bay for the normal and storm conditions.

The objectives of this investigation are: i) to find the effects that storms may have on the evolution of the bathymetry of the Luebeck Bay, and ii) to determine characteristic morphological changes of the Luebeck Bay during the medium-term period.

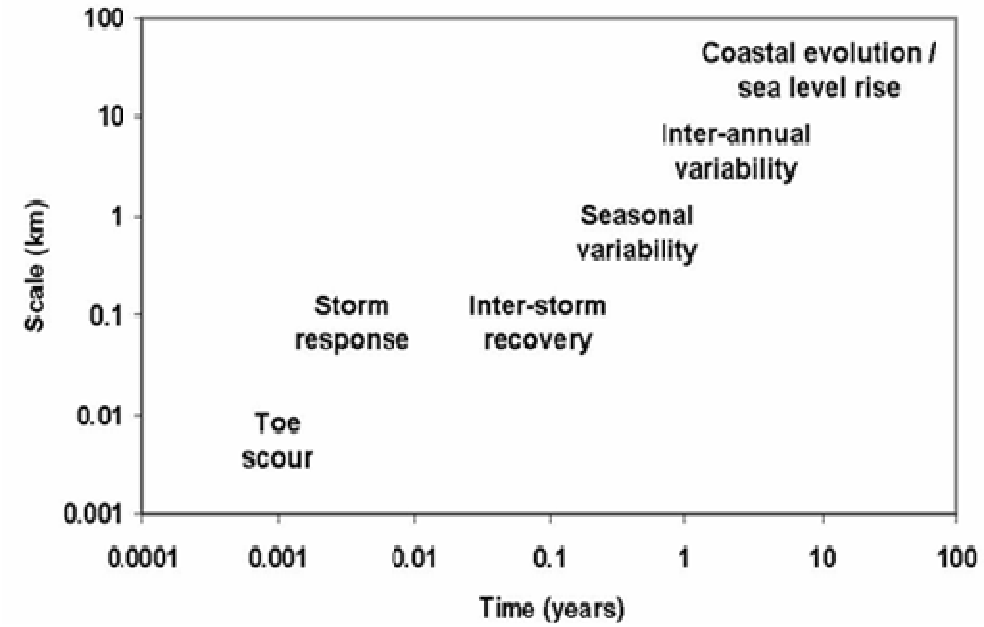

Figure 1-1. Spatial and temporal morphodynamic scales (after Magar V., 2009)

1.2 Thesis topic

The present thesis work comprises of the following: i) definition of the study area, ii) setup of numerical models used in this investigation, iii) assessment of the medium-term bathymetrical changes in the Luebeck Bay including the effects of storms and normal conditions.

1.2.1 The study area

Figure 1-2 shows the position of the inner Luebeck Bay along the German Baltic Sea coastline. In Kannenberg (1952) a number of initial studies about hydrodynamics and geomorphology of the Luebeck Bay are presented. During the last decades, habitants and stakeholders in the Luebeck Bay have expressed increasing concern for the threats of the erosion processes and flooding. In this investigation the first attempt to simulate the morphodynamics of that study area with the use of numerical models has been presented. The results that are obtained from this investigation are expected to explain the localization of areas of deposition and erosion that are observed in the Luebeck Bay. In Chapter 3 a detailed description of the study area is presented.

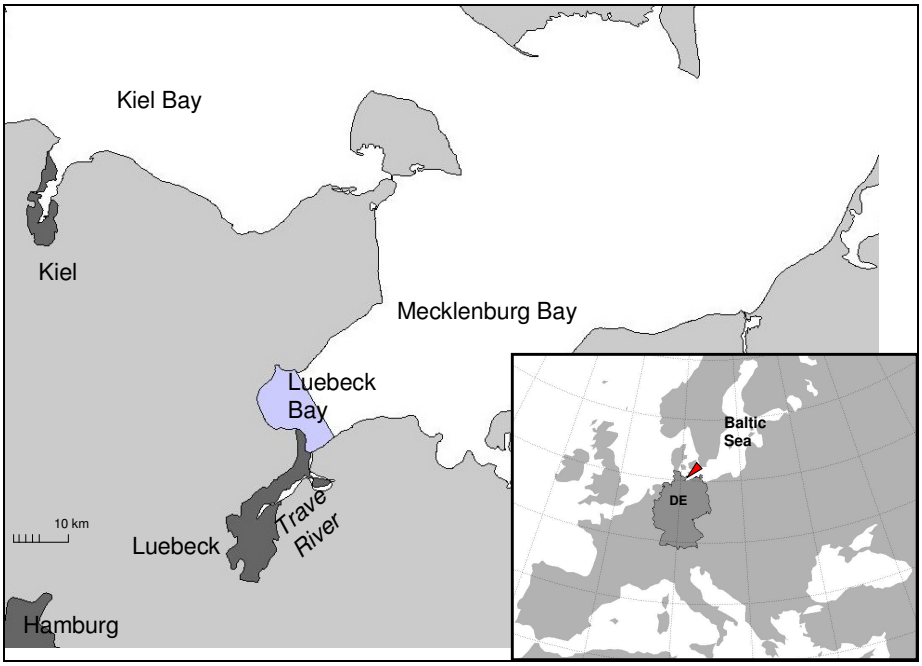

Figure 1-2. Study area

1.2.2 Numerical models

The development of numerical models including, sediment transport, waves and currents, have shown significant progress during the last 50 years (Grasmeijer, 2002). Supported by an increasing capacity in the computational resources, the applications of numerical models are nowadays the breakthrough in the investigations of the coastal zones around the world (Wilkens, 2004). Numerical models have proven to be a very practical tool in the analysis of coastal processes, giving the modellers the possibility to setup different conditions in the same domain area. It should be born in mind that the performance of the numerical models is highly dependent on the available information collected from the field. A proper calibration and validation of the model is only possible as long as measurement data is available (Reeve, D. et al., 2004).

Most of the accuracy that is expected from process-based numerical simulations depends on the assumptions and the applied methods in the model (Martin. et al., 2004). In this study the implementation of the morphodynamic model (i.e. including simulations of hydrodynamics and bathymetrical changes) corresponds to the medium term model classification found in De Vriend et al. (1993). The model has the capacity to simulate interactively all the processes that one morphological cycle may contain (i.e. flows, waves, advection-dispersion and sediment transport). In those models, a series of multiple morphological cycles are integrated to complete a period of simulation. The morphological evolution is updated once all the aforementioned processes are synchronized at the defined time step for the overall cycle of the bathymetry update.

In this study the MIKE 21/3 modelling system developed by DHI (Danish Hydraulics Institute) in Denmark was used. MIKE 21/3 is a coastal numerical model used for the simulation of flows, waves and sediment transport combining the effects that are produced out of the interaction between these three modules. The basic physical concepts are similarly applied to other systems of coastal numerical models, like Delft 3D at Delft Hydraulics, Netherlands. The main differences between both models are found in the spatial formulation and the solution of the sediment transport module in the way the bed and suspended load are considered (for more information see in: http://www.wldelft.nl and http://www.dhigroup.com , for Delft Hydraulics and DHI institute , respectively).

Waves, currents and sediments transport modules are integrated in this investigation. Separate simulations are carried out for each module during sensitivity analysis and calibration. Once the modules perform acceptably, the coupling of flow, wave and sediment transport is executed to validate the model.

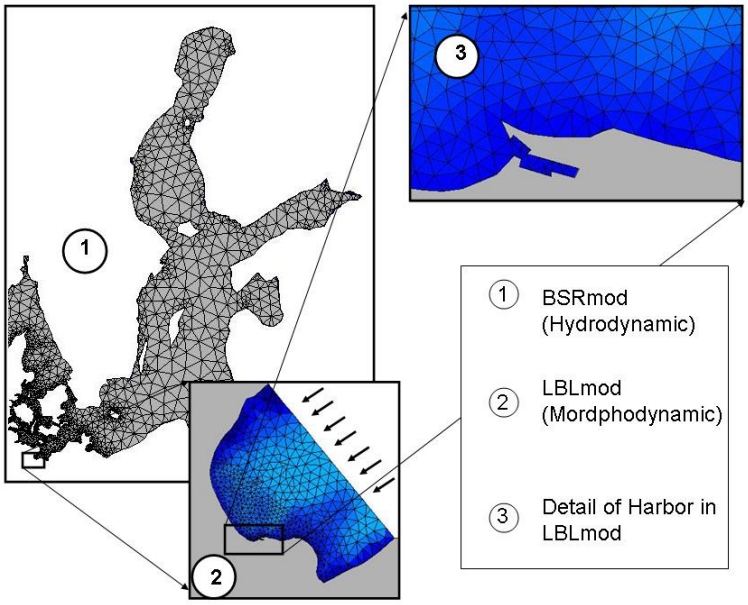

Figure 1-3. Schematization of nesting procedure adapted in this study. Arrows in LBLmod indicate the position of boundary conditions transferred from BSRmod to LBLmod.

Two numerical models (i.e. in the regional and local scale) were developed. The first case corresponds to the Baltic Sea Regional hydrodynamic model (BSRmod). The BSRmod was used to provide boundary conditions for the local areas close to the Luebeck Bay. It is driven by water levels in the Kattegat strait (on the west) and wind fields covering the whole region. The second model that has been developed in this investigation is the Luebeck Bay Local model (LBLmod). This model has

been included to simulate bathymetrical changes in the coastal area. Figure 1-3 shows the nesting sequence from BSRmod to LBLmod. In Figure 1-3, the unstructured mesh is shown illustrating how efficient the triangular elements accommodate the curvy sectors of the shoreline.

1.2.3 Methodology

This morphological study has been carried out in the following order of activities: i) acquisition and processing of data used as input of the numerical models, ii) setup, calibration and validation of the regional and local numerical models, iii) morphodynamic simulations and analysis of storm scenarios, and vi) morphodynamic simulations of medium-term morphodynamics including storm and normal conditions.

1.3 The thesis outlines

In total, 8 chapters have been included in this thesis. In the following an overview from chapter 2 until chapter 8 is presented.

Chapter 2

General concepts are presented in this chapter. The principles of morphodynamics in the coastal areas are explained. It also presents the technique of acceleration factor used in the morphodynamic models. In addition to that, the method of empirical orthogonal functions and the system of equations to determine the period of normal conditions is also explained in this chapter.

Chapter 3

In this chapter there is an overview of previous investigations in the Luebeck Bay. It presents different aspects about the geology, sedimentology and hydrodynamics of the study area. Additionally, it also mentions the most recent investigations that have contributed to a better understanding of its geomorphologic evolution.

Chapter 4

In chapter 4 the setup of the regional Baltic Sea Model including the online coupling of flows and waves, driven by currents, water levels and wind fields is introduced. A sensitivity analysis is carried out for wave and flow parameters, mesh resolution and time step of the model in the regional scale. The model is also calibrated and validated covering the entire Baltic Sea region. With the use of this model, water levels and current velocities are simulated generating the boundary conditions for the morphodynamic local model in the Luebeck Bay.

Chapter 5

General aspects of sensitivity analysis, calibration and validation of the Luebeck Bay Local Model are presented in chapter 5. The set-up and calibration of each module of this model has been presented separately. At the end, all modules are coupled for validation.

Chapter 6

This chapter includes a definition of storm conditions in the study area. In addition to that, the numerical results of the morphodynamics based on 16 extreme scenarios are analyzed. An analysis of empirical orthogonal functions used to produce a map of tendencies in the distribution of areas of erosion and sedimentation in the Luebeck Bay is presented.

Chapter 7

In this chapter the medium-term morphological simulations are analyzed based on the results of the sequential simulation of storms flowed by the calm period. The numerical results will contribute to have a better understanding about the tendencies in the evolution of the coastal areas of the Luebeck Bay in the medium-term period.

Chapter 8

The final conclusions and recommendations are included in this chapter.

Chapter 2

Literature Review

2.1 Studies on the morphological evolution of the coast

Interests on the morphology of the coastal areas can be traced back to the 15th century by the time Leonardo da Vinci drew plans to drain the Pontine marshes (Woodroffe, 2002). During the World War II, the emphasis of the investigations about the morphological process on the beaches began as a result of complications of landing on beaches (Williams, 1960). In most recent investigations the observations and empirical formulations have been fundamental to understand the processes that shape the coastal areas (Van Rijn et al, 2003).

Coasts can adopt distinct geometrical patterns in its platform and profile. Compartments along the coastlines are composed of drifted-aligned beaches, embayed beaches, pocket beaches or swash-aligned beaches (see Figure 2-1). Drifted-aligned beaches are the result of long-drift transport of sediment generated by the waves that have an angle of incidence different than 90°. Swash-aligned beaches, on the other hand, are shaped by the effects of the cross-shore transport generated by incident waves that are normal to the shoreline. Pocket and embayed beaches are enclosed beaches that have a combination of both, long-shore and cross-shore sediment transport. The origin of the sediment also plays a role in the evolution of the coast; cliff erosion, river input and in-situ availability of sediment are decisive for the sustainability of the beach.

The cross-shore section in (Figure 2-2) includes four main zones on the basis of the characteristics of the waves, including, shoaling-waves zone, breaking-waves zone, surf zone, and a swash zone.

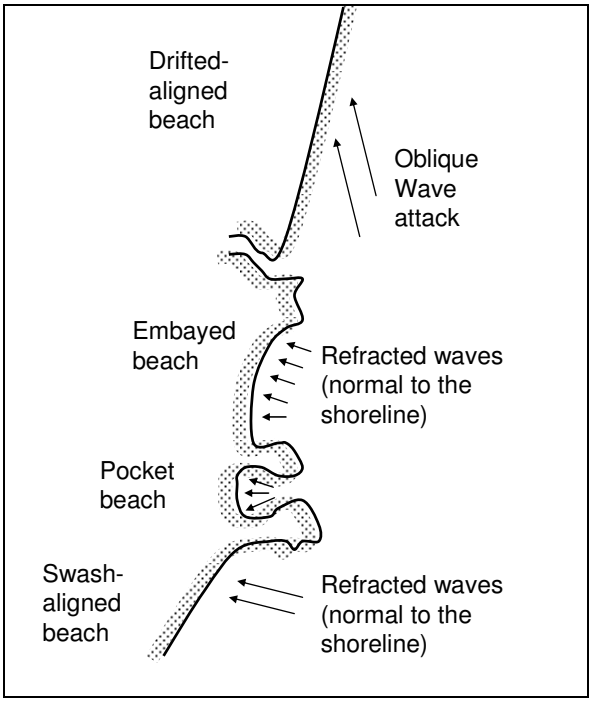

Figure 2-1. Definition of beach compartments in the planview (after Woodroffe, 2003)

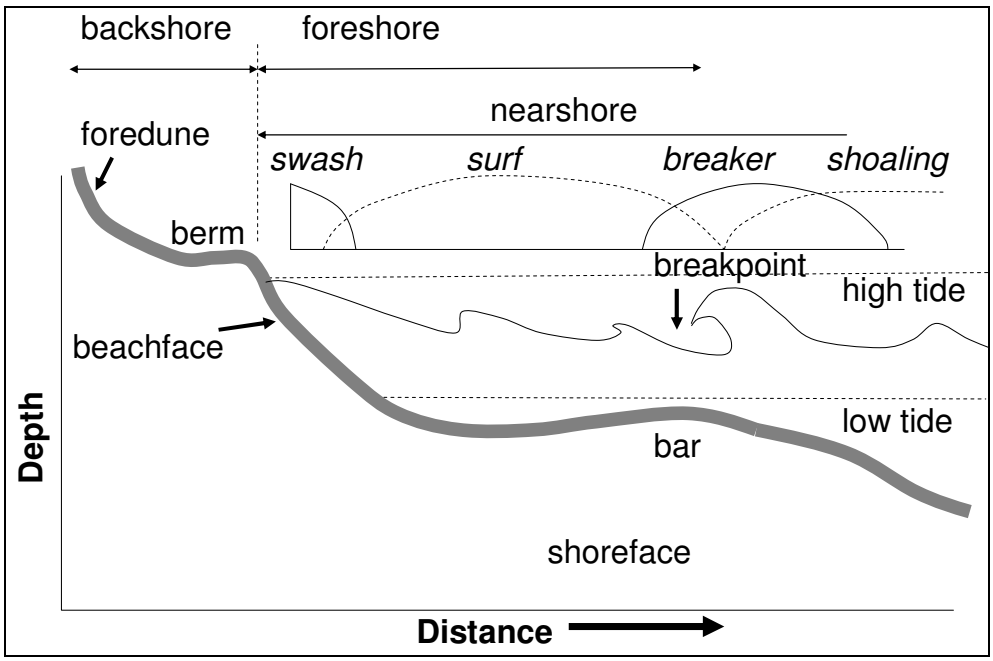

Figure 2-2. Definition of a typical beach profile (after Woodroffe, 2003)

The changes on the bathymetry of the coasts have been studied for many years. The initial investigations on the morphology of the coast were focused on the concept of cross-shore equilibrium profile (Woodroffe, 2002). Many years, the long- and medium-term development of the costal areas has been one of the most investigated fields of coastal morphodynamics. A major problem in those investigations is the limitations of the available data. In most of the cases, the effects of the extreme events on the medium- and long-term morphological changes are normally disregarded due to the low frequency of measurements in the bathymetry.

The principal approaches used to analyze the morphological development of the coastal areas are mainly based on statistical analysis of the available information and model applications. In the first approach, the available data in terms of series of bathymetries are statistically analyzed. Through this method the computation of average bathymetrical changes and the application of more sophisticated approaches are used to determine the tendencies of evolution of coastal areas. In one example of data analysis, Wijnberg (1995) combined analysis of bathymetrical changes along the coast of Holland using measurement from 1963 until 1990. In that investigation the EOF technique is combined with a moving window approach to define large-scale coastal behavior regions. In another application of statistical techniques, Lane (2004) determined the tendency of loss of volume of the Mersey Estuary in UK based on the bathymetries from 1906 to 1997. In another investigation a complete analysis of the morphology in five coastal areas, including: Noordwijk beach in Netherlands, Duck in North Carolina (USA), Sylt in Germany, Lubiatowo in Poland and Winterton in UK, is presented in Kroon, et al. (2008). In that work the bulk statistics (mean, standard deviation, correlation, etc.) and more sophisticated methods, including empirical orthogonal functions (EOF), canonical correlation analysis (CCA), complex EOF and singular spectrum analysis (SSA) were applied to identify the most relevant characteristics of the morphological changes in those coastal regions.

Through the analysis of historical data the knowledge of the morphological evolution of the coastal areas can be improved. Those investigations are based on the information that is collected by means of different techniques, including measurements of cross-sections, shoreline observations and satellite images. The possibility given by numerical simulations integrated with the collected data is the breakthrough of the coastal engineering applications during the last years. In the work from Ruggiero et al. (2003), one example of investigations of morphological changes applying numerical models is presented. In that approach seasonal morphological changes are studied to determine both, the physical mechanisms governing the morphological changes and the links of short-term measurements to the coastal change at management scales. The effects of long-term morphological changes in the short-term simulations have been investigated in the study of Bochev-van der Burgh (2008). The contribution of that investigation is focused on the morphological numerical simulations of short-term including the long-term tendency of the bathymetry evolution along the coastline. Longer periods of simulations of morphological changes applying numerical models have been

studied by Dastgheib et al. (2008). In that work the approach consisted of the 'online approach' applying morphological factors. In that study insight is given into the tendencies of the morphological changes of the Dutch Wadden Sea by considering equilibrium and non-equilibrium conditions. The most extensive data ever collected of the morphology of the sandbanks at Great Yarmouth, UK, is investigated by Reeve, D.E., et al. (2008). In that investigation, a data-driven model has been developed based on historical survey charts reaching back to 1848, in order to produce forecasting with regard to the movement of the sandbanks in the long-term.

The morphological changes in the coastal areas that are produced by storm events and the role that these events might play over longer periods of time is still a matter of debate. At the Egmond site (The Netherlands), one of those studies has been carried out with the aim to validate the predictability of the process-based models that simulate the bed evolution of sandy beaches (van Rijn, et al., 2003). The results from that study showed the importance that 3D morphodynamic effects have on the simulations of the beaches. The models were accurate enough to simulate the storm effects that influence the offshore displacement of bars, contrasting with the low accuracy in the results during the simulation of the recovery processes over periods of calm conditions. A more detailed analysis of the effects of storms on the offshore/onshore movement on the nearshore was investigated by Houser and Greenwood (2005). They discover important relationships between the system of bars in the southern beaches of the Lake Huron, indicating a feedback mechanism between the pre-existing morphology and the wave forcing. Research on the shoreline erosion and barrier island response to the extreme events has been carried out by Houser et al. (2008). In that investigation the effects of one particular extreme event (Hurricane Ivan) on the morphology of the Santa Rosa Island in northwest Florida are analyzed to identify the alongshore patterns in the rate-change of the morphology of the island. The time of coastal areas to recover may take several years and in some cases the recovery is not total; Maspataud et al. (2009) have investigated the pre-storm and post-storm beach recovery process in northern France. In that study it was found that post-storm conditions are not uniform along the coastal areas; in some sector the beaches may recover during calm periods, whilst in the others the cumulative effects of the storms might remain. In a recent research on the effects of the storms on artificial embayed beaches, Ojeda et al. (2010) indicated the relevance of distinct factors different from the wave condition in the evolution of the coast during storm events. In that investigation the authors urge for to consider several factors that affect the response of the beaches to the storms, including the morphodynamic configuration of the beach before the storm event (sediment availability, sandbar morphology and shoreline orientation), storm sequence and human intervention.

The German coast in the Baltic Sea is in permanent geomorphologic evolution; the meteorological and hydrodynamic conditions affect the shoreline and bathymetry in the coastal zone. For more than 100 years the risk of floods and the progressive erosion have been studied in many locations along the coastline of the German Baltic Sea (Kannenberg, 1952). During the second half of the last century,

governmental authorities and stakeholders have made efforts to protect the coastal areas around the bay. In this thesis these previous investigations of the morphological changes in the Luebeck Bay are complemented by the development of a morphodynamic numerical model.

In the 1950s several research projects were carried out (e.g. Dietrich and Weidemann 1952, and Seifert 1952). The results of those investigations about the hydraulic and geologic conditions of the Luebeck Bay have been used to develop methods of coastal protection against flooding of the low lands of the lake of Hemmelsdorf and the erosion of the exposed Brodten cliff-coasts. Several geomorphologic studies have shed light on the bathymetrical evolution of the Luebeck Bay (Bayerl et al., 1992 and Schwarzer, 1995). In one of the most recent studies Schrottke (2001) carried out investigations intended to investigate the systematic erosion in areas close to the cliff-coasts along the German Baltic Sea shoreline.

During the execution of the MUSTOK-SEBOK-A project (Bruss et al., 2009) a hydrodynamic model covering the entire Baltic Sea Region was developed to simulate more than 60 synthetic scenarios. The results of that project were used to assess the efficiency of coastal-protection structures and to evaluate the traditional methods of design of dikes along the German Baltic Sea coast (see Bruss et al., 2008).

2.2 Brief introduction to morphodynamic numerical models

The evolution of the coast is the result of the balance between the counteracting forces that are constantly shaping and modifying the morphology through erosion, transportation, and deposition of sediment. These forces comprise of hydrodynamic processes due to tides, currents, and waves. The interaction of such forces generates transport of sediment as a permanent process that ends up in the morphological change of the coast. At present the investigations of numerical models are focussed on the improvement of t he accuracy, including a wide range of temporal and spatial scales (Martin and McCutcheon, 1998). Although relevant advances in the morphodynamic modelling has been made during the last years (e.g. Rakha, 1998), there are still computational limitations that do not permit the precise representation of the morphological changes including all scales over medium and long term simulations. Woodroffe (2002) indicates the importance of defining the temporal and spatial scales according to the relevance of processes that matters to the morphological investigations. In Figure 2-3 a simplified schematization of the geomorphologic processes and their corresponding temporal and spatial scales is presented.

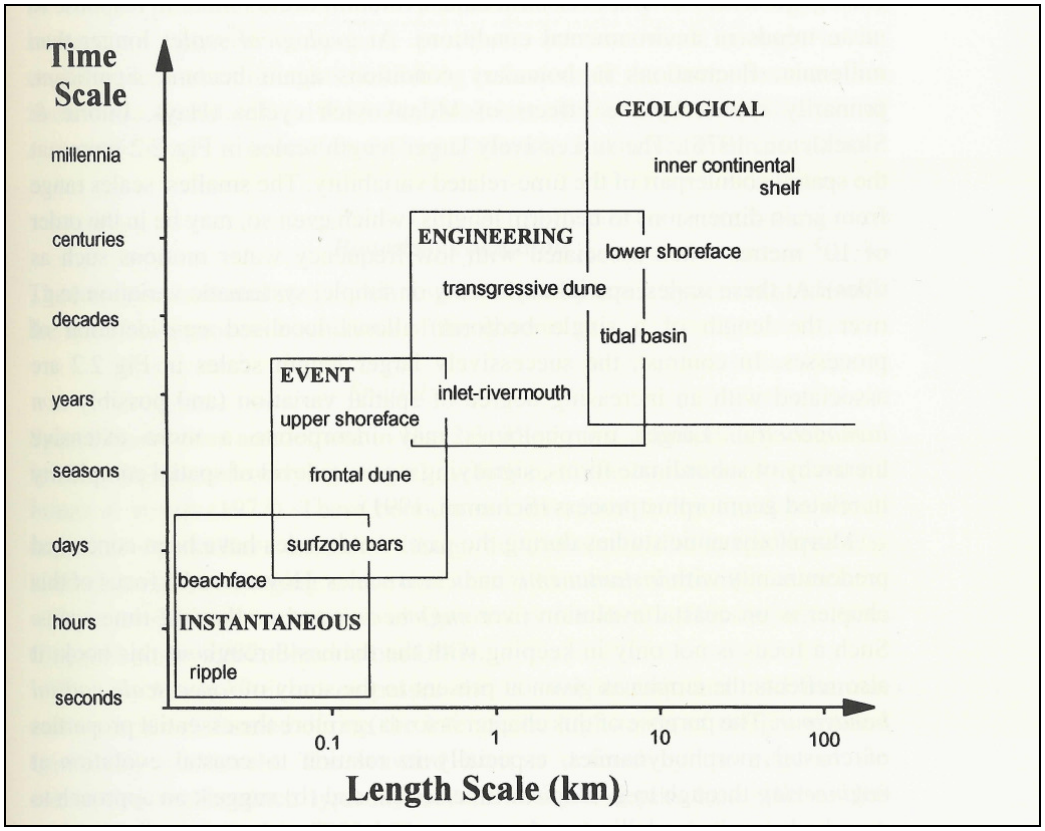

Figure 2-3. Spatial and temporal morphodynamic scales (after Cowell and Thom, 1994)

Most of the processes that are included in the instantaneous scales in Figure 2-3 cannot be exactly represented by the numerical models. Nowadays most of the formulations that are used to solve the physical processes that take place in such scales consist of stochastic and empirical methods (Rakha, 1998). In contrast to the processes that are observed in the instantaneous scales, in the event scales other techniques are applied in order to make longer periods of simulation feasible (Roelvink, 2006). In the engineering scales, for example, the average of the hydrodynamics for one tidal cycle, the simulations of one representative storm event, and the experience and previous knowledge about trends for seasonal variations can provide a background about the typical conditions for morphological simulations of medium- and long-term. Within the scope of this thesis work, the numerical simulations will be run for the analysis of cases within the engineering scale.

In Figure 2-4 a flow chart shows the numerical-model scheme used in the morphodynamic simulations of MIKE 21/3 FM model. The model makes part of the marine package of numerical models developed at Danish Hydraulics Institute

in Denmark (www.dhigroup.com). The bathymetry and driving forces arising from wind fields, flows, water levels and wave conditions, are provided into the hydrodynamic modules of the numerical model. Subsequently, the on-line coupling of waves and flows enables the system to work as one single hydrodynamic module. The sediment transport formulations are integrated in the system. The bed load and sediment in suspension are combined together. More details about the modules are presented below.

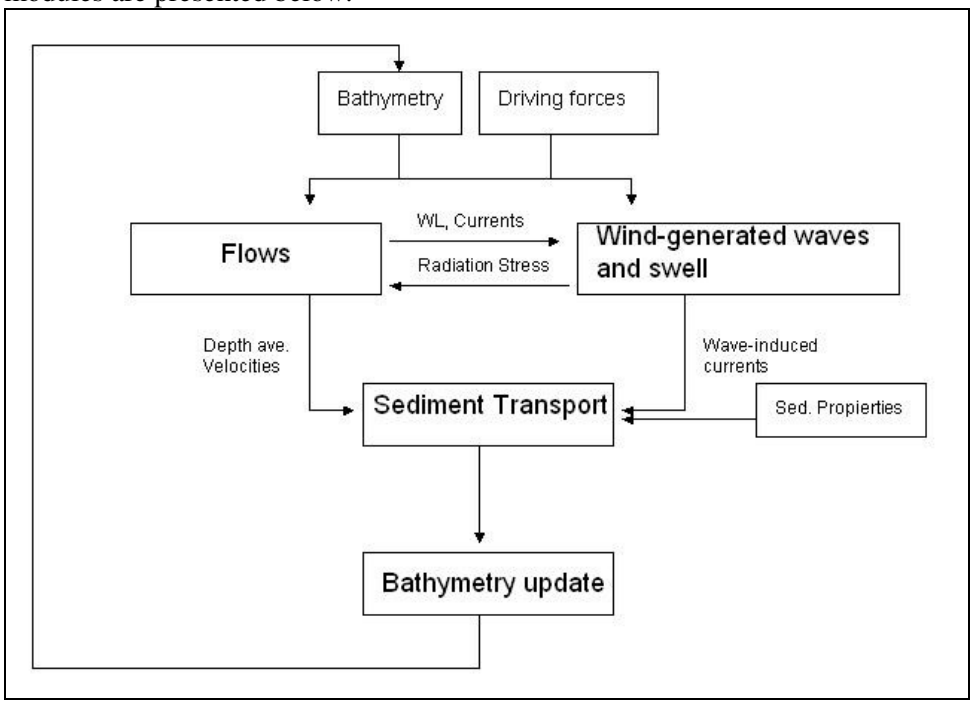

Figure 2-4. Basic computational updating of the bathymetry within MIKE 21/3 Coupled Model

The simulations of morphodynamics using the DHI system are carried out by coupling the three basic modules online: first, hydrodynamics, then, sediment transport, and finally changes in the morphology are computed. In Figure 2-4, one computational cycle of the morphodynamic model is illustrated.

The basics of the formulations and equations of the model system are presented in Appendix A. A more complete explanation of the concepts included in the numerical model is presented in the available documentation at http://www.dhigroup.com.

2.3 Acceleration techniques in morphodynamic numerical simulations

In recent investigations of numerical morphodynamic models applied for medium and long term, the techniques to accelerate the simulations of morphological changes have been validated (see Roelvink, 2006). Those techniques can be

summarized in two main groups as follows: i) the averaging of hydrodynamic conditions and ii) the introduction of acceleration factors applied to a representative period of time.

The technique in the first group consists of the application of the hydrodynamic conditions that may be found during one tide-average period to reduce the computation of the equation of the sediment transport and bathymetrical changes. The key aspect of the procedure is the adjustment of the hydrodynamic conditions during the tide period (i.e. the continuity correction technique on wave action and flows). For these kinds of methods a fixed bathymetry is assumed.

The tide average technique is not the best choice for cases where important effects of the bathymetry-changes on the flow rate and patterns of currents are expected. For example, high errors might appear when the area becomes shallower and the flow velocity continues to increase every time the correction is applied. In such cases, the depth-currents relation should be revaluated during iterative procedures.

In order to overcome the difficulties posed by the "continuity correction" assumptions, another approach can be integrated to the "tide-average" technique through the RAM method (Rapid Assessment of Morphology). Basically, the two methods, i.e. continuity correction and RAM, are different to each other in the procedure used to simplify the sediment transport formulation. While the intention of the "continuity correction" approach is to adjust new hydrodynamic conditions to the morphological changes; the technique of RAM on the other hand, considers several hydrodynamic conditions in such a way that the final changes of the bathymetry are the results of the most representative morphological patterns.

Lesser et al. (2004) presented a new method based on the application of a morphology factor (morfac). It consists of online simulations of flow, sediment transport and bathymetry updating. With this method it is possible to find a way to represent with more accuracy the bathymetrical changes. These techniques consist of increasing the bathymetry-change rate by a constant factor, which proportionally allows the bathymetry to change faster. The simulations using morphological factors should be carefully carried out. It is important to have enough information about the morphological evolution of the study area in order to compare the observations with the results of the numerical models.

Figure 2-5 shows the tide-averaging and online method. In this investigation the application of 'morfac' (MF) will be considered in the way presented by the online method shown on the right side of Figure 2-5.

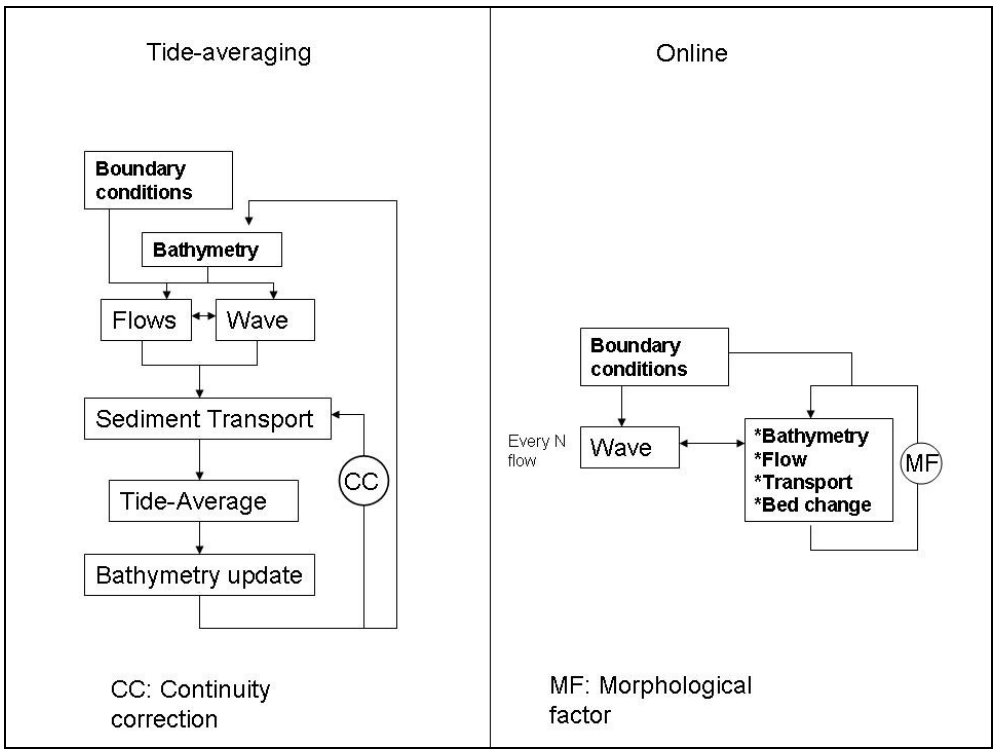

Figure 2-5. Diagrams of techniques to accelerate medium- and long -term morphological simulations.

2.4 Methods used in the definition of the representative hydrodynamic and meteorological conditions

In the acceleration methods mentioned above, it is required to define the period of normal conditions of water levels, waves and winds. Steijn (1992), for example, shows a method to define the tide-and wave-climate representative conditions. The method begins with the definition of the representative tide with amplitude 10 % longer than that of the average tide, which has been calculated out of the set of tides included in the selected neap-spring tide-cycle. In order to adapt the input conditions to the steady-state nature of the wave and sediment transport models, the representative tide had to be discretisized in a block wise sequence of flows and surface elevations. The discretization of the tide followed a multi-criteria analysis. The wave-climate average conditions had to be also found. The main directions of the waves are divided into a few sectors and weights are given to the wave conditions based on the long shore power and the stirring parameter.

The tide average technique has been extensively studied by previous theses at CORELAB (Coastal Research Laboratory-University of Kiel). The most recent studies are found in Wilkens (2004), Wilkens and Mayerle (2005), and Etri (2007). Their topic of investigation has been focused on the application of morphodynamic

models on the German Bight area. Basically, the principal aim of the aforementioned investigations was the analysis of bathymetrical changes during medium-term periods in the tidal flats area. Wilkens (2004) in his thesis introduces the average-tide technique during the calibration and validation of the Dithmarschen Bight Model (DBM). Advances on the application of the DBM using a more detailed process-based model are the contributions implemented in Etri (2007). The former thesis-work differentiates from the later in the way how the morphological time schematization is applied. Initially, the approach implemented consisted on the continuity correction technique during the updating of the bathymetrical changes. Etri (2007) implemented the morphological factor, which is the most recent method on time-evolution morphological techniques developed at Delf-Hydraulics. One distinctive aspect between the aforementioned studies is the differences as to how storms should be represented during medium-term simulations. By applying the continuity corrections scheme, the limitations were clear in those cases where storms may play an important role during medium-term simulations. In order to solve that problem, the morphological factor approach has been introduced as an alternative to compensate for the lack of information of the storm events in the morphodynamic model.

For this particular study, no average-tide approach is proposed. The clear semidiurnal tidal cycle that is present in the German North Sea has made such scheme suitable during the above mentioned studies; in contrast, in this particular study, the lack of a clear water-level oscillation regime of the German Baltic Sea precludes all methods that are dependent on application of representative tides in the medium-term-simulation studies. In the German Baltic sea region the most important aspects that should be considered are the wave climate and extreme events conditions that may affect the bathymetrical changes during short-and medium-term durations.

The uncertainty that lies behind extreme events of short duration constitutes the most difficult aspect for numerical simulation. There are many factors that contribute to the increment of such uncertainty during the simulation of bathymetrical changes on coastal areas. Winds, for instance, are driving forces that sometime behave quite unpredictable by generating effects on the morphodynamics that are not easy to understand. The wind effects along with the hydrodynamics and sediment characteristics are important in the morphodynamics and always have to be accounted for.

In this study the normal conditions and storm events are considered together in order to carry out medium term morphodynamic simulations. As mentioned above, the acceleration methods are applied considering a representative period of normal conditions. Until now no clear procedure has been documented in which the effects of the storms are included in combination with the acceleration methods. Thus, in this thesis work, it is intended to propose a method to simulate morphodynamics over medium-term periods through a combination of two techniques. The first one, i.e., the Cost Functions method, is the procedure to determine the period of normal conditions. The ‘Coast Functions’ is a technique that helps to find a period of time (e.g. seasonal durations) that represents most of the conditions that are normal for a

specific variable. The storm effects on the other hand, are implemented through the principal components analysis technique or Empirical Orthogonal Functions (EOFs) applied to the morphological changes. The EOFs method has been used to analyze the variability of bathymetrical changes. In the work of Houser et al. (2008), for example, the EOFs technique has been used to characterize the changes in the morphology of island barriers that were produced by Hurricane Ivan in Santa Rosa Island in Florida. One more example of EOFs application is presented by Bochev-van der Burgh (2008), in which the EOFs were used in the characterization of long-term morphological changes, which were included in cross-shore dune erosion models.

In the following the theoretical fundamentals of cost functions and EOFs are described.

2.4.1 Cost Functions

Representative periods within the available data are useful whenever it is possible to obtain a significant reduction in the computing time. The 'cost functions' method is a tool to reduce the time series of data through the comparison of statistical properties between sets of data of different duration (Boon et al., 2002). In other words, if the value of a statistical property (e.g. mean, standard deviation) of a larger set of data is similar to that of a predefined fraction included in it, it is likely that that fraction of the original set of data represents the conditions of the total. The approach of 'cost functions' can be briefly illustrated by the particular application to wind velocity as indicated by Boon (2002). The difference between the monthly average wind components (i.e., Wn and We; where, *n*: north, *e*: east) and the long-term average wind components (i.e., Wn_lt and We_lt) produces the first cost function (see below, equation 1). Additionally, a second cost function (see equation (2)) can be estimated by the differences between the standard deviations of the monthly average (i.e., σ_{Wn} and σ_{We}) and long-term average standard deviations (i.e., σ_{Wn_lt} and σ_{We_lt}, respectively).

$$C1 = \left(Wn - Wn\_lt\right)^2 + \left(We - We\_lt\right)^2 \tag{1}$$

$$C2 = \left(\sigma_{Wn} - \sigma_{Wn\_lt}\right)^2 + \left(\sigma_{We} - \sigma_{We\_lt}\right)^2 \tag{2}$$

Finally, C1 and C2 are normalized and summed up in order to estimate the level of similarity that exists between the periods that are compared, i.e. total and fraction respectively:

$$C3 = \frac{C1}{\sigma_{C1}} + \frac{C2}{\sigma_{C2}} \tag{3}$$

2.4.2 Empirical Orthogonal Functions (EOF)

The simulation of bathymetrical changes is prone to uncertainties and limitations due to the complexity of the processes involved. The availability of data is crucial to reduce such uncertainties at the very initial stages, when boundary conditions, bathymetry and driving forces are defined, and during the calibration, when the model results are compared with the measurements. Unfortunately, measurements of bathymetries before and after the impact of storms in coastal areas are usually not available. The measurements of bathymetry are limited and just a few, if any, of them might have been collected exactly at the beginning and end of an extreme event. In addition to that, the lack of temporal resolution makes it almost impossible to see the real bathymetrical evolution during the storm. The most detailed bathymetrical measurements might be able to indicate how the morphology evolves in a seasonal scale, but this kind of data usually misses important patterns in the transformation of the bathymetry that can only happen during storms. In the underlying work, it is intended to evaluate the method of EOFs analysis to generate a representative morphological evolution based on the results obtained from a series of synthetic storms. The following is an introduction to the EOFs technique and the way it has been implemented in the methodology.

Empirical Orthogonal Functions, also named Principal Components Analysis (PCA), is a method used to analyze the spatial and temporal variability of geophysical fields. Through this method, spatial distribution-patterns of any kind of variable may be identified, while most of its principal features are sorted out following the relevance of each of them among the vast possibility of combinations.

Many authors strongly recommend the use of simpler methods before applying EOFs (von Storch and Navarra, 1995). In doing so, the data is previously reviewed and knowledge about the variability of the field can lead to a better understanding of the spatial distribution of the parameter. For example, contour plots and simple correlations would be useful for recognizing how the physical variable is distributed over the domain, and whether the physical parameters correspond to the variability of the modes.

For a detailed introduction to the EOFs method, Preisendorfer (1988) presents a complete definition of the procedures and its applications. Another useful literature is the textbook from Von Storch and Navarra (1995.

2.4.2.1 Input data of EOFs

In this investigation representative conditions of the storm in the Luebeck Bay are defined as differences of the bathymetrical changes given in meters during the storm. For the EOFs analysis the variable is represented as a ‘map’, i.e. a 2D-horizontal distribution of the bathymetrical changes given in meters (see Figure 2-6).

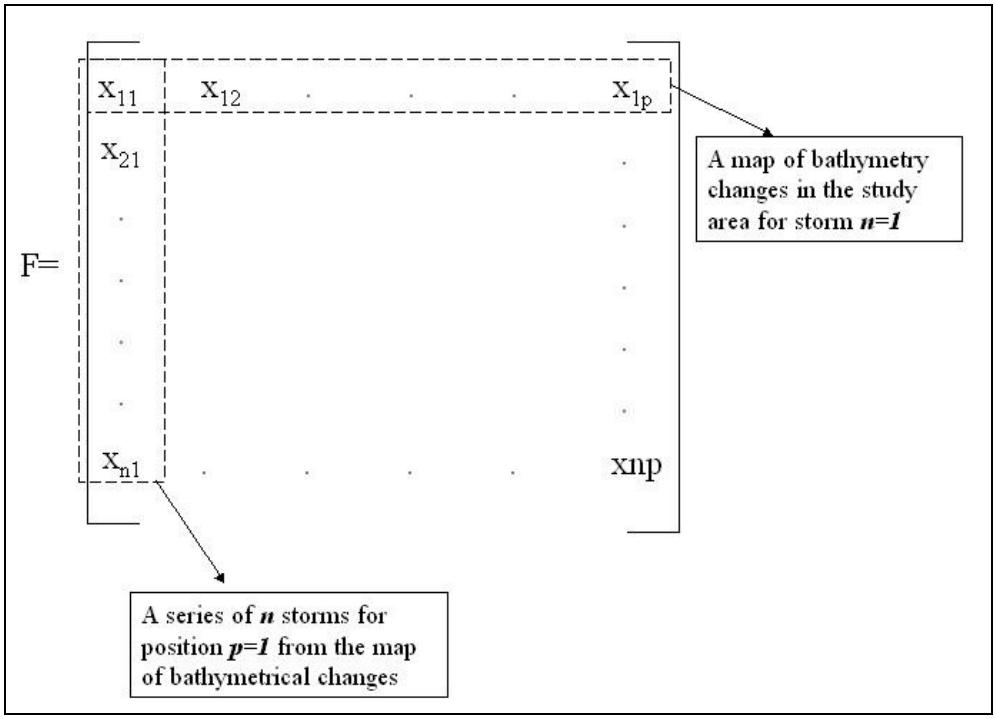

Figure 2-6. Matrix of input data for the application of the Empirical Orthogonal Functions.

In Figure 2-6 the rows in matrix F correspond to each of the maps that contain the two-dimensional set of bathymetrical changes (i.e. $X_{i,j}$=bathymetrical changes in meters). For each map, i.e. the scenario of one single storm, the original 2D array shape of the data is rearranged in vectors (i.e. rows in the matrix) keeping the locations of each cell along the vertical at the same column for every storm (i.e., columns in the matrix) included in this study. Finally, a n-by-p matrix represents the field of storm scenarios of the bathymetrical changes.

2.4.2.2 Eigenvalues (λ)

The expression eigenvalues is taken from the German expression 'eigen', which means proper. This parameter represents the weights of the components of the equations that are formulated by the 'eigen' decomposition theorem (see Annex B). In this context the eigenvalues are expressed in terms of percentage. Thus, through the eigenvalues the information about the relevance of the set of patterns that are present in the bathymetry changes resulting from the set of storm scenarios are determined.

2.4.2.3 Eigenvectors (EOFs)

It has been already indicated that the eigenvectors are related to a corresponding eigenvalue. It was also mentioned that both quantities are the result of the procedure derived from the 'eigen' decomposition theorem. Both quantities, i.e. eigenvalues and eigenvectors, make part of the system of three matrices shown in the equation (4). The matrix *C* contains the eigenvectors; also known as EOFs. Through the decomposition of the 'eigenvector' matrix the solution of equation (4) is carried out, i.e. the solution of the eigenvalue problem. The resulting vectors are uncorrelated (i.e. orthogonal) in space among different EOFs. In this context it is said that, the EOFs represents the spatial variability of a finite number of trends (i.e. scenarios) of the bathymetrical changes.

System of equations in the solution of the eigenvalue problem

$$RC = C\Lambda \tag{4}$$

$$R = F^t F \tag{5}$$

R is the covariance matrix of F, C is the matrix containing the eigenvectors of R, and Λ *is the vector of eigenvalues.*

2.4.2.4 Expansion coefficients (EC)

While eigenvectors represent the spatial distribution of the bathymetry changes, expansion coefficients are the solution in the temporal dimension. For this particular case, there is no temporal dimension of the bathymetry changes; instead of that, there is a set of scenarios that are associated to each EOF through the ECs.

Equation 6 shows the ECs (i.e. vectors $\vec{a}$) as a projection of the maps (i.e. bathymetrical changes) onto the EOFs. Through the application of equation (6) large quantities of data may be significantly reduced, i.e., by including the most representative eigenvectors and its corresponding expansion coefficients, a new map of bathymetrical changes can be created after filtering the patterns that are less relevant. For a step-by-step description of the EOFs technique, details are included in the annexes (Annex B).

$$F = \sum_{j=1}^{p} a_j \left(EOF_j \right) \tag{6}$$

Chapter 3

Study Area: Luebeck Bay

Figure 3-1 shows the localization of the Luebeck Bay in the German Baltic Sea (between 10°45' and 11° Longitude, and 53°54' and 54°6' Latitude). The area is situated in the Schleswig-Holstein state of Germany, to the northeast of the city of Hamburg. The bay constitutes the innermost region of the Mecklenburg Bay along the German Baltic Sea coast.

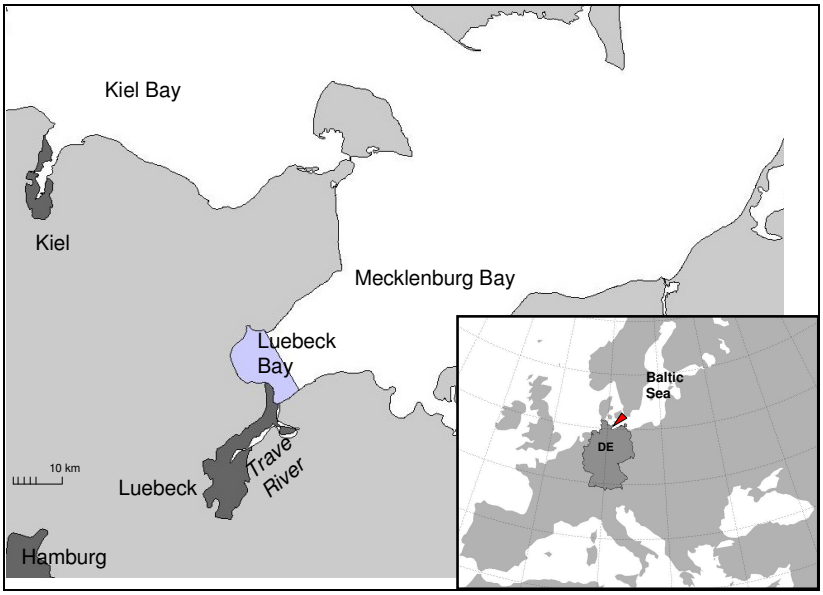

Figure 3-1. Study area.

Meteorological and hydrodynamic conditions affect the shoreline and bathymetry in the coastal zone of the Luebeck Bay. The risk of floods and the progressive erosion along the coastline of the German Baltic Sea can be a threat to the residents and the commercial use. Efforts have to be done to protect the coastal areas around the bay. In this study morphodynamic numerical-models are proposed as a tool to help to prevent critical hydrodynamic and morphological conditions in the study area.

3.1 Geology

The origins of the Luebeck Bay can be traced to more than 115.000 years, during the last Pleistocene-deglaciation period (i.e. Eem-warm period) (Duphorn et al., 1995). The basin of the bay originated from the melting of ice that existed in the southern areas, where nowadays the Lake of Hemmelsdorf is found. During the Frankfurt glaciation-stage, the Luebeck glacial-snout started expanding southwards reaching the outskirts of Hamburg City. A number of consecutive glacial-snouts during the following glaciation stages, like the Pommerian and Mecklenburg glaciation-stages, led to the formation of Hemmelsdorf Lake and Travemuende fjord. The evidence of such process can be clearly seen through the Rosenthal glacial boundaries that were left in the area like footprints of the colossal forces that helped to shape the Luebeck Bay (see Figure 3-2).

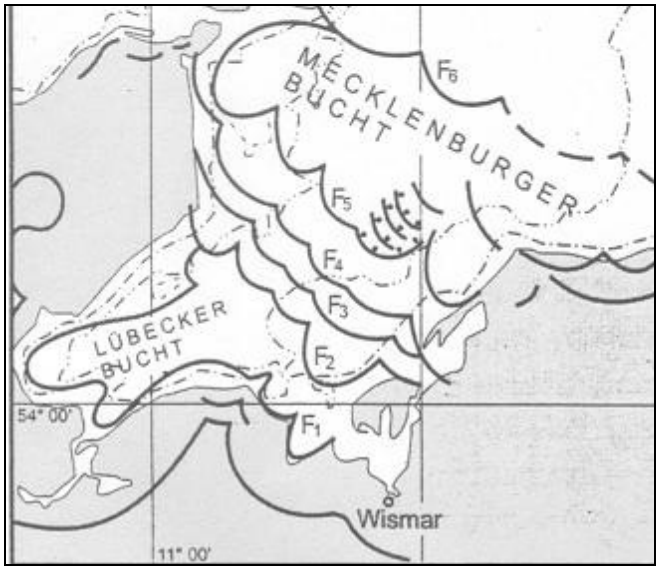

Figure 3-2. Glacial boundaries in the south-western Baltic Sea after Lange (1984) (from Lemke, 1998). F: Rosenthal glacial boundaries.

At the beginning of the Holocene, a recently-formed moraine between the Hemmelsdorf Lake and the Travemuende became the principal source of sediment in the area. With an extension of 6 km, north of the Brodten cliff-coast, the remains of the moraine are still visible in the bathymetry of the Luebeck Bay. The hydrodynamic condition of the area generated the erosion of the moraine, transporting the loose sediment to the Timmendorf –Niendorf beaches and the eastern Travemuende fjord (Ruck 1952). A schematic representation of the Holocene geomorphologic-evolution of the Luebeck Bay is given in Figure 3-3.

The bathymetry of the actual inner Luebeck Bay comprises four main characteristic features (see Figure 3-4). Two channels in the south-north direction are well defined in the western and eastern sub-domains. These channels have been the result of the water produced by the melting of ice during the Holocene. The Kuhlbrook channel is situated on the western side of the bay. This channel is ca. 15m deep with abundant sand and residual sediment on its bottom. The second channel, the Aalbeek channel, is found on the eastern side of the bay. In the Aalbeek channel the deepest areas are about 19 m deep, which are mostly covered by silt and clay. In the middle of the bay, just in front of the Niendorf harbor, a shallow area separates both channels. The exchange of sediment between both channels is considered restricted; there is no evidence that the main source of the sediment that is deposited in the Kuhlbrook channel comes from the Aalbeek channel (Bayerl, et al, 1992). Another geologic feature that characterizes the inner Luebeck Bay is the ridge in font of the Brodten cliff-coast, which is still under erosion. In the investigation of Schrottke (2001) it is shown that the ridge is retreating. It is possible that the erosion produced along the Brodten-Cliffcoast constitute a source of sediment that is deposited in the Niendorf and Timmendorf coastal zone; there is no definite evidence that such pattern of the sediment transport has indeed taken place in that direction.

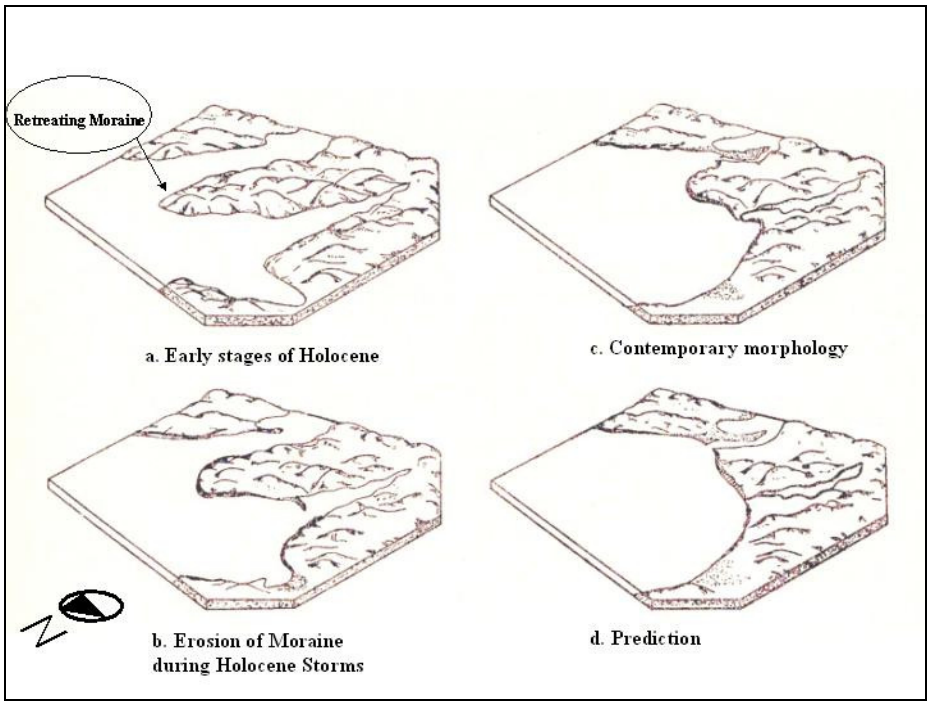

Figure 3-3. Geological evolution of the Luebeck bay during the Holocene (after Schmitz, 1951)

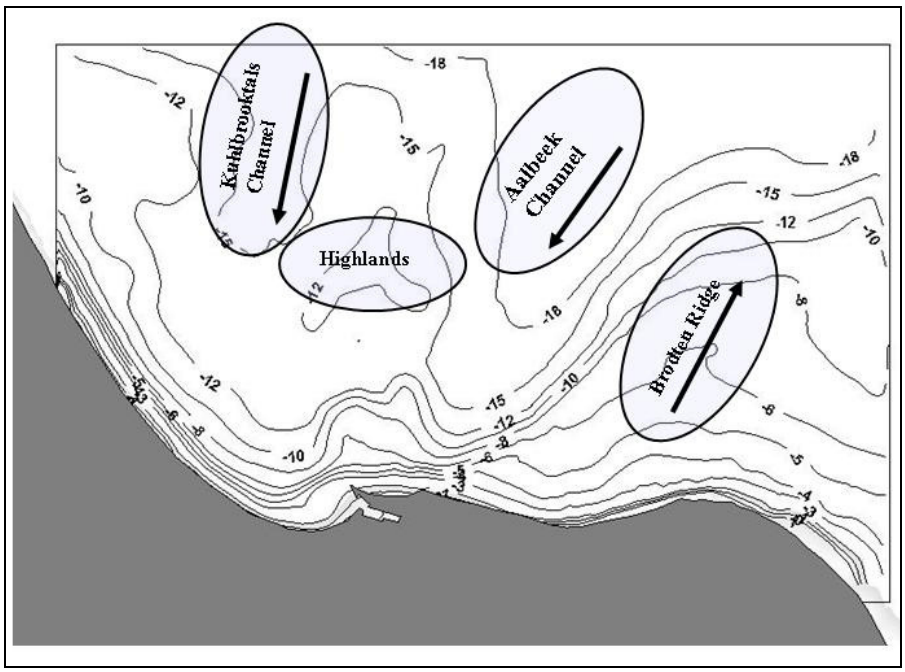

Figure 3-4. Representing geomorphologic elements in the interior Luebeck Bay.

3.2 Hydrodynamics

The hydrodynamic conditions of the Baltic Sea are characterized by its low tidal range with tides as high as 5 cm in the northern bays and 20 cm in the Danish straits (Sterr et al., 1998). It is possible that increases of water level in the southwestern Baltic Sea can be boosted by strong northerly and easterly winds (~3.5 m + NN). The opposite effects might happen when southwesterly winds push the waters offshore the coastline producing water levels as low as 1.5 m below NN.

The flows along the coastline of the Luebeck Bay commonly produce well-defined convergence-divergence patterns (Dietrich and Weidemann, 1952). Right in front of the Brodten Cliff-coasts a divergence of flows is normally seen, and to the west of the Brodten Cliff-coasts, several points of convergence were observed at different locations.

The waves are also a factor that affects the bathymetrical changes in the Luebeck Bay. The retreat of the ridge in front of the Brodten cliff-coasts can be associated with the impact of waves in that area. A higher frequency of waves coming from the northeast sector is most probably the factor that triggers the erosion of the ridge and the cliff-coasts of Brodten (Schwarzer et al., 2000).

Nowadays the hydrodynamic conditions of the Luebeck Bay are continually measured and analyzed in terms of waves and water levels. The ADCP units in Figure 3-5 provide information of the hydrodynamics in the study area. Those data have been collected by FTZ-CORELAB. During this investigation, three ADCP

units are used in the interior of Luebeck Bay for calibration and validation of the regional and local models.

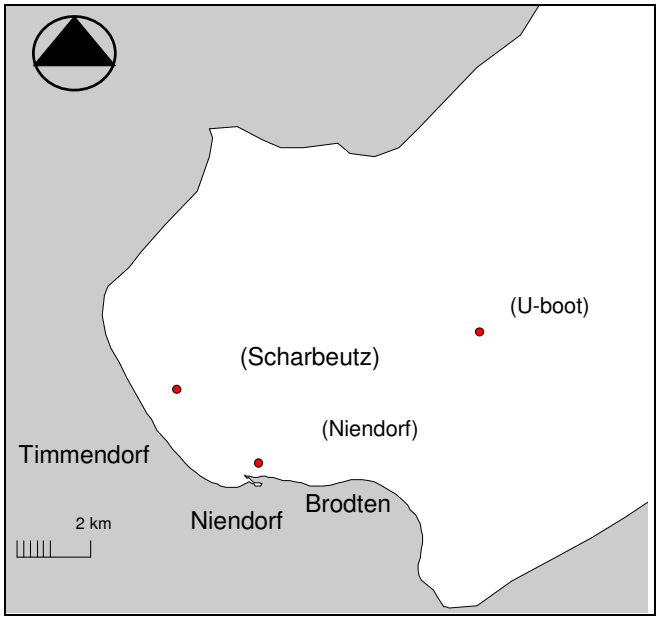

Figure 3-5. ADCP stations in the Luebeck bay.

3.3 Morphodynamics

The most complete information about the morphodynamics in the study area is found in the geology department of the University of Kiel, in Germany. A number of profile-measurements give us an idea about erosion and sedimentation rates near the Brodten Cliff-coast. The research projects of the sedimentology and morphology in the Luebeck Bay provide information about the correlation between the meteorological and hydrodynamic conditions. It was found that the ridge is currently retreating between 1.5 and 2.8 cm/year (Schrottke, 2001).

Chapter 4

BSRmod: Baltic Sea Regional Model

In this chapter a hydrodynamic model for the region of the Baltic Sea has been setup, calibrated and validated. The results provided by this model are in the local area of the inner Luebeck Bay in order to be used as boundary conditions in the local model (see LBLmod in Chap. 5). Through the simulations with the regional model, the most important hydrodynamic effects that might be originated in the offshore regions are transferred to the near-shore areas along the German Baltic Sea coasts. The optimal unstructured mesh approach used in the system of MIKE 21/3-FM, has been very efficient in carrying out simulations with different resolutions in an integrated domain scheme. Through the flexible (unstructured) mesh scheme it has been possible to adapt the numerical solutions for hydrodynamic and morphodynamic formulations to complex geomorphologic features near the coast, keeping acceptable cost-efficient computations during medium- and long-term simulations.

In this chapter BSRmod is presented, including the model set-up, definition of boundary conditions, sensitivity analysis, calibration and validation. Additionally, the simulation and the study of synthetic storm scenarios in the Baltic Sea region, and the generation of boundary conditions for the nesting approach of the Luebeck Bay model are explained.

4.1 Model setup

The aim of the Baltic Sea regional hydrodynamic model (BSRmod) is to generate the boundary conditions for the Luebeck Bay local morphodynamic model (LBLmod). In the following, the domain of BSRmod is introduced, including the specifications of the mesh and the general aspects of the study area. An overview of the meteorological and hydrodynamic conditions applied during the simulations is also included. The procedure to set up the model is explained along with a description of the boundary conditions and their implementation.

4.1.1 Regional model domain

The Baltic Sea region is the inland sea of the northern European continent, which is linked to the North Sea through the straits of Skagerrak and Kattegat. The whole area of the Baltic Sea is 415.266 km^2, extending between 53° N and 66° N, and 9° E and 30° E. Almost half of this area (45%) is covered by ice during the average winter seasons. All through the year the salty waters from the North Sea are mixed with the brackish waters of the Baltic Sea.

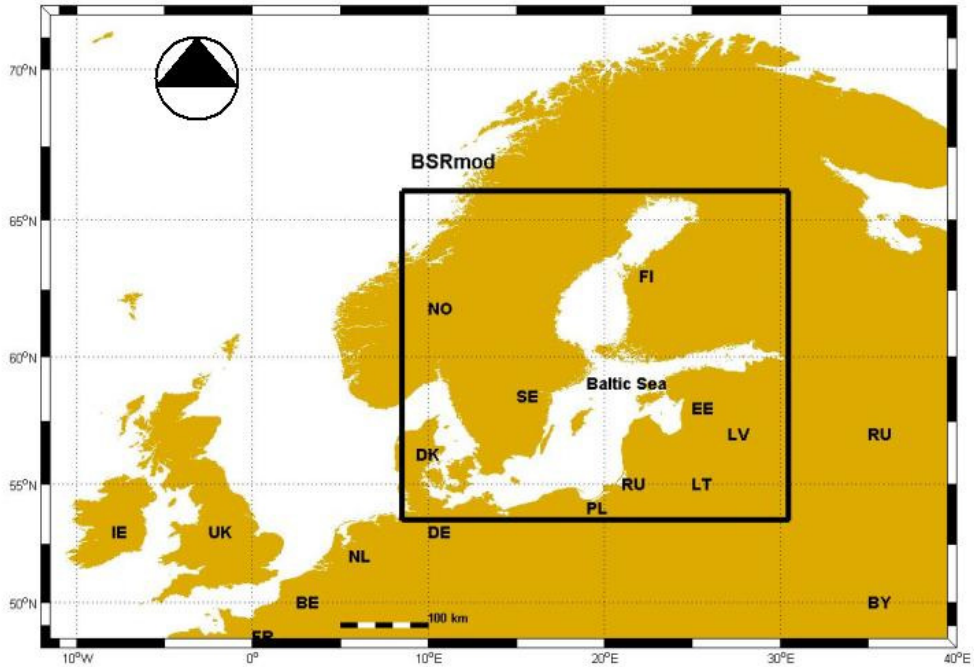

Figure 4-1. Location of the domain

During most of the year, ice is present in the northern Baltic Sea. In the middle domain, the deepest areas (~200 m deep) are localized off the coast of Sweden, Finland, Russia, Estonia and Latvia. In the southwest of the Baltic Sea region, the German coastline is found containing the bays of Kiel, Mecklenburg and Pomerania. The simulations would be mainly focused in the coastal areas, especially in the Mecklenburg Bay (inner Luebeck Bay), where the morphodynamics are investigated in detail by means of a local model.

4.1.2 Basic mesh

In the latest version of the hydrodynamic numerical models by DHI (MIKE 21/3 FM), the computational domain is represented by triangular elements that together form the unstructured mesh used for the solution of the hydrodynamic formulations. The finite element method is applied to solve the equations of momentum, continuity, and energy balance that are formulated in the flow and

wave modules. By means of unstructured meshes, the resolution in the domain is efficiently increased for those areas where details in the results may be required. On the other hand, in regions where details are not that relevant, computing time may be saved through using a coarser mesh. In Figure 4-2 the triangular grid created in the south-western Baltic Sea for BSRmod is presented.

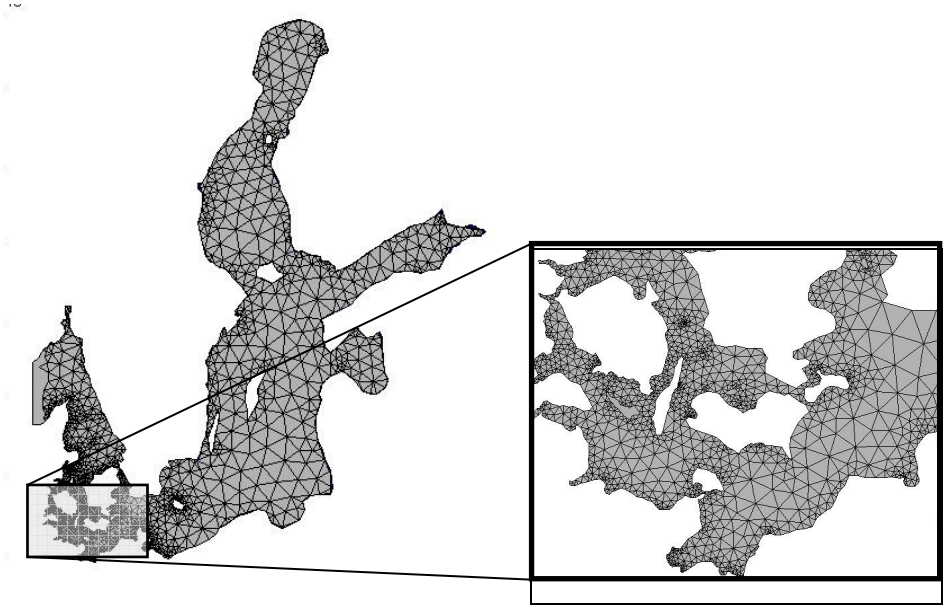

Figure 4-2. Unstructured basic mesh of the Baltic Sea Regional model.

Table 4-1 presents the mesh in the Baltic Sea regional model. The 'basic' mesh comprises 5140 triangular elements with an average side-longitude of 5 meters near the Luebeck bay. Several modifications of the mesh have been tried to investigate the effects of the mesh resolution for the computation of the hydrodynamic parameters. During the sensitivity analysis, a redistribution of the domain in two, three and four levels of resolution is implemented. Different conditions of mesh resolution are compared; especially, in the area near the location of the open boundaries that correspond to the Luebeck Bight Local model.

Table 4-1. Mesh properties of the basic Baltic Sea regional model.

Number of elements	Length of the element side close to BC. [Km]	Area of the element close to BC. [Km2]
5140	~5	~10.7

4.1.3 Bathymetry of the Baltic Sea

The bathymetry data in the Baltic Sea region has been originally used in the execution of hydrodynamic simulations within the framework of the MUSTOK-SEBOK-A project (Bruss et al. 2009 and Jimenez et al., 2009). In that project, the effects that extreme events have on the hydrodynamic conditions of the German Baltic Sea coast were investigated (Bruss et al., 2009). Figure 4-3 shows the bathymetry of the Baltic Sea, which has been measured in the year 2004 (data provided by Danish Hydraulic Institute, DHI).

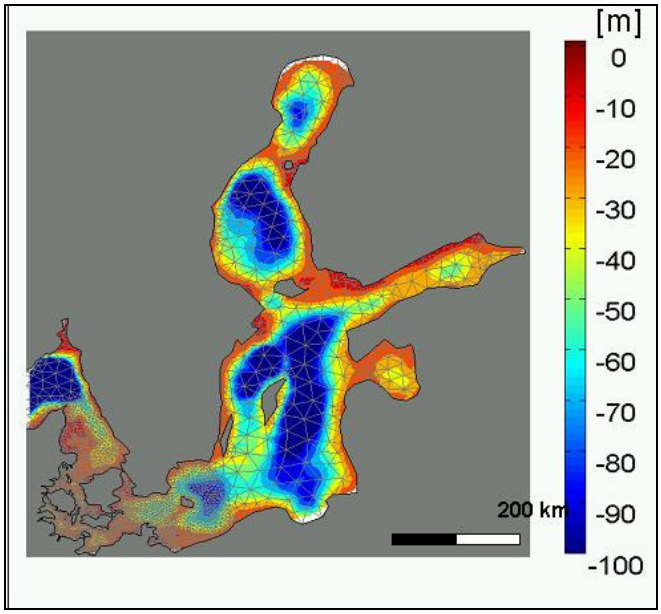

Figure 4-3. Water depths of the Baltic Sea Regional model.

Most of the deepest areas in the Baltic Sea region are found in the central and northern sectors of the region. Figure 4-3 shows the central Baltic Sea where water depths can be deeper than 150 meters, while in the northern regions, inside the Gulf of Bothnia, the depths are close to 100 meters. High gradients in the bathymetry can be seen in the area where the Baltic Sea is 'connected' to the North Sea, i.e., crossing the straits of Skagerrak and Kattegat. 500 meters of depth can be seen in the Skagerrak strait, while in the eastern side of the Kattegat Strait a much shallower bathymetry, close to 50 meters depth, is observed. Close to the German coast, in the south-western Baltic Sea region, the shallowest areas are found (25 meters deep, approximately). In the south-western Baltic Sea a detailed bathymetry is used for the simulations of the hydrodynamics in the coastal zones of the German Baltic Sea. Thus, a high resolution of the mesh is applied along the coasts for representing properly the processes involved in the wave-energy transformation that takes place during the transition from the offshore to the coastal areas.

4.1.4 Driving forces

The driving forces applied in the regional model have been selected for three independent periods of simulation. Each period corresponded to the main steps that have been considered in the study implementing the Baltic Sea Regional model (i.e. sensitivity analysis, calibration and validation). The sensitivity analysis has been carried out considering a period in November 2006. During the simulations water levels close to 0.6 meters above N.N. and significant wave heights that reached 0.8 m have been observed in the Luebeck Bay. During the calibration a period between October and November in 2006, was defined. For that period, the significant wave height observed in the area close to the Luebeck Bay reached its highest value of 1.4 meters during the calibration, and the highest water level was 2.0 m above N.N. A period of simulations within February 2002 has been selected for validation of BSRmod. Particularly interesting in this period is the extreme event on February 21st, in which the water levels were close to 1.8 meters and the maximum significant wave height was close to 2.2 meters.

4.1.4.1 Boundary conditions

The boundary conditions in the Baltic Sea regional model are applied in the area between the Skagerrak and Kattegat straits (see position of BC in Figure 4-4). Time series of water levels from a measuring station close to 10°E on the western open boundary of BSRmod are provided along the boundary as indicated in Figure 4-5. This data has been collected and prepared by the Swedish Meteorological and Hydrologic Institute (SMHI), and provided as input data to the flow model implemented by CORELAB-FTZ during the execution of the MUSTOK-SEBOK-A project (Bruss et al., 2009 and Jimenez et al., 2009).

Figure 4-5 shows the time series of water levels available for the western open boundary of BSRmod. The time series of water levels during the sensitivity analysis comprises two months of measurements in which water levels not higher than 0.6 meters were observed. During calibration, the water levels were slightly higher when compared to the period of sensitivity analysis. In the former, the surface elevation was close to 1 m above normal null. The third period presented in Figure 4-5 corresponded to the validation of BSRmod. Within that period, water levels were close to one meter at the peak of the storm on 21st February in 2002.

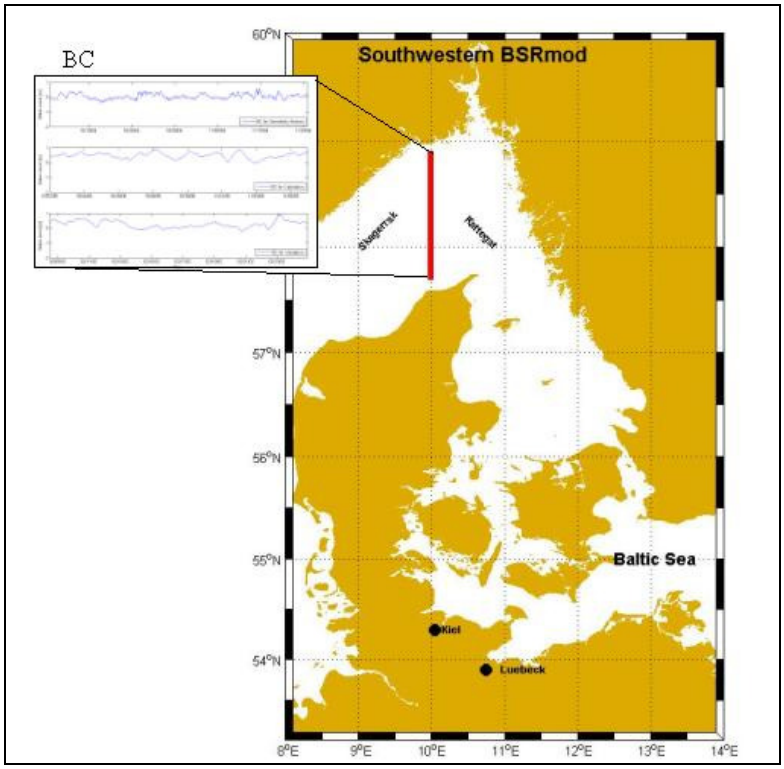

Figure 4-4. Position of BC in the BSRmod.

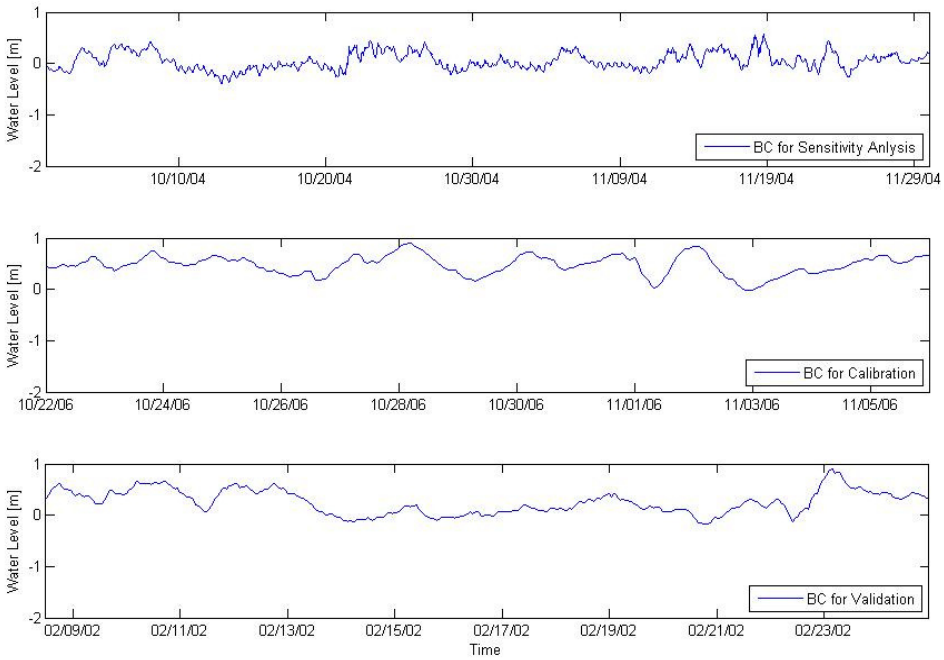

Figure 4-5. Water level measured at station Ringhals used as input for the boundary conditions

4.1.4.2 Winds

Winds induce friction on the surface of the water generating currents and waves. The effects of the winds are particularly important in the simulation of swell, local wind-waves and surges. Winds are also important in the simulation of water levels, principally, in the design of coastal protection structures. Many authors comment on the influence of winds on the water levels of the Baltic Sea; for example, Hupfer et al. (2003) mentioned that the main factors related to the wind that can affect the occurrence of extreme water levels in the Baltic Sea region are: atmospheric pressure, wind distribution, especially, shifts in the direction and velocity of air-fronts.

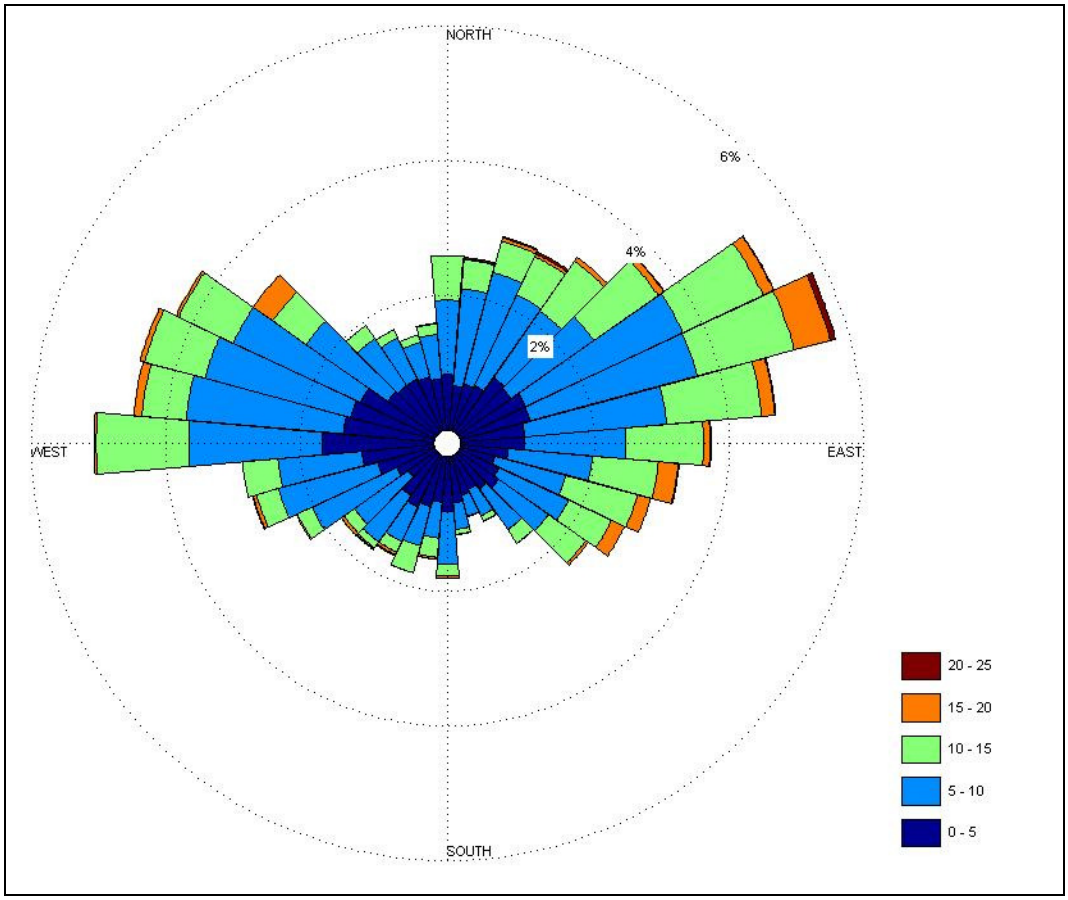

Figure 4-6. Wind direction (nautical convention) and magnitude given in terms of frequency in the Luebeck Bay area. Data provided by BSH for the year 2002.

In the previous investigations the effects of the winds field on the hydrodynamics of the Baltic Sea have been studied bay means of numerical models. Two of these investigations were recently conducted at CORELAB (University of Kiel, Germany). One of them consisted in the development of a hydrodynamic model

covering the Kiel Bight (Fischer, 2005). In the other study, a hydrodynamic model in the Mecklenburg Bay was set up (Bruss, 2006). In both investigations the authors concluded about the advantages of using the correct spatial distribution of the wind fields instead of taking one single values for the entire domain.

Figure 4-6 shows the yearly distribution of the frequency of magnitude and direction of winds in the Luebeck Bay during the year 2002. The distribution of winds in that year showed the highest frequency in the northeast direction. Westerly winds were less frequent than the north-easterly winds. The southerly and northerly winds, in contrast, appeared to be insignificant.

4.1.4.3 Waves

Winds generate waves and the surge of water. Waves transmit the shear stress to the sea bed along the water column. In that process the morphology of the seabed is constantly transformed due to the transport of sediment resulting from the shear stress exerted on the seabed.

In this investigation waves and currents are taken into account in the simulation of sediment transport. In the regional model of the Baltic Sea, the wind fields are provided by a complete set of data containing the wind-velocity vectors varying in time and space. Waves are simulated covering the entire region of the Baltic Sea.

The frequency distribution of the waves in terms of combined magnitude and direction in year 2002 in the Luebeck Bay is shown in Figure 4-7. In Figure 4-7 a clear tendency of the waves in the southeast direction for that particular period is observed. A high concentration of waves in that direction is expected due to the morphological distribution of the land that encloses the Mecklenbrug Bay. In the same direction, the wind has the longest fetch along which waves gain energy. That energy is transported to the coastal area of the Luebeck Bay where the dissipation of waves starts due to the effects of the bottom roughness and breaking of the waves.

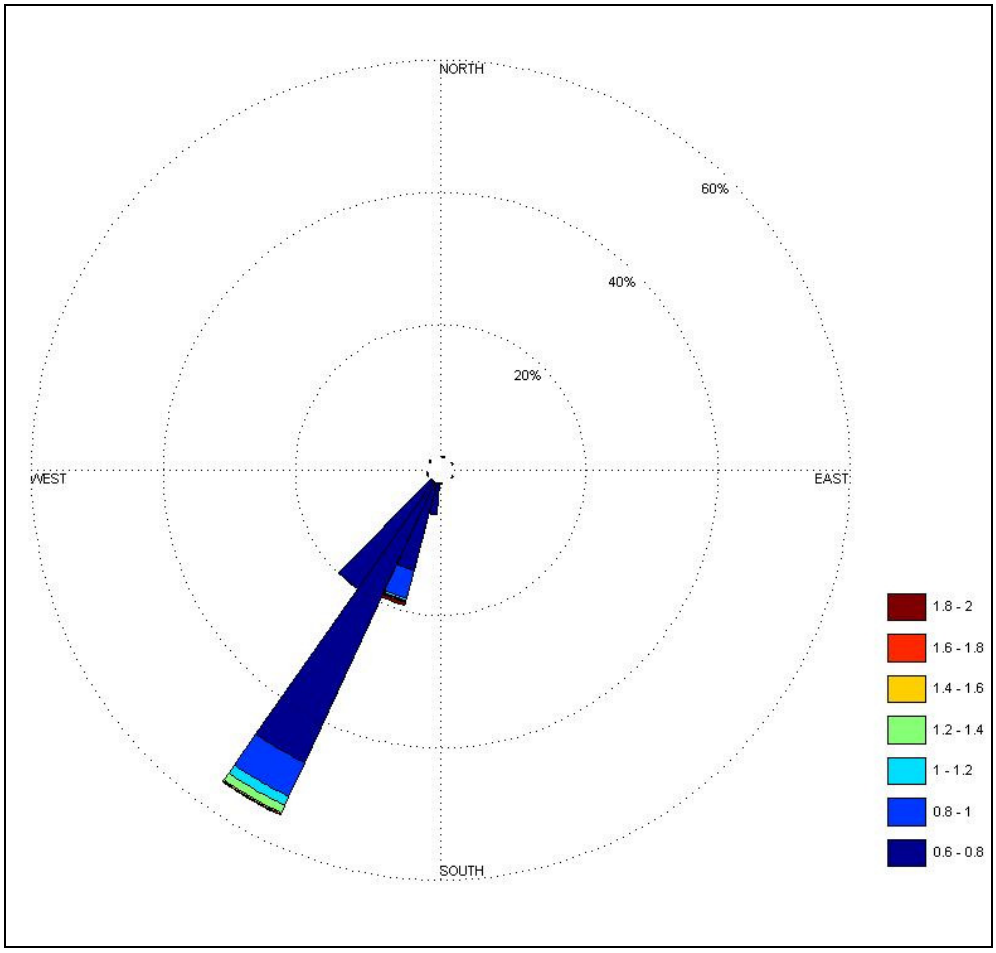

Figure 4-7. Wave direction and significant wave height in terms of frequency of occurrence in the Luebeck Bay. Data provided by WSA for the year 2002

4.2 Model sensitivity analysis

In the application of the numerical models, the sensitivity analysis is the term that makes reference to the assessment of the effects on the computed results due to the systematic change of various parameters. The conclusions about the sensitivity of the model to those parameters affecting the processes would be used for the calibration of the model. Below, the scheme applied for the sensitivity analysis in the regional model (BSRmod) is explained in detail.

At the beginning of the sensitivity analysis of BSRmod it is considered to study the effects on the simulation results that are produced by changing the mesh resolution. Subsequently, the duration of the time step is accounted for as a second parameter in the sensitivity analysis. The effects on the water surface produced by modifying the wind conditions, as well as the physical and numerical parameters in the flow

and wave module, will be investigated during the final stages of this sensitivity analysis.

4.2.1 Mesh resolution

Figure 4-8 shows the four cases of different mesh configurations that are studied during the sensitivity analysis. The summary of the characteristics of each case is presented in Table 4-2. A systematic modification of 'Mesh 4' is applied in such a way that all of the remaining cases, i.e. from 'Mesh 1' to 'Mesh 3', have a finer resolution than 'Mesh 4'. In that regard, 'Mesh 3' is the result of increasing the resolution in the south-western Baltic Sea, 'Mesh 2' is conformed by increasing the resolution of 'Mesh 3' in the German Baltic Sea, i.e. including, the Kiel, Mecklenburg and part of the Pomeranian Bay. Finally, 'Mesh 2' is modified by increasing the resolution in the local area close to the Luebeck Bay conforming a third cases called 'Mesh 1'.

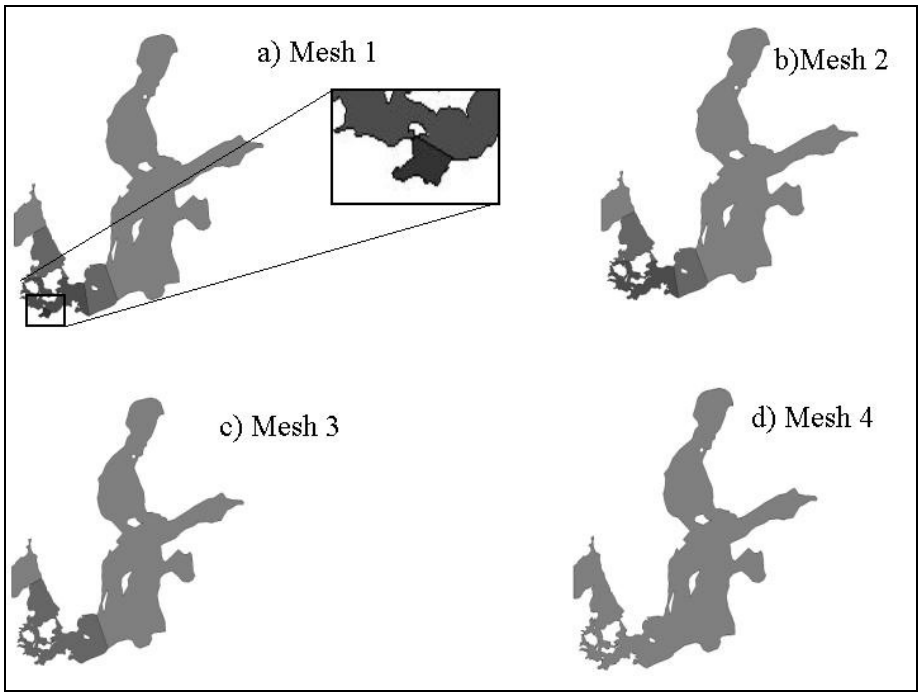

Figure 4-8. Distribution of areas for four different mesh configurations in the BSRmod

Column 1 in Table 4-2 contains the total number of elements from each case studied in this sensitivity analysis. In addition to that, in Column 2, the area (in kilometres) of the largest mesh-element is presented. In order to give an idea about the resolution of the mesh close to the area of interest in the Luebeck Bay, the length of one side of the elements in that location is shown in Column 4. Finally, in

columns 5 and 6, the computational time of flows and waves for one month of simulations is shown.

Table 4-2. Summary of mesh settings in the BSRmod.

	Number Elements	Max. Area of Element inside Polygon of Highest Resol. [Km2]	Approx. Length of Side Element close to the BC of LBLmod [km]	Computing Time [hours/month]	
				Flows	**Waves**
Mesh 1	9854	1	1	2.0	16
Mesh 2	7523	20	4	1.6	12.5
Mesh 3	6545	50	4.5	1.35	12
Mesh 4	5140	200	5	1	5.2

The configuration using ‘Mesh 1’ represents the highest resolution in the area close to the Luebeck Bay. Note that the flow simulations using that mesh-configuration take almost as much as twice the computing time when compared to the configuration using ‘Mesh 4’. In the wave module the application of ‘Mesh 1’ increases excessively the computation time, in which one single simulation of waves can take more than 3 times of computing time if the ‘Mesh 4’ is applied. Considering only the computing time as the only criterion to decide on which configuration is suitable, might not be adequate for the specific objectives of the model application. The main motive of the Baltic Sea Regional model is the generation of boundary conditions in the Luebeck Bay area for the local model. The model satisfies the requirements as long as the resolution in the area of interest provides reasonable results to drive the local model. Hence, in this specific model application, ‘Mesh 4’ can be considered adequate to be used for generating boundary conditions to the local model in the Luebeck Bay. A further comparison between ‘Mesh 1’ and the remaining mesh configurations using statistical parameters shows no relevant differences. Based on that, it is decided to apply ‘Mesh 4’ in the following simulation of BSRmod during this investigation.

Table 4-3. Summary of statistical parameters between the case using the mesh of highest resolution (Mesh 1) and each of the 3 remaining mesh configurations (Mesh 2-4).

	WL [m]			Hs [m]		
	Bias	MAE	StdDev.	Bias	MAE	StdDev.
Mesh 2	5.0 E-04	8.0 E-04	9.0 E-04	-0.006	0.012	0.016
Mesh 3	0.002	0.004	0.005	-0.008	0.013	0.016
Mesh 4	0.003	0.007	0.007	-0.010	0.015	0.016

4.2.2 Time step

In the analysis of sensitivity of BSRmod, the time step used in each of its two modules (i.e. flows and wave) has been carried out according to the particular temporal discretization-scheme of each module. On the one hand, the sensitivity of the time step applied on the flow module has been based on the maximum CFL (Crouant-Fiedrich-Lewy number) given by each of the three settings presented in Table 4-4. On the other hand, in the wave module, the maximum CFL is based on the time step given to the wave simulations. In the latter, the maximum time step has a corresponding CFL value that is calculated during each interval in the instationary scheme.

Table 4-4. Time discretization in the flow (gray cells) and wave module.

	Flows			Waves		
	Maximum CFL	Average Time Step [s]	CPU time [hrs]	Maximum time step [s]	Maximum CFL	CPU time [hrs]
1st Setting	1	9	1	600 s	0.8	11
2nd Setting	0.8	6	2.3	30 s	0.4	17
3rd Setting	0.4	3	5	50 s	0.3	27

Table 4-5. Summary of statistical parameters for sensitivity analysis of time step using the differences between the 1st setting and each of the 2 remaining settings of the flows and waves module for the BSRmod (i.e. 2nd and 3rd Setting)

	WL [m]			Hs [m]		
	Bias	MAE	StdDev.	Bias	MAE	StdDev.
2nd Setting	4.0 E-6	5.0 E-5	7.0 E-5	2.3 E-4	4.2 E-4	6.5 E-4
3rd Setting	5.0 E–6	8.0 E-5	1.0 E-4	3.0 E-4	5.2 E-4	6.5 E-4

Table 4-5, shows the results of the accuracy of water levels and significant wave heights based on the simulation results, defining the time step according to the 1st setting and then comparing with respect to the cases using the 3rd and 2nd settings. Note in Table 4-4 that the results of the 2nd setting and 3rd setting are not that different when compared to the reference case (1st Setting). No significant improvement in the results is expected by increasing the temporal resolution based on those results. Hence, the 1st setting for the following simulations of flows and waves will be applied in this investigation.

4.2.3 Wind

The effects of the wind are represented in a manner different from the waves and flows modules. In the sensitivity analysis of the effects of the wind in the flow module, a friction coefficient is provided depending on the wind velocity. In the wave module, on the other hand, the sensitivity analysis is based on the two formulations applied in the simulation of the waves-wind interaction (coupled and uncoupled). In Table 4-6 three different settings are indicated. The analysis of the wind effects on flows is based on three settings, in which the lower (Ca) and upper (Cb) limits of the wind friction coefficient are defined. These two coefficients are the thresholds that define the values of the wind that are taken into account in order to avoid extremes of wind velocities. The wind-wave interaction is analyzed including the following three cases: i) wind-wave uncoupled scheme, ii) wind-wave coupled scheme (0.01), and iii) wind-wave coupled scheme (0.1).

Table 4-6. Configuration for wind effects on flows (gray cells) and waves.

	Flows	Waves
	Wind-friction Coefficients (Ca - Cb) for low U_{10} and high $U_{10.}$	Wind Formulation
1st Setting	0.00125-0.006	Uncoupled
2nd Setting	0.00125-0.003	Coupled (0.01)
3rd Setting	0.003-0.006	Coupled (0.1)

Table 4-7 shows the results of the sensitivity analysis of the wind effects on the flows and waves. Flows are evidently affected when the friction coefficient is increased in its lower limit changing 'Ca' from 0.00125 to 0.003. The differences showed that the higher values of the 'Ca' coefficient produced lower water levels. In this regard, the 'Ca' coefficient is considered important for the setup of the regional model, in which calm conditions should be also taken into account including very low wind velocities. The wave module, on the other hand, proved to be sensitive to the modification of the wind-wave formulation. By applying the coupled formulation the waves tend to be larger than those produced by the uncoupled alternatives.

Table 4-7. Summary of statistical parameters during sensitivity analysis of winds, based on the differences in the flows and waves module, between the 1st setting and each of the 2 remaining settings (i.e. 2nd and 3rd Setting)

	WL [m]			Hs [m]		
	Bias	MAE	StdDev.	Bias	MAE	StdDev.
2nd Setting	-0.007	0.02	0.05	-0.14	0.14	0.11
3rd Setting	0.14	0.21	0.3	-0.11	0.13	0.14

4.2.4 Physical parameters

In this section the sensitivity analysis consists of the study of the most important physical parameters that are included in the flows and wave module. The settings of the model are summarized in Table 4-8 and Table 4-10. The bed roughness and eddy viscosity for the flow module are presented in Table 4-8. Table 4-10, on the other hand, shows the model parameters that affect the transformation of the wave energy of the wave module.

4.2.4.1 Flow module

The effects of eddy viscosity and bed roughness are analyzed by comparing the 1st setting with the other two cases presented in Table 4-8. Note in Table 4-9 (column 2 and3) that the differences between the 1st and the 2nd setting are larger than the differences observed between the 1st and the 3rd setting in the eddy-viscosity sensitivity analysis. Thus, it is expected that the model results are affected by changing the values of the vertical eddy viscosity more than in the case the horizontal eddy viscosity is modified. By changing the bed roughness in the flow module the simulation results were similarly affected by the modifications applied to the 1st setting. Eddy viscosity and bed roughness, are thus important for the calibration of BSRmod.

Table 4-8. Configurations for two physical parameters (i.e. eddy viscosity and bed roughness) during sensitivity analysis of flows module

	Eddy Viscosity		Bed Roughness [m]
	Horizontal [m^2/s]	Vertical [m^2/s]	
1st Setting	0.002	0.002	0.1
2nd Setting	0.002	0.04	0.01
3rd Setting	0.04	0.002	0.5

Table 4-9. Summary of statistics of sensitivity analysis for physical parameters of the flow model, calculated using the differences between the 1st setting and each of the 2 remaining settings (i.e. 2nd and 3rd Setting) in BSRmod

	Eddy Viscosity WL [m]			Bed Roughness WL [m]		
	Bias [m]	MAE [m]	StdDev [m]	Bias [m]	MAE [m]	StdDev [m]
2nd Setting	-0.04	0.09	0.15	0.10	0.13	0.15
3rd Setting	4.0 E-8	5.2 E-7	6.5 E-7	0.11	0.15	0.20

4.2.4.2 Waves module

In the following the effects that the wave breaking and wave-bottom-interaction scheme have on the final results are studied. The settings of the cases that are studied are presented in Table 4-10. It can be seen in Table 4-11 that wave breaking and wave-bottom-interaction in the wave height are not that relevant for the numerical results of the waves. The mean absolute differences (MAE) were in the order of 4 mm, while the mean differences (Bias) were lower than 3 mm.

Table 4-10. Separate configurations for two wave-dissipators (i.e. weave breaking and wave-bottom interaction) during sensitivity analysis of wave module

	Wave Breaking	Wave Bottom Interaction
1st Setting	Included	Included
2nd Setting	Not included	Not included

Table 4-11. Summary of statistics for sensitivity analysis of physical parameters in the waves modules based on the differences between two cases: i) including and ii) with out including wave braking and bottom interaction in BSRmod.

	Hs [m]		
	Bias [m]	MAE [m]	StdDev [m]
Wave Breaking	-0.003	0.004	0.01
Wave-Bottom interaction	-3.0 E-4	0.004	0.01

4.2.5 Coupling of flows and waves

In this study the sensitivity analysis of the hydrodynamic modules of BSRmod was presented for separate modules, i.e., waves and flows. In the following, the sensitivity analysis is made with the study on the effects of coupling flows and waves.

The different settings to be compared in this analysis are presented in Table 4-12. In the 1st setting, waves and flows are coupled. Both modules are setup on-line, exchanging radiation stresses, currents, and water levels. The other two settings are defined implementing wave and flows independently in the same way that it was carried out in the previous sections.

Table 4-12. Hydrodynamic module settings: i) total dynamic coupling of waves and flows, ii) running waves with no flows and iii) running flows without waves in the BSRmod.

	Waves	Flows
1st Setting	Included	Included
2nd Setting	Included	Not included
3rd Setting	Not included	Included

In Table 4-13 the differences observed in the sensitivity analysis of coupling waves and flows is presented. According to the observed discrepancies in terms of significant wave height between the simulations of waves alone and the coupled model (2nd Setting in Table 4-13), the effects of the flows on the waves in the area close to the Luebeck Bay are very important. It is expected that waves may be underestimated if flows are not properly coupled to the waves. In contrast, waves have proven to be not that relevant for the mean water levels computation as indicated in the last row of Table 4-13. According to the results in Table 4-13, if waves are not coupled to the flow module the differences with respect to a full-coupled simulation might not be relevant for the water levels computation.

Table 4-13. Statistical parameters to compare the individual output of the waves and flows modules with respect to the full coupled simulation in terms of significant wave height and water levels, respectively.

	Bias [m]	MAE [m]	StdDev [m]
2nd Setting (Hs [m])	0.360	0.360	0.380
3rd Setting (WL [m])	0.003	0.004	0.006

4.3 Model calibration

In a second phase in the development of numerical models, once the sensitivity analysis is finished, a further step needs to be implemented to execute the calibration of the parameters. In the calibration of a model the results of the simulations are compared to the available measurements; subsequently, the parameters are change systematically in order to produce model results that come closer to those measurements. In this section, the calibration of BSRmod is presented including: i) available data, ii) model results and ii) statistics.

Measurements of water levels and wave properties have been used for the calibration of BSRmod. Figure 4-9 shows the positions of the measurements for calibration and validation. German and Swedish authorities (WSA and SMHI) have been collecting information at gauge stations that are shown in Figure 4-9. In the inner Luebeck Bay close to the harbour of Niendorf (i.e., station #2), water levels, currents and wave properties have been collected during the years 2006, 2007 and

2008 using ADCP measurements. That equipment has been deployed and operated by FTZ-Corelab institute.

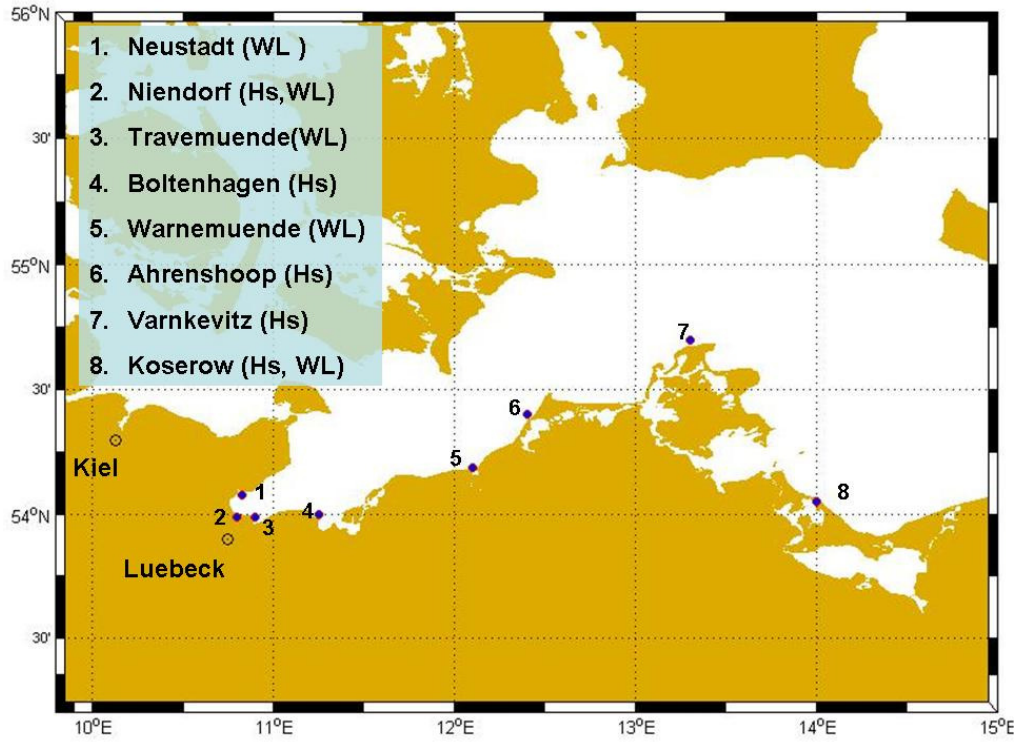

Figure 4-9. Location of water-levels and waves-monitoring stations used for calibration and validation of BSRmod

During calibration, the statistics based on Mean Absolute Error (MAE), standard deviation, and Adjusted Relative Mean Absolute Error (ARMAE) are determined. The comparisons of model results with measurements are carried out for the data collected at Travemuende, Koserow and Niendorf.

In the calibration of BSRmod the lowest limit of the wind-drag coefficient ('C_a') is determined executing simulations with three values of that parameter (i.e. 0.001, 0.00125 and 0.003). Concerning the highest limit of the wind-drag coefficient ('C_b'), a constant value (0.002) was considered. Equations 7 and 8 show the relations of the wind-drag coefficient and the wind-friction that is generated on the water surface. The results of the calibration of the wind-drag coefficients are shown in Figure 4-10. In the figure it can be seen the way the surface elevation is affected by 'C_a' during the calibration.

$$\bar{\tau}_s = \rho_a C_d |u_w| \overline{u_w} \tag{7}$$

Where:

$\bar{\tau}_s$ *: Surface stress*

ρ_a : *Density of air*

C_d : *Empirical drag coefficient of air*

u_w : *Wind velocity 10 m above the water surface*

$$C_d = \begin{cases} C_a & W_{10} < W_a \\ C_a + \dfrac{C_b - C_a}{W_b - W_a} \cdot (W_{10} - W_a) & W_a \le W_{10} \le W_b \\ C_a & W_{10} > W_b \end{cases} \quad (8)$$

Where:

C_d, C_a, C_b : *Drag coefficient for air ('a' and 'b' sub indices indicates lower and higher limit, respectively).*

W_a, W_b : *Wind velocities limits ('a' and ' b' indicates lower and higher velocity limits of the wind)*

W_{10} : *Wind velocity 10 m above water surface.*

Figure 4-10 shows how wind drag coefficient affects the water levels. The simulation of water levels using a drag coefficient of 0.003 boosted the effects of the wind on the water surface. Much closer results to the measurements were obtained applying lower values on that parameter. The results for the first and second setting (i.e., Ca=0.001 and Ca=0.00125) were comparable.

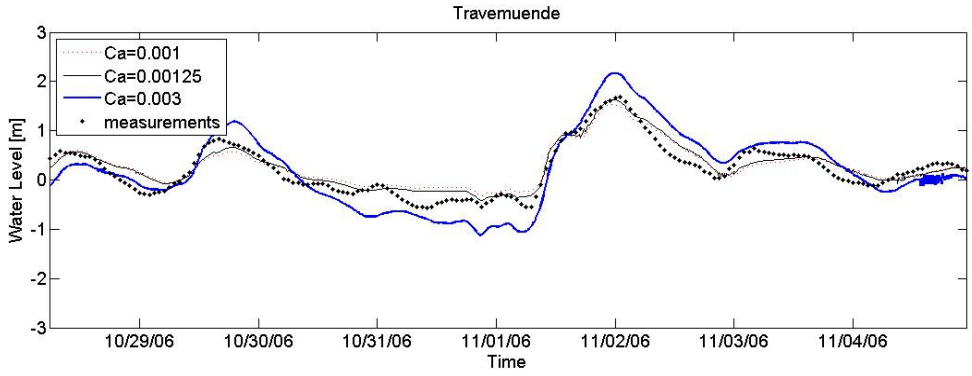

Figure 4-10. Measurements and simulation of water level for three different settings of wind drag coefficient at the Travemuende gauge station.

In Table 4-14 the statistics based on the calibration of the wind-drag coefficient are presented. By comparing the differences between the first two settings no major improvement was observed; the model came slightly closer to the measurements when the value of the wind-drag coefficient was increased from 0.001 to 0.00125. It is also observed in Table 4-14 that the highest value of this calibration parameter gives the worst results regarding the water levels (see Figure 4-10).

Table 4-14. Statistical analysis base on the wind drag coefficient for three different settings

Lower wind coefficient	Statistics	Stations		
		Travemuende	Koserow	Niendorf
Ca= 0.001	MAE [m]	0.13	0.15	0.17
	StdDev [m]	0.16	0.20	0.22
	ARMAE [m]	0.17	0.25	0.26
Ca= 0.00125	MAE [m]	0.12	0.16	0.16
	StdDev [m]	0.15	0.21	0.20
	ARMAE [m]	0.14	0.28	0.22
Ca= 0.003	MAE [m]	0.30	0.40	0.20
	StdDev [m]	0.32	0.45	0.20
	ARMAE	0.64	1.02	0.32

The calibration of the BSRmod has been executed for the wind-drag coefficient. It was observed that the flow model is in better agreement when C_a=0.00125. In this section, the vertical eddy viscosity (Ev) in the calibration of the flow model is presented.

In Figure 4-11, the results of the simulations calculated using three values for the vertical eddy viscosity (0.001 m^2/s, 0.04 m^2/s, 0.08 m^2/s) are compared with the measurements of water levels. The computed water levels were quite similar. The measured and computed water levels shown in Figure 4-11 are keeping similar trends and no major improvements are expected with the calibration of the eddy viscosity.

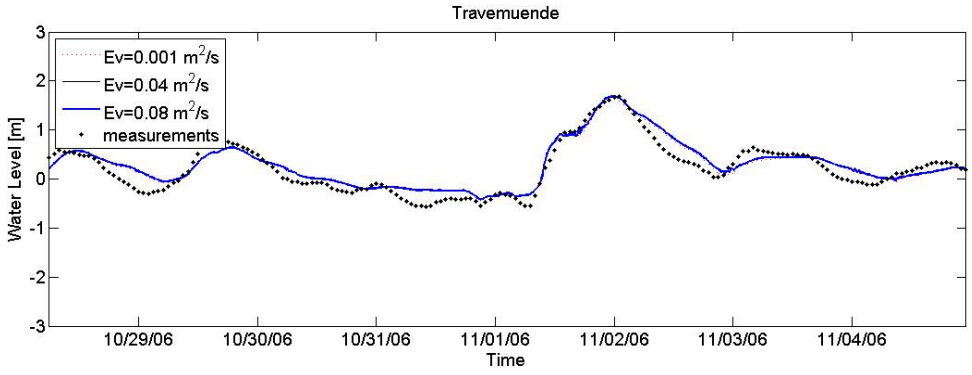

Figure 4-11. Measurements and simulation of water level for three different settings of vertical eddy viscosity at the Travemuende gauge station.

Table 4-15 shows the results of the effects of the eddy viscosity on the water levels. The first setting barely shows an improvement in terms of ARMAE when compared to the other two options, specially, for the Travemuende station, inside Luebeck Bay. In this regard, it is decided that in the following application of the BSRmod, the eddy viscosity value will be 0.001 m^2/s.

Table 4-15. Statistical analysis base on the vertical eddy viscosity for three different settings

Vertical Eddy viscosity [m^2/s]	Statistics	Stations		
		Travemuende	Koserow	Niendorf
Ev= 0.001	MAE [m]	0.12	0.16	0.16
	StdDev [m]	0.15	0.21	0.20
	ARMAE [m]	0.14	0.28	0.22
Ev= 0.04	MAE [m]	0.12	0.16	0.16
	StdDev [m]	0.15	0.22	0.20
	ARMAE [m]	0.15	0.29	0.22
Ev= 0.08	MAE [m]	0.12	0.16	0.16
	StdDev [m]	0.15	0.22	0.20
	ARMAE [m]	0.15	0.29	0.22

In the following, the calibration of the BSRmod continues with the wave module. The wave module is calibrated considering two parameters, i.e., wind friction and air-water roughness coefficient.

Figure 4-12 shows the significant wave height at the Varnkewitz station. Two basic formulations of wind-wave growth rate are initially compared. In the coupled formulation overestimations were observed, whereas, the uncoupled alternative showed better agreement with the measurements.

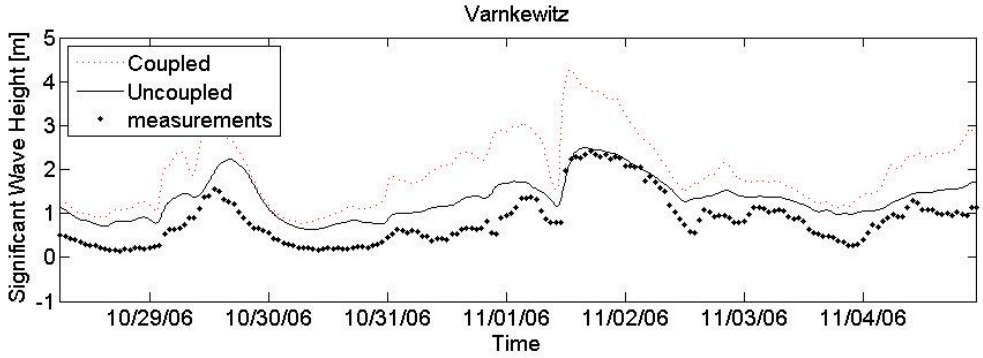

Figure 4-12. Measurements and simulation of significant wave height at Varnkewitz station. Coupled and uncoupled settings in the BSRmod to compute significant wave height.

A more detailed analysis of the differences between the uncoupled and coupled formulation is presented in Table 4-16. Notice the better agreement of the simulated significant-wave-height values when the uncoupled alternative is applied. The three statistical parameters were almost duplicated when the coupled formulation was implemented. Based on that, in the later applications of the BSRmod the uncoupled wind-wave-interaction has been selected.

Table 4-16. Statistical analysis for the calibration of the wave module. Uncoupled and coupled wind-wave-interaction.

Wave-wind interaction	Statistics	Stations		
		Varnkewitz	Koserow	Niendorf
Uncoupled	MAE [m]	0.41	0.27	0.23
	StdDev [m]	0.24	0.37	0.20
	RMAE [m]	0.34	0.45	0.46
Coupled	AMAE [m]	1.02	0.41	0.30
	StdDev [m]	0.51	0.43	0.41
	ARMAE [m]	1.24	0.80	1.16

One last parameter that was considered in this calibration is the Charnock's parameter. With the implementation of the Charnock's parameter the sea-air-roughness effects are taken into account. In equation 9 the parameter appears as a multiplying factor in the equation to calculate the sea air roughness. The effects of this parameter are directly proportional to the wave growth. In Figure 4-13 that tendency is observed in the simulation results, where the option with the maximum Charnock's parameter showed the highest values of significant wave height (blue line). The three simulations are showing similar tendencies, and no major discrepancies are observed. Just during the picks of significant-wave-height values the first option presents much lower values when compared with the other two options.

$$Z_0 = Z_{Charnock} \times \frac{u_*^2}{g} \tag{9}$$

Where:

Z_0 *: sea-air roughness*

$Z_{charnock}$ *: Charnock's parameter*

u_* *: wind friction velocity*

g *: Gravitational acceleration*

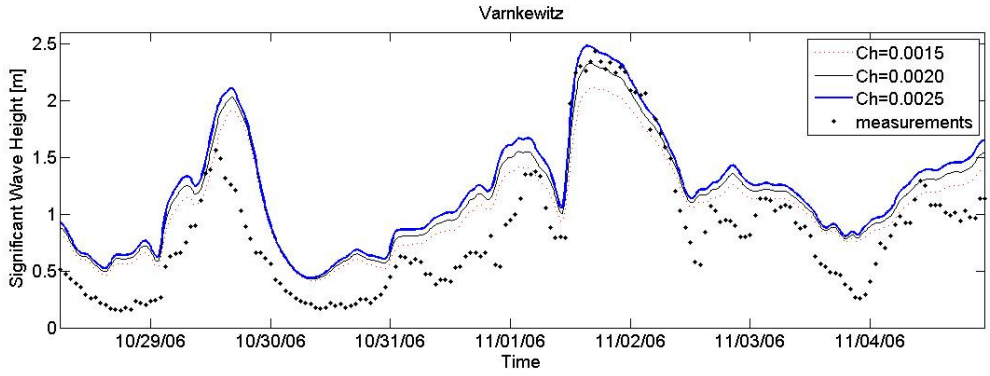

Figure 4-13. Measurements and simulation of significant wave height, comparing three different settings by changing the Charnock's parameter in the computation of the sea-air roughness at Varnkewitz station

Table 4-17 presents in more detail the discrepancies in terms of significant-wave-height values obtained applying the settings for the Charnock's parameter. According to the statistical parameters, the first option was the closest to the measurements. All the simulations implementing the three available settings followed the trend of the significant wave height and were also close to the measurements. Although the wave module of BSRmod was overestimating the lower values of significant wave height, it is expected that the accuracy obtained with the BSRmod is adequate to provide hydrodynamic boundary conditions in the inner Luebeck Bay area.

Table 4-17. Statistical analysis base on the vertical eddy viscosity for three different settings

Uncoupled wave-wind interaction Parameter	Statistics	Stations		
		Varnkewitz	Koserow	Niendorf
Ch= 0.0015	MAE [m]	0.41	0.27	0.23
	StdDev [m]	0.24	0.37	0.20
	ARMAE [m]	0.34	0.45	0.46
Ch= 0.0020	MAE [m]	0.48	0.27	0.23
	StdDev [m]	0.25	0.37	0.20
	ARMAE [m]	0.43	0.44	0.41
Ch= 0.0025	MAE [m]	0.53	0.27	0.22
	StdDev [m]	0.26	0.37	0.20
	ARMAE [m]	0.51	0.45	0.37

4.4 Model validation

In all applications of numerical simulations, a proper validation is always recommended. Through the use of a statistical analysis based on the differences between measurements and computed results, the users can estimate the capacity of the model to simulate the physics of the natural processes. For most of the cases, the possibilities to validate a model are dependent on the quality of the available data. In the present work, two periods of measurements are available for the year 2002, from the 19th until the 22nd of February, and 2006, from the 1st until the 4th of November.

In the validation of the BSRmod, water levels and significant wave height (Hs) are accounted for. Initially, the computed water levels are compared with the measurements at four stations (i.e., Neustadt, Travemuende, Niendorf and Koserow). In the second part of the validation, the simulated significant wave height is also compared to the measured data at the following four stations: Ahrenshoop, Varnkewitz, Niendorf and Boltenhagen.

In Figure 4-14 and Figure 4-15 measured and computed water levels are compared. In the inner Luebeck Bay three stations were considered for the validation (see Figure 4-9). A fourth station was also taken into account for this validation in the Pomeranian Bay (Koserow). Neustadt is the station in which the data was compared during part of the month of February 2002; the data in the other three stations comprised of the waters levels at the beginning of the month of November 2006. In the former the simulated water levels shows its maximum values close to the end of the validation period, while in the later the maximum values of water levels are closer to the beginning of its validation period. The maximum value of water levels was close to 2 m.

The results of the simulations, in all four stations, and the two periods of the validation, showed good agreement with the measurements. An acceptable estimation of the temporal distribution of water levels was observed.

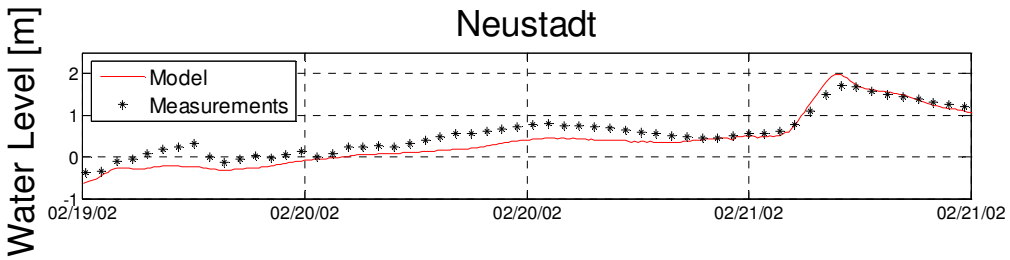

Figure 4-14. Measurements and results of simulation of water levels at Neustadt station

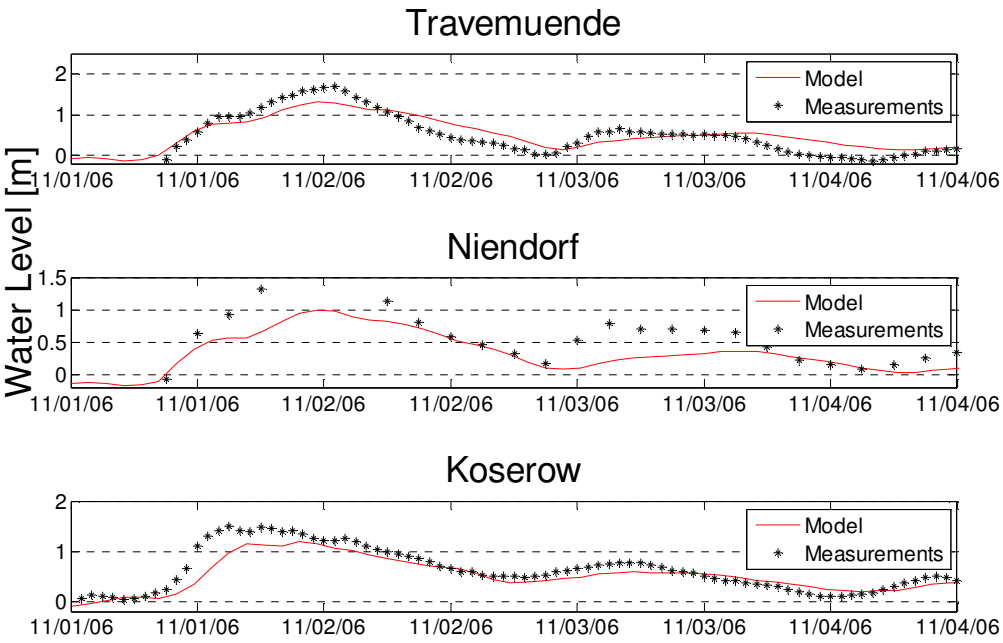

Figure 4-15. Measurements and results of simulation of water levels at Travemuende, Niendorf and Koserow stations

The statistical analysis of the validation is summarized in Table 4-18. In general, the flow model for the Baltic Sea is performing well. Nonetheless, it was observed that a considerable underestimation in the water levels took place close to the Niendorf station, showing highest discrepancies when compared with the other two stations. That inaccuracy in the computational results is due to the low resolution of the model in that location. In contrast, the values obtained at Neustadt and Koserow showed the best agreement with the measurements.

Table 4-18. Statistical analysis for validation of the flow module included in the BSRmod

	Neustadt	Travemuende	Niendorf	Koserow
MAE [m]	0.13	0.17	0.22	0.14
StdDev [m]	0.17	0.25	0.37	0.21
ARMAE [m]	0.09	0.16	0.28	0.07

In the second part of the validation process, the computed significant wave height is compared with the measurements collected at the four stations shown below. During the validation of the wave module of the BSRmod two periods of measurements were provided. At the Ahrenshoop station, the data covers part of February in 2002; for the rest of the stations the data covers the first days of November, in 2006.

According to Figures 4-16 and 4-17, during the period in February 2002, a maximum significant wave height close to 1.5 m was observed; while in November

2006, the significant wave height reached values ca. 2.5 m at the Varnkewitz station.

In general, the wave module in the Baltic Sea region followed the trend of the measurements observed in all four stations for the two periods of validation. Note that the higher the waves the closer the model results were to the measurements. This validation proved that the Baltic Sea regional model is good enough to be considered reliable close to coastal areas.

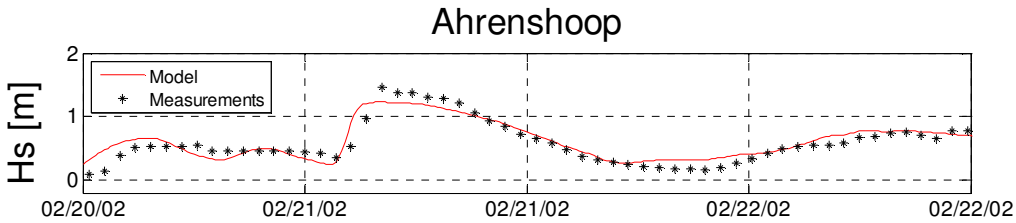

Figure 4-16. Measurements and results of simulation of significant wave height at Ahrenshoop stations

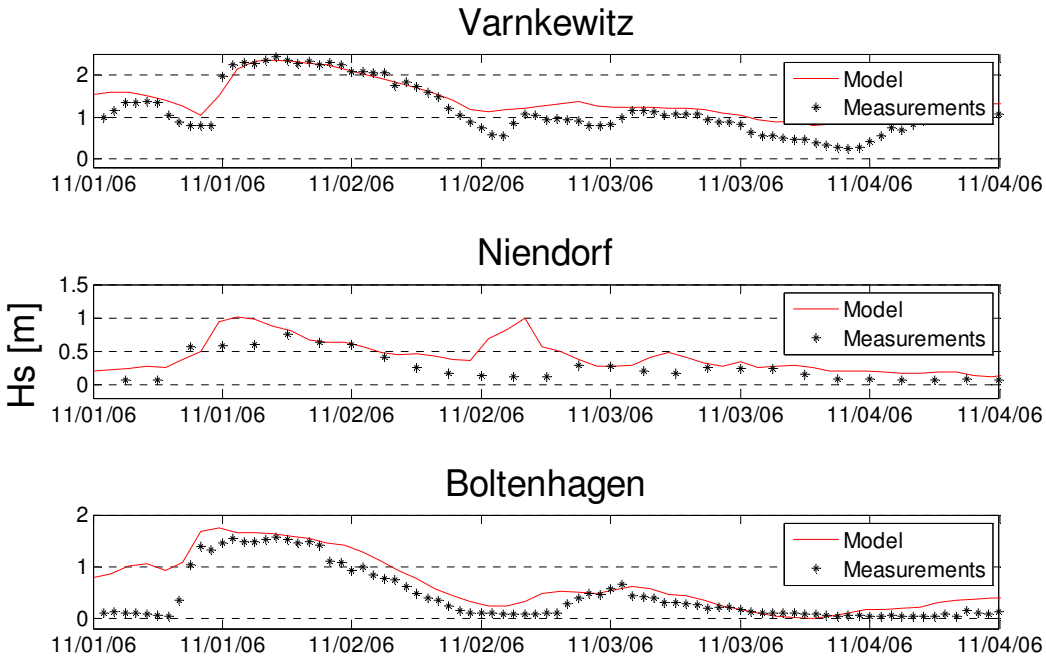

Figure 4-17. Measurements and results of simulation of significant wave height at Varnkewitz, Niendorf and Boltenhagen stations

In Table 4-19 the statistics showed that the model at Ahrenshoop and Varnekewitz performed with the most accurate results among all four stations. At Niendorf and Boltenhagen the results were comparable. The lowest ARMAE was 0.09 m, while at Boltenhagen, the highest values of that statistical parameter reached 0.23 m. In the simulation of the waves the computational schemes include complex formulations that are strongly dependent on the resolution of the model. The area close to the beaches of Boltenhagen and Niendorf constituted different conditions in which the depth and the shape of the coastline might have played a major role in the transformation and orientation of the waves. Ahrenshoop is a location in which the conditions corresponded to the regular hydrodynamics of the Luebeck Bay, which were well captured by the stationary scheme applied in the BSRmod.

Table 4-19. Statistical analysis for validation of the wave module included in the BSRmod

	Ahrenshoop	Varnkewitz	Niendorf	Boltenhagen
MAE [m]	0.22	0.22	0.25	0.23
StdDev [m]	0.21	0.24	0.25	0.24
ARMAE [m]	0.09	0.09	0.18	0.23

4.5 The applications of BSRmod

In this chapter the development of the BSRmod has been explained in detail; i.e. each step during the setup, calibration and validation of the model was presented. By means of the BSRmod, the boundary conditions in the local areas of the Luebeck Bay are generated through the nesting of a local model in that particular area. In the final application of this system of models, a whole number of simulations is designed for extreme events and medium-term simulations during the hindcasting of the morphodynamics in the inner Luebeck Bay. In the following a brief introduction of these two types of simulations is presented.

4.5.1 Reproducing extreme events in the Baltic Sea

In order to generate extreme meteorological and hydrodynamic conditions in the German Baltic Sea, a method to simulate climatologic extreme conditions in the Baltic Sea has been used in the MUSTOK-SEBOK-A project (Bruss et al., 2009 and Jimenez et al., 2009). The model simulations were driven by physically-consistent atmospheric scenarios that were generated by the German Meteorological Service (DWD: Deutscher Wetterdienst) (Schmitz, 2007). Those scenarios were generated using the ‘Super-Ensembles’ method. That method consists of a combination of numerical forecasting models and extensive

measurements of meteorological parameters used to find a set of extreme events that might have occurred during the last century in the Baltic Sea region.

The 'Super-Ensembles' method is based on the weather forecast modelling system (EPS: Ensemble Prediction System) created at ECMW (European Centre for Medium-Range Weather Forecasts) (ECMWF, 2001 and ECMWF, 2004). The EPS is a daily-basis operational model system that is nowadays considered the best meteorological-simulation tool for the middle atmosphere conditions (i.e. 500hPa; see ECMW-Annual report 2006). The simulation system consists of fifty members. Each member differentiates from each other in the way the formulations of the model are considered. Additional to the modification in the formulations of the model, a systematic application of sequential initial conditions is conducted in order to begin individual simulations. The entire evolution of the storm that is supposed to be reproduced in the Baltic Sea region is eventually contained along the period covered by the aforementioned set of simulations (see Annex D).

Each EPS-member would generate one scenario that might have happened around the date that is intended to be reproduced. In this way 31900 scenarios have been generated; among them, a number of scenarios have been pre-selected based on the highest wind surge produced. The wind surge is calculated based on the formulation from the statistical analysis of storms conducted by Schmager (1984) in the coastal area of the German Baltic Sea.

It is worth mentioning that the dates considered in the 'Super-Ensembles' simulations are dates of storms that indeed happened in the region. The initial conditions to simulate such events are set-up through meteorological analyses conducted during the European Reanalysis Project (ERA40). ERA40 is a project in which the possible meteorological conditions of the area have been reproduced based on measurements during a period of 45 years approximately (i.e. 1957-2002).

Once the preselected extreme scenarios from the EPS are processed to obtain the wind speed and atmospheric pressure, the BSRmod is driven by these meteorological extreme conditions in order to reproduce the hydrodynamic conditions in the regional scale.

4.5.2 Downscaling

The simulation of the morphodynamics in the Luebeck Bay will be eventually driven by the hydrodynamic conditions that are created in the regional scales. In order to simulate bathymetrical changes in the Luebeck Bay, the hydrodynamic conditions have to be driven at the boundaries of the LBLmod. The BSRmod provides water levels, currents and wave parameters to the LBLmod during the execution of extreme events and during the medium-term hindcasting of the morphodynamics. In the following chapter, the Luebeck Bay Local model is presented in detail considering all steps necessary for the setup, calibration and validation of the morphodynamic model.

Chapter 5

LBLmod: Luebeck Bay Local Model

In this chapter, the most important aspects about the setup, sensitivity analysis, calibration and validation of the local model in the inner Luebeck Bay are presented. The LBLmod is a model created to fulfill the requirements to simulate the morphodynamics in the inner Luebeck Bay. The spatial resolution of this local model is significantly higher than the BSRmod. In contrast to the BSRmod, the finer mesh of the LBLmod is expected to have better computational resolution to simulate the morphodynamics within the coastal area of the inner Luebeck Bay.

Each time a morphodynamic simulation has to be carried out with LBLmod, in which no measured data for boundary conditions is available, the flows and wave conditions are numerically generated. Therefore, a parallel simulation of the BSRmod had to be executed to generate the conditions at the open boundaries of the LBLmod. Below, in Figure 5-1 the nesting procedure of the two models is schematized. Note in Figure 5-1 the differences in the dimensions of the domains. The domain area of LBLmod is significantly smaller, in contrast with that of the BSRmod.

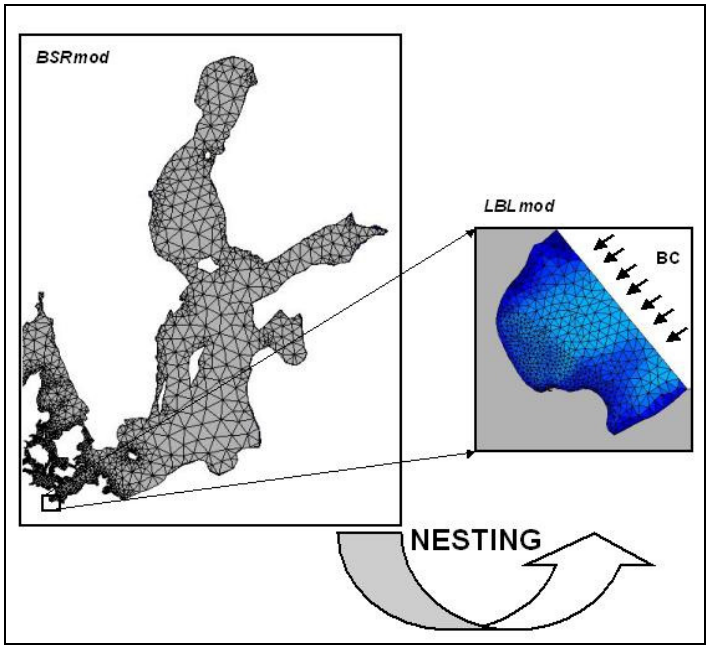

Figure 5-1. Nesting sequence of LBLmod into BSRmod

5.1 Domain and driving forces

This part of the thesis is intended to give an overview of the main aspects that were considered during the development of the LBLmod. This section contains special information about the model, including the domain specifications, characteristic hydrodynamic conditions in the area, meteorological patterns and representative sediment properties. Special features about the morphodynamics of the Luebeck Bay that are relevant in that area, are also included in this discussion.

5.1.1 Domain

The local-model domain is found in the southernmost area of the Mecklenburg Bay. That area is particularly known as the inner Luebeck Bay (see Figure 5-2). The extension of the domain begins in the west at 10°43'and ends at 11°00' longitude in the east. In the south-north direction, the area begins at 53°56' and ends at 54°05' latitude. There is a distance of ca. 11 km between the open boundary in the NE and the beaches of Timmendorf in the SW. In the east-west direction, a distance of ca. 15 km, between Neustadt, in the NW, and Travemuende in the SE is found. The local model contains a total area of ca. 128 km^2.

Two types of boundaries are applied in the LBLmod, as follows: i) an open boundary on the NE side of the domain which connects the inner Luebeck Bay with the Southwestern Baltic Sea, and ii) a land boundary in the south, west and east, where the shoreline is affected by the flooding and drying of cells due to the oscillations of the water levels.

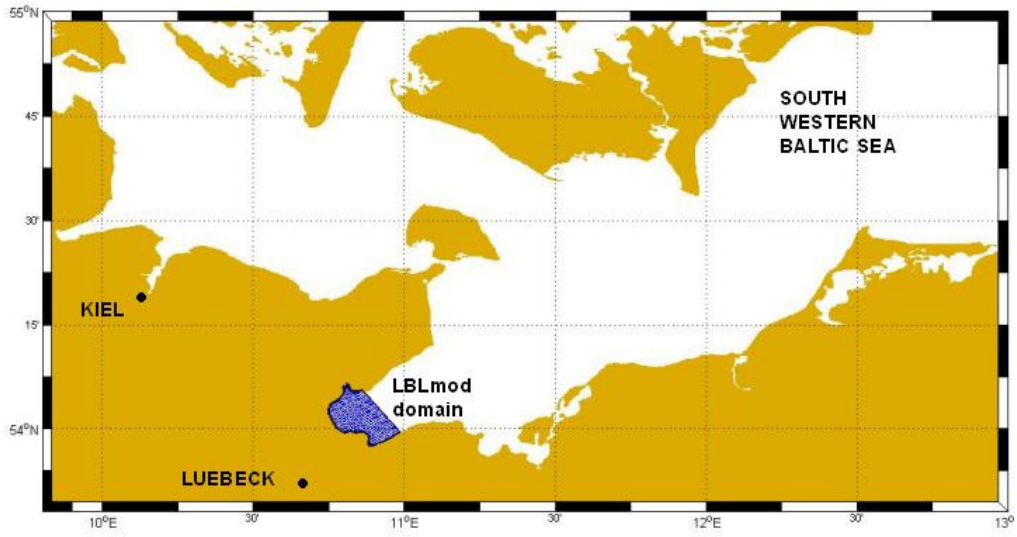

Figure 5-2. South-western Baltic Sea (LBLmod domain)

5.1.2 Bathymetry

The bathymetry of the inner Luebeck Bay is shown in Figure 5-3. Offshore of the beaches of Timmendorf, Niendorf and Brodten Cliff-coasts, the maximum depth can reach about 20 m along the open boundary. Some elevations can be distinguished in the middle area and in the eastern side of the Luebeck Bay. There are bathymetrical features in the Luebeck Bay that can be related to the geological structures that lie underneath. For example, in Figure 5-3 the distinction of shallow and deep channels in the inner Luebeck Bay can be associated with the characteristics of the geology that is found in those locations. In most cases of the shallow areas, till and agglomerates are found, while in the deeper areas the accumulation of fine sediment takes place.

The deep areas of the inner Luebeck Bay are formed by two main channels. The first one, the Kuhlbrooktals channel is found on the west side of the domain with a maximum depth of ca. 17 m. The second channel -and the deepest- is the Aalbeek channel, which is localized in the eastern domain; the maximum depths observed in this channel are close to 20 m.

In the coastal area of the inner Luebeck Bay sandy beaches with gentle crossing-slopes on the west and steep cliffs-coasts on the east are observed. The cliffs are rapidly transformed under the erosion due to waves and winds. In this way, the sediment is distributed westwards along the shoreline, until reaching the entrance of the harbor of Niendorf.

In the Luebeck Bay, anthropogenic factors have also contributed to the transformation of the coasts in the Luebeck Bay; especially, in front of the harbor of Niendorf, where the deposited sediment is periodically dredged.

There are two kinds of bathymetries used in this investigation. The first one is the one collected by BSH (Federal Maritime and Hydrographic Agency of Germany) in 1997 and the one collected by the Sedimentology Institute at the University of Kiel in 2007. In addition to that, the topography along the coast has been provided by ALR (Office of Rural Management in Kiel). These data have mixed resolutions from 5 to 15 meters of spacing between samples.

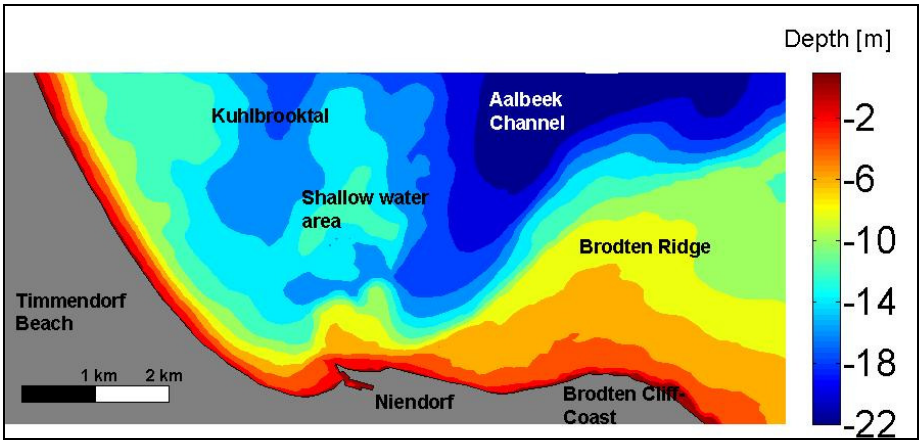

Figure 5-3. Bathymetry in the LBLmod (Source: Sedimentology, Coastal and Continental Shelf Research Group, University of Kiel –Schwarzer and Krause, 2008)

5.1.3 Winds

The direction and magnitude of the wind in year 2007 is presented in Figure 5-4. In that year the northeasterly winds were the most frequent wind direction. In the Luebeck Bay the northeasterly winds are important in the generation of waves that travel to beaches of Timmendorf and Niendorf. Under extreme meteorological conditions, wind-surges and high waves in the inner Luebeck can be important along the coastline.

5.1.4 Waves and currents

Figure 5-5 shows the frequency and direction of waves in year 2007. In the inner Luebeck Bay it was observed that during that year the waves were mostly driven to the southeast. In that period a large proportion of the data collected consisted of waves lower than 1 m; in very few cases the maximum of significant wave height was larger than 2.5 m.

In the LBLmod, waves are quite important in the simulation of the processes of erosion and sedimentation in the nearshore zone. The waves start breaking inducing currents to transport the sediment in the shallow areas. The capacity of the waves to initiate the sediment transport is affected by the shear stress generated by the hydrodynamics of the waves.

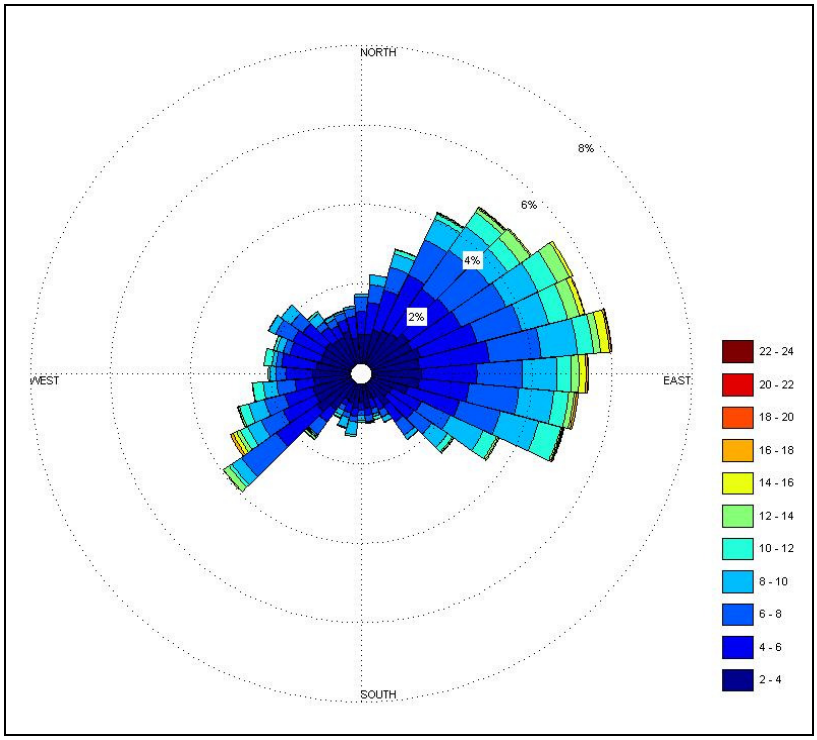

Figure 5-4. Frequency of wind speed and direction (nautical convention) in the Luebeck Bay (year 2007)

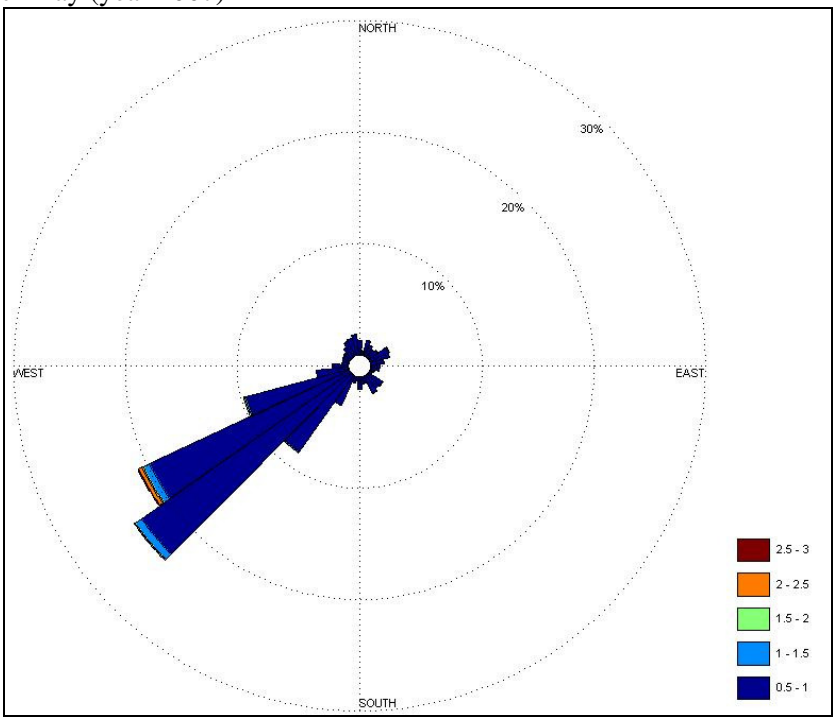

Figure 5-5. Frequency distribution of significant wave height and direction in the Luebeck Bay in the year 2007

In 1950 Dietrich and Weidemann analyzed the magnitude and direction of currents based on measurements (Dietrich and Weidemann, 1952). In that investigation a 6-days period of currents was analyzed, determining the main patterns of currents in the Luebeck Bay. Figure 5-6 shows the observed flows and wind conditions every two days during six days of measurements. A particular relation between meteorological conditions and the flows can be observed. The strongest winds are making the currents converge and diverge along the coastline (see in Figure 5-6, days: June the 6th and 8th). In contrast to that, the weakest winds were more likely to drive the currents in a dominant direction, i.e. either eastwards or westwards (see in Figure 5-6, days: June the 4th and 10th). A trend in the transformation of the Luebeck Bay might be predictable with the results of investigations like that of Dietrich and Weidemann (1952); specially, when medium- and long-term periods are included. In this study, with the use of numerical models it is intended to know more about the medium-term morphological evolution of the Luebeck Bay.

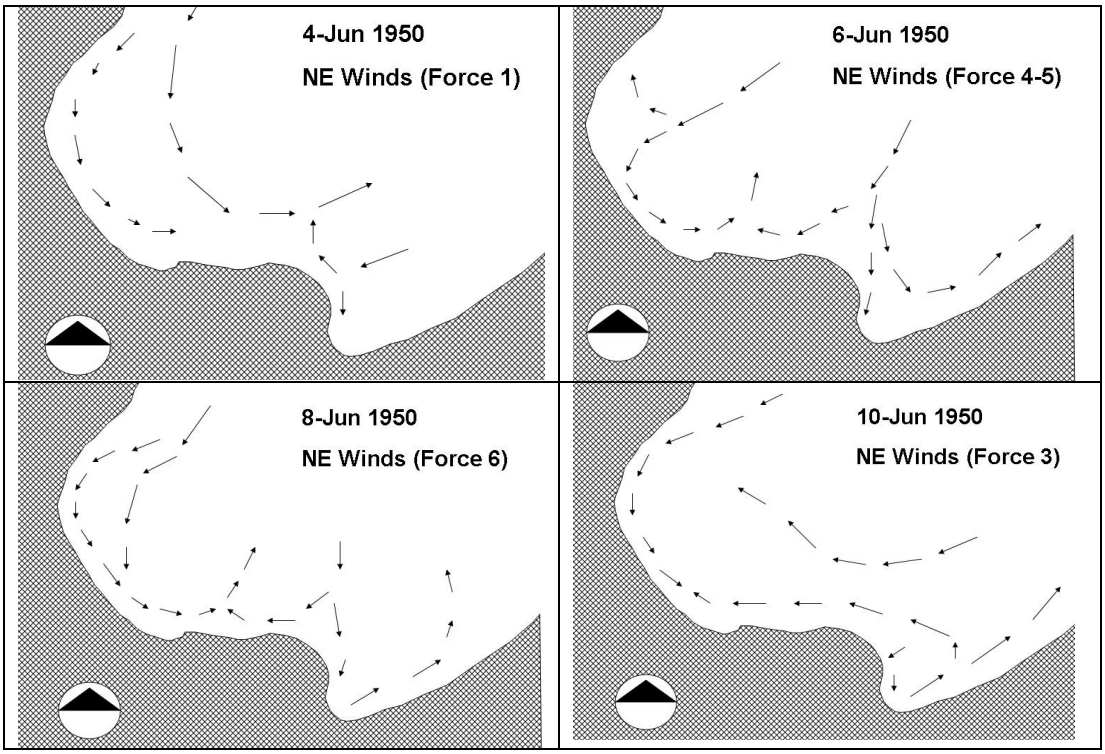

Figure 5-6. Patterns of flow currents in the Luebeck Bay based on hydrodynamic study by Dietrich and Weidemann in June 1950 (Dietrich et al., 1952).

5.1.5 Sediment properties

The data about sediment properties in the LBLmod has been collected during the years 2006 and 2007. At the University of Kiel (institute of sedimentology department) the collection and posterior analysis of sediment samples in the area of

the Luebeck Bay were carried out (Schwarzer und Krause, 2008). Using the 'Side-Scan-Sonar' and 'Boomer' technology mounted in the research vessels FK Littorina and FB Seston, from IFM-Geomar and FTZ-Corelab, respectively, the aforementioned institutions provided the most ever complete information related to sediment gradation and thickness in the study area. Additional to that, in 2007, the research-diving group at the University of Kiel conducted several campaigns of data collection including nine profiles in the nearshore area to complement the measurements executed by the vessels. The resulting sediment properties are used in the LBLmod.

Figure 5-7 presents the mean grain size distribution in the area of interest. In the Luebeck Bay the fine-sand material is commonly observed in the deep areas, while coarser residual of conglomerates is found in the shallow areas. Along the coastline medium-sand sediment is commonly found.

The available sediment on top of the deposits of conglomerates usually presents very thin layers of sediment (<0.05 m). The rate of erosion of the material that constitutes the conglomerates is relatively low. Schrottke (2001) estimated an annual erosion rate between 1.2-4.6 cm/a in the eastern Luebeck Bay (Schrottke, 2001).

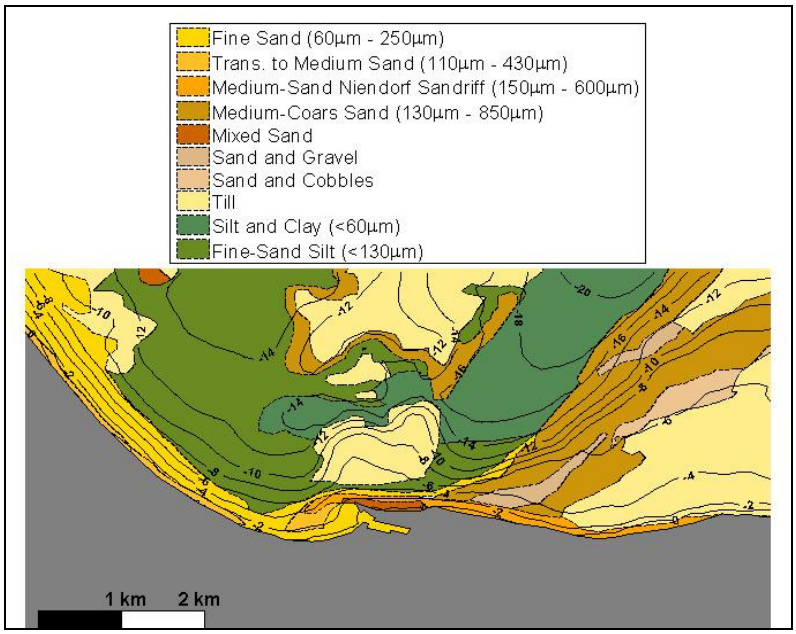

Figure 5-7. Mean grain size distribution (Source: Sedimentology, Coastal and Continental Shelf Research Group, University of Kiel –Schwarzer and Krause, 2008)

In the context of this study the sediment availability makes reference to the thickness of the layer of sediment. The distribution of sediment availability of the LBLmod is shown in Figure 5-8. In most part of the area the sediment availability ranges between 5 and 30 centimeters. Three principal areas can be distinguished. Firstly, in the shallow areas, the availability of the sediment has low values with a

maximum of 5 cm. Secondly, close to the coastline the layer of sediment availability is roughly found in the order of 25 cm, which is mostly constituted by medium-sand material. A third area is characterized by fine sand, localized in the deep areas along the channels of Aalbeek and Kuhlbrookstal. For the later, very thick layers of sediments are observed which suggests long periods of deposition with few, if any, erosion intervals of time in between.

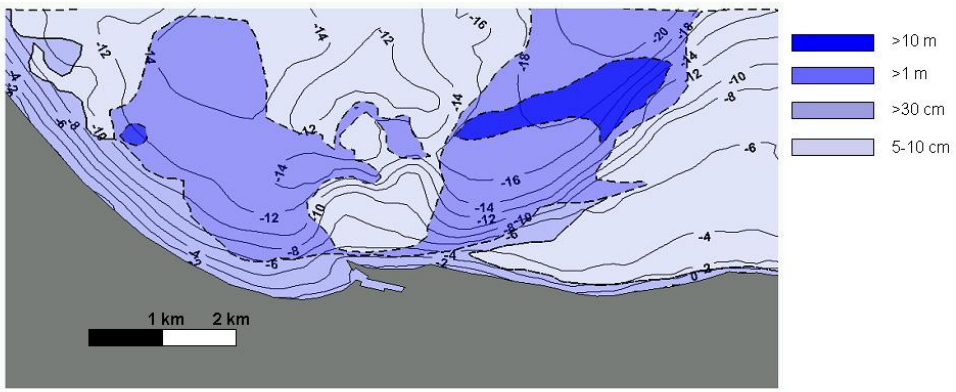

Figure 5-8. Sediment availability (Source: Sedimentology, Coastal and Continental Shelf Research Group, University of Kiel –Schwarzer and Krause, 2008)

5.1.6 Boundary conditions

The data provided in the open boundary of LBLmod can be either generated by numerical models or collected by measurements. In the first case, the boundary conditions of LBLmod are provided by numerical simulations applying BSRmod. In the second case, measurements collected at one station close to the open boundary of LBLmod are used to drive the model. Figure 5-9 shows the two periods of water levels used as boundary conditions. In the first one, i.e. during the sensitivity analysis, a maximum value of water levels not higher than 0.8 m is observed. As for the second period, i.e. in the calibration and validation of LBLmod, the maximum value of water levels is close to 1.5 m.

For the module of spectral-waves, the wave conditions, such as, significant wave height, wave period, and wave direction, are provided in the open boundary of LBLmod.

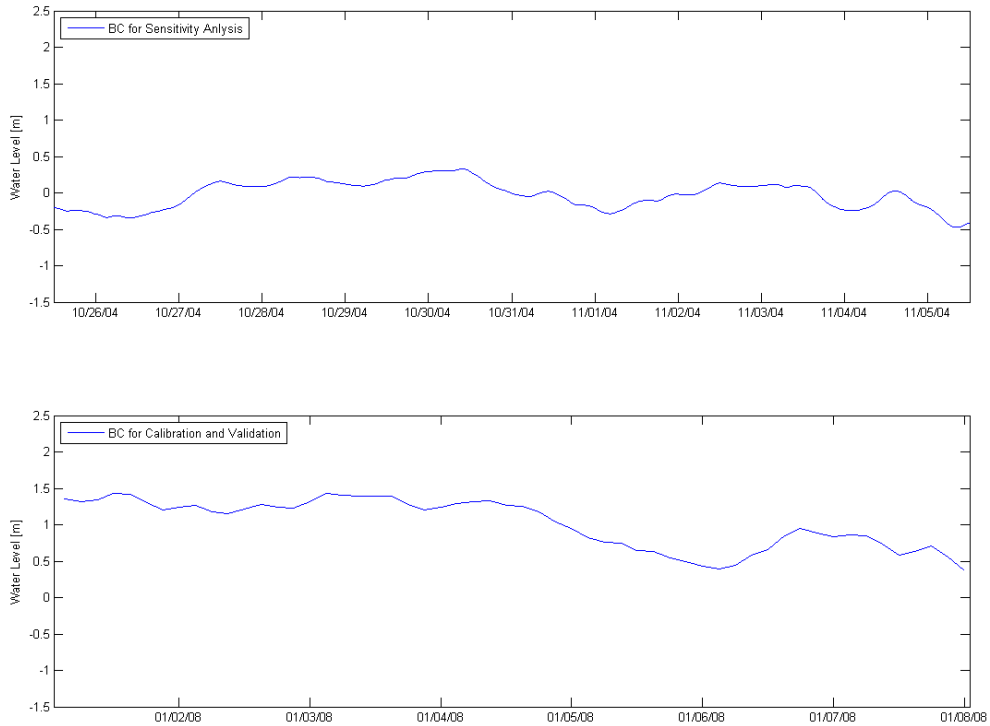

Figure 5-9. Water-levels boundary conditions in LBLmod [m]

5.2 Model setup

5.2.1 Mesh resolution

In the design of the computing mesh of numerical models there are several criteria that should be evaluated. First of all, the areas of interest must be identified in the model according to the objectives of the investigation. In the Luebeck Bay there are important sectors in the domain for the study of its morphological evolution, including: i) the deep areas of Kuhlbrookstal and Aalbeek channels, ii) the elevation in the middle of the bay and iii) the eastern shallow areas in front of the 'Brodtener' cliff coast. The beaches of Timmendorf and Niendorf are also considered important for the definition of the mesh.

The scale of the phenomena studied is also an important consideration for the design of the mesh of a numerical model. An important aim in this investigation is the analysis of the bathymetrical changes of the areas mentioned above. Therefore, a node-spacing would be in range between 10 and 100 meters, in order to evaluate the morphological evolution of the bay during and after storm events.

Figure 5-10 shows three polygons that enclose the areas with different mesh resolutions in the LBLmod. Note that the closer the polygons are to the coastline, the finer the structure of the mesh.

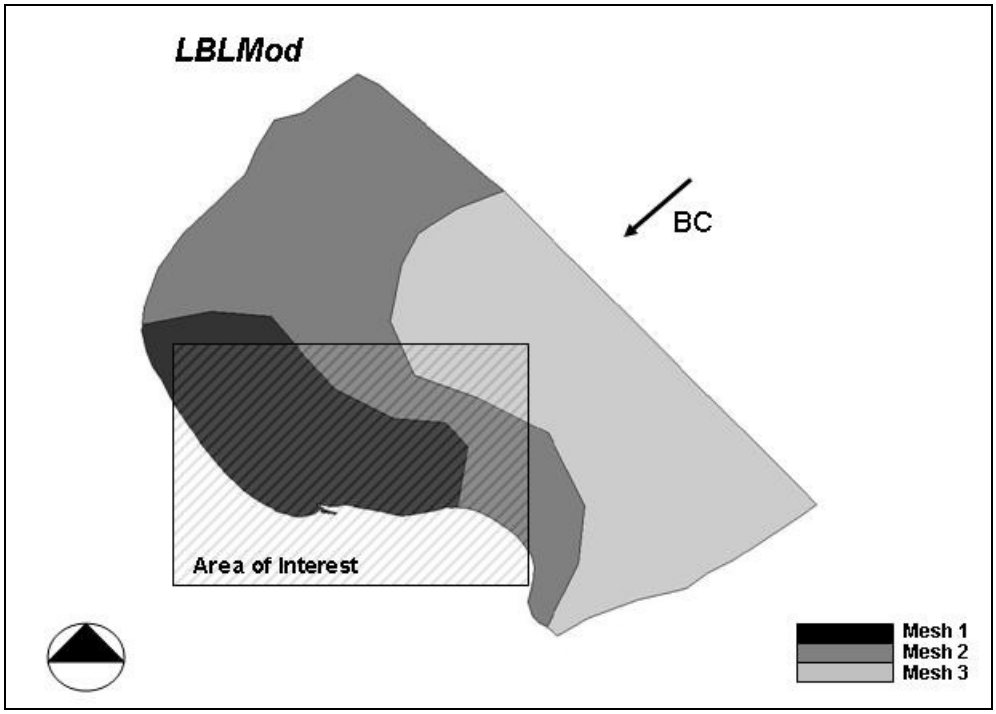

Figure 5-10. Mesh definition in the Luebeck Bay Local model (LBLmod)

Table 5-1 shows the configurations of the polygons with different resolutions (see Figure 5-10). A total of 9040 elements constituted the mesh of the LBLmod. The nodes in the zone of highest resolution have a spacing of ca. 80 m. The definition of a region of high resolution must be consequent to the necessity of covering the most important morphological features of the study area. In areas that are less important for the general objective of this investigation, the mesh resolution of the mesh was reduced (node-spacing of ca. 280).

Table 5-1. Mesh specifications for the LBLmod.

	No. Elements	Ave. Side of Element [m]	Ave. Area of element [m^2]
Mesh 1	9040	80	2700
Mesh 2		140	8470
Mesh 3		280	33880

5.2.2 Time step

In the previous chapter the different forms of the time discretization that are implemented in the flow and wave module of BSRmod were explained (cf. chap. 4). It has been mentioned that the CFL-stability condition is applied to both wave and flow module in order to restrict the time step to ensure the numerical stability of the model. In contrast, the approach applied in the regional model (BSRmod), in the local model (LBLmod) the stationary condition is assumed in the numerical solution of the wave module; therefore, instead of searching for the stability CFL-condition of the instationary approach, the results obtained while assuming the stationary conditions of the local wave model depends on the convergence of the solutions according to a predefined tolerance of residuals and maximum number of iterations.

Table 5-2 shows the basic settings in the configuration of the time step in both, flows and waves. The time step in the flow module is setup depending on the CFL-stability condition. Three values of the maximum CFL-number in the flow module are provided. As for the wave module, the stationary solution is depending on the value provided to the maximum tolerance. At the end, the different settings in both modules are compared based on the CPU time required to finalize the simulations.

In Table 5-2 the computing time taken by each simulation of flows and waves is shown in columns 4th and 7th respectively. As expected, the computing time in both modules is proportionally increased when the more accurate settings were implemented.

Table 5-2. Settings of time discretization of LBLmod for the uncoupled flow and wave modules

	Flows			**Waves**		
	Maximum CFL	**Average Time Step [s]**	**CPU time [hrs]**	**Tolerance value [m]**	**Max. Num. Of iterations**	**CPU time [hrs]**
1st Setting	0.4	1.0	16.8	0.001	500	2.2
2nd Setting	0.8	1.2	11.8	0.01	500	0.5
3rd Setting	1	1.5	8.8	0.08	27	0.2

From Table 5-2, it is observed that the computing time is significantly sensitive to the changes in the restrictions of accuracy in both modules. For example, if the CFL-number is changed from 1 to 0.4, the CPU time is double. The computing time of the wave module on the other hand, was significantly increased with the application of more restrictive conditions in the precision of the computations. By using the 2nd Setting in the wave module the conditions for an efficient and accurate numerical model are found. Concerning the flows modules, the conditions of stability of the model are guaranteed by implementing the 3rd Setting.

5.3 Sensitivity analysis

In the following, the sensitivity analyses of several parameters in the LBLmod are investigated. A systematic modification of some of the most important parameters of the LBLmod and their effects on the results during the simulations is presented in this section. The effects of each parameter are individually analyzed, avoiding interaction between them.

In chapter 4, flows and waves were not coupled during the sensitivity analysis of the BSRmod, in a similar way, in this chapter, the waves and flows modules were also considered independent from each other in the sensitivity analysis of the LBLmod.

In the final stages of the sensitivity analysis, the sediment transport is driven by flows and waves that are coupled during the analysis of the morphodynamic module in the LBLmod. The location of the observation points where the information was collected to compare the different settings in this investigation is shown in Figure 5-11.

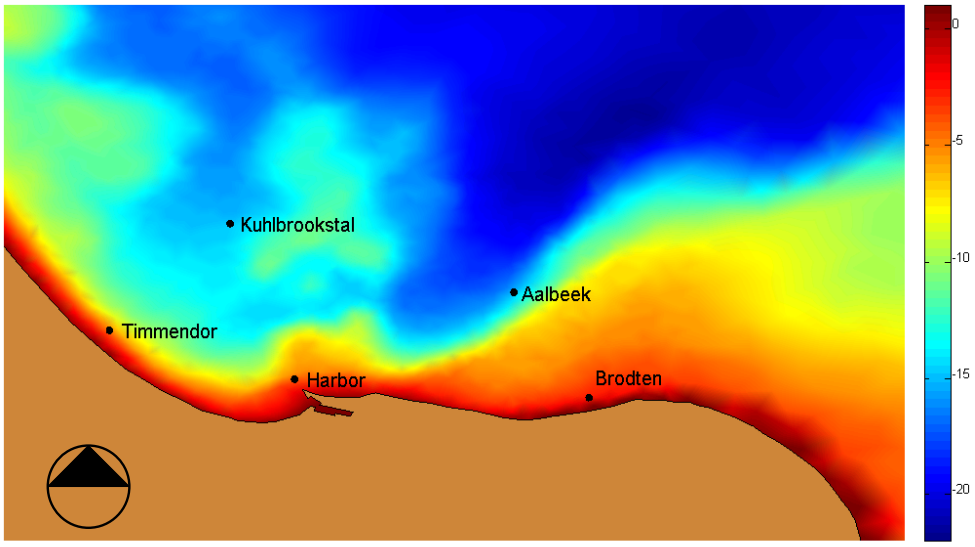

Figure 5-11. Locations for sensitivity analysis in the LBLmod

5.3.1 Flow module

In this section the sensitivity analyses of the most important parameters of the flow module are presented. The analysis begins with the bed roughness by considering the three values presented in the second column of Table 5-3. Additionally, in this investigation three values of eddy-viscosity are considered for horizontal and vertical eddy viscosity. Finally, the effects of the winds are taken into account in

the sensitivity analysis for three values of drag coefficient shown in the last column of Table 5-3. For the analysis of sensitivity each parameter is changed systematically as the remaining parameters are kept fixed in the values of the first setting of Table 5-3.

Table 5-3. Settings for sensitivity analysis of the flow module

	Parameters			
	Bed roughness [m]	Eddy viscosity [m^2/s]		Wind drag coefficient
		Hor.	Ver.	
1st Setting	0.01	0.002	0.002	0.00125
2nd Setting	0.05	0.008	0.002	0.005
3rd Setting	0.2	0.002	0.008	0.010

The results used in the analysis of the first flow parameter (bed roughness) are shown in Table 5-4. The 2nd and 3rd Settings are compared to the 1st Setting at each position shown in Figure 5-11. As for the other two parameters, their values are fixed in 0.002 m^2/s, 0.002 m^2/s and 0.00125 for Eddy viscosity (horizontal and vertical) and wind drag coefficient respectively. The depth-average current velocity is the numerically-simulated variable used in this analysis.

The effects of the bed roughness have shown to be more important for the simulation of currents velocities in the observation points close to the east coast and middle area in the Luebeck Bay (i.e. Brodten and Harbor). The results indicated a clear tendency of the differences of currents velocities to increase when the bed roughness is changed. The bed roughness in the Luebeck Bay is an important parameter to be considered for the calibration of the LBLmod, specially, in the shallow areas in the east and center locations of the domain.

Table 5-4. Sensitivity analysis of the flow-module with respect to the bed roughness. A comparison of the basic setting (1st setting in Table 5-3) and two additional variations (2nd and 3rd settings in Table 5-3).

		Statistics of Current magnitude [m/s]				
		Aalbeek	Brodten	Kuhl.	Harbor	Timm.
2nd Setting	MAE [m/s]	0.005	0.017	0.003	0.011	0.006
	ME [m/s]	0.003	0.016	0.001	0.010	0.005
	StdDev [m/s]	0.006	0.013	0.004	0.007	0.004
3rd Setting	MAE [m/s]	0.010	0.033	0.005	0.022	0.011
	ME [m/s]	0.008	0.032	0.002	0.021	0.011
	StdDev.[m/s]	0.010	0.024	0.007	0.014	0.007

In this sensitivity analysis of the LBLmod the effects of the eddy-viscosity on the simulated currents are also investigated. The results are compared in Table 5-5 considering the three settings of eddy-viscosity presented in Table 5-3 (columns 3 and 4 in). Similar to the procedure of sensitivity analysis of the previous parameter, in this case, the remaining parameters are fixed in 0.01 and 0.00125, which corresponds to the values of bed roughness and wind drag coefficient. Note that the differences were higher for the vertical eddy viscosity (3rd Setting) than for the horizontal eddy viscosity (2nd Setting). In addition to that, it was also observed that at those locations from the eastern side of the domain (i.e. Aalbeek and Brodten) the differences where higher when compared to the differences found at the western locations.

Table 5-5. Sensitivity analysis of the flow-module with respect to the eddy viscosity. A comparison of the reference setting (1st setting in Table 5-3) and two additional variations (2nd and 3rd settings in Table 5-3).

		Statistics of Current magnitude [m/s]				
		Aalbeek	Brodten	Kuhl.	Harbor	Timm.
2nd Setting	MAE [m/s]	0.011	0.012	0.008	0.007	0.005
	ME [m/s]	0.010	0.011	0.002	0.002	-0.002
	StdDev [m/s]	0.012	0.012	0.012	0.011	0.008
3rd Setting	MAE [m/s]	0.014	0.014	0.009	0.009	0.005
	ME [m/s]	0.013	0.013	0.000	0.003	-0.002
	StdDev.[m/s]	0.015	0.014	0.012	0.012	0.009

In the sensitivity analysis of the wind-drag coefficient, the simulation results of water levels are compared in Table 5-6. The three settings with different wind-drag coefficient are presented in Table 5-3. The other two parameters, i.e. bed roughness and eddy viscosity (horizontal and vertical), are kept constant with 0.01, 0.002 m^2/s and 0.002 m^2/s, respectively. For most of the locations the differences between the settings were relatively low. It is probable that the domain in the LBLmod was not large enough for the winds to develop a relevant effect on the water surface. In contrast with the BSRmod, the LBLmod contains a smaller domain where the water levels are less affected by the local wind, when compared to the wind conditions in the BSRmod.

Table 5-6. Sensitivity analysis of the flow-module with respect to the wind drag coefficient. A comparison of the basic setting (1st setting in Table 5-3) and two additional variations (2nd and 3rd settings in Table 5-3).

		Statistics of Water Levels [m]				
		Aalbeek	Brodten	Kuhl.	Harbor	Timm.
2nd Setting	MAE [m]	0.009	0.010	0.010	0.011	0.012
	ME [m]	0.003	0.001	0.005	0.004	0.006
	StdDev [m]	0.012	0.014	0.015	0.016	0.017
3rd Setting	MAE [m]	0.021	0.023	0.025	0.027	0.029
	ME [m]	0.006	0.002	0.013	0.010	0.015
	StdDev.[m]	0.029	0.033	0.035	0.037	0.040

5.3.2 Wave module

In this section, the sensitivity analysis is focused on the most important parameters of the wave module of the LBLmod. The analysis begins by comparing the differences in the significant wave height using five schemes with a different formulation of the wind-wave interaction. In this analysis the wave-breaking and bottom-friction are also considered. The parameters that have been already studied in the previous sections are kept constant with the values of the first setting of Table 5-3.

Table 5-7a and Table 5-7b show the configuration of the cases that are compared in the sensitivity analysis of the wave module. The formulations in the generation of waves by wind are presented in Table 5-7a. The second and third parameters are in Table 5-7b. Table 5-7b contains only two settings for the analysis of both parameters; for these two parameters the results of significant wave height are compared including and not including the parameter in the wave-energy equation.

Table 5-7. Settings for sensitivity analysis of wave module

a)

Cases	**Parameter**
	Wave Wind-generation Scheme
1st Setting	JONSWAP
2nd Setting	Kahma & Calkoen
3rd Setting	SPM73
4th Setting	SPM73_HBH
5th Setting	SPM84

b)

Cases	**Parameters**	
	Wave Breaking	**Bottom Friction**
1st Setting	Included	Included
2nd Setting	Not Included	Not Included

The formulations in the wind-waves generation have been compared based on the differences of significant wave height. With the same statistical parameters and the same positions, as it was carried out in the previous analyses of the flow module, the effects of the parameters on the model results are analyzed. In Table 5-8 the first option (JONSWAP) and the other four settings of wind-wave generation are compared. In general, the values calculated with the JONSWAP setting are less than 10 cm lower than those computed using the other choices. The formulation of SPM84 proved to be the closest to the JONSWAP formulation. Concerning the spatial distribution of the differences, it can be observed that the maximum effects of changing the wind-wave-generation scheme is slightly higher in the Aalbeek channel when compared to the other locations.

Table 5-8. Sensitivity analysis of wave-module with respect to the formulation of the wave wind-generation scheme. A comparison of the basic setting (1st setting in Table 5-7a) and four additional schemes (2nd, 3rd, 4th and 5th settings in Table 5-7a)

		Statistics of Significant Wave Height [m]				
		Aalbeek	Brodten	Kuhl.	Harbor	Timm.
2nd Setting	MAE [m]	0.087	0.065	0.077	0.066	0.058
	ME [m]	-0.086	-0.064	-0.075	-0.066	-0.056
	StdDev [m]	0.124	0.103	0.111	0.092	0.097
3rd Setting	MAE [m]	0.088	0.062	0.078	0.068	0.060
	ME [m]	-0.087	-0.061	-0.076	-0.066	-0.058
	StdDev.[m]	0.129	0.106	0.116	0.095	0.100
4th Setting	MAE [m]	0.092	0.066	0.084	0.070	0.062
	ME [m]	-0.091	-0.065	-0.083	-0.070	-0.061
	StdDev [m]	0.128	0.109	0.116	0.096	0.100
5th Setting	MAE [m]	0.059	0.054	0.055	0.049	0.044
	ME [m]	-0.055	-0.053	-0.052	-0.048	-0.041
	StdDev.[m]	0.120	0.109	0.107	0.089	0.095

The waves-breaking parameter in the wave module represents the dissipation of the energy of waves when they approach the shallow nearshore zones. The results of the simulations showed differences close to 4 cm in the significant wave height between the two settings (see Table 5-9). Table 5-9 shows those differences in all five positions in the area of the inner Luebeck Bay. In general, the differences have shown that the wave-breaking parameter is important in the calibration of the model, especially for those areas with shallow depths.

Table 5-9. Sensitivity analysis of wave-module with respect to the exclusion of wave breaking. A comparison between including (1st setting in Table 5-7b) and not including wave breaking (2nd setting in Table 5-7b)

		Statistics of Significant Wave Height [m]				
		Aalbeek	Brodten	Kuhl.	Harbor	Timm.
2nd Setting	MAE [m]	0.044	0.044	0.043	0.038	0.039
	ME [m]	-0.042	-0.043	-0.041	-0.038	-0.038
	StdDev [m]	0.112	0.107	0.102	0.084	0.094

The differences in the results when comparing the results of significant wave height between no-bottom-roughness and including the bottom roughness are presented in Table 5-10. The effects of not including the bottom friction are generally the tendency to 'overestimate' wave heights. The differences had a maximum close to 7 cm in the area close to the Brodten Cliff-coast. In contrast with the BSRmod, in the LBLmod it has been proven that the bottom friction plays an important role in the computation of the waves in the Luebeck Bay.

Table 5-10. Sensitivity analysis of wave-module sensitivity with respect to the exclusion of bottom fiction. A comparison between including (1st setting in Table 5-7b) and not including bottom friction (2nd setting in Table 5-7b)

		Statistics of Significant Wave Height [m]				
		Aalbeek	Brodten	Kuhl.	Harbor	Timm.
2nd Setting	MAE [m]	0.021	0.069	0.010	0.029	0.015
	ME [m]	-0.018	-0.069	-0.009	-0.029	-0.014
	StdDev [m]	0.047	0.075	0.025	0.046	0.028

5.3.3 Coupled hydrodynamic modules

In the previous sections the numerical results of the LBLmod were obtained carrying out simulations of flows and waves as individual modules. In the following the simulations of the hydrodynamic variables are executed using not only the individual modules but the coupled flow-waves modules as well. Table 5-11 shows the scheme of the analysis including three model configurations. The first one is the coupled LBLmod; the second and third configurations are waves without flows and flow without waves, respectively.

This analysis is aimed to determine the extent to which one module affects the final results of the other. In this way, current velocities and significant wave heights are calculated using wave and flow modules separately. The results of the coupled LBLmod are compared with those previously obtained by separate runs.

Table 5-11. Settings for analysis of differences between simulations of coupled and non-coupled hydrodynamic modules

	Parameters	
	Sig, Wave Height	Currents Magnitude
Coupled	Included	Included
Only Wave	Included	Not Included
Only Flow	Not Included	Included

The statistics presented in Table 5-12 shows the differences based on the significant wave height between the coupled model and the model including only waves. By applying the wave module alone the waves are computed under hydrodynamic conditions that are significantly different from those generated in the coupled version of LBLmod. In the only-wave setting the water levels were considered constant and no currents were applied in the computing of waves. In contrast, by coupling flows and waves, the variations of currents and variations in the surface elevation are taken into account in the computation of waves.

The results shown in Table 5-12 indicate that when currents and water levels are included in the computations, higher waves are expected in the Luebeck Bay. When compared to the wave-only configuration, the differences at the location close to the Brodten Cliff-coast presented the highest discrepancies. In the Luebeck Bay currents and water levels are important in the simulation of waves.

Table 5-12. Statistical analysis comparing simulated significant wave heights from coupled hydrodynamic modules and non-coupled wave module (Only Wave)

		Statistics of Sig. Wave Height [m]				
		Aalbeek	Brodten	Kuhl.	Harbor	Timm.
Only Wave	MAE [m]	0.033	0.072	0.026	0.039	0.030
	ME [m]	-0.011	-0.065	-0.008	-0.032	-0.020
	StdDev [m]	0.052	0.078	0.038	0.051	0.042

In the second part of this analysis the effects of the waves on the computation of current velocities are assessed. The ‘only-flow’ setting and the coupled LBLmod are compared in this section. Table 5-13 contains the statistical values of the differences based on currents velocities. In general, the difference between the results from the flow module and the coupled LBLmod confirmed that the effects of the waves on the computation of flows are not relevant. In the shallow area close to the Brodten Cliff-coast, maximum differences were observed.

Table 5-13. Statistical analysis comparing simulated current magnitudes from coupled hydrodynamic modules and non-coupled flow module (Only Flow)

		Statistics of Current Magnitude [m/s]				
		Aalbeek	Brodten	Kuhl.	Harbor	Timm.
Only Flow	MAE [m]	0.005	0.029	0.003	0.023	0.007
	ME [m]	0.001	0.006	0.002	0.005	0.001
	StdDev [m]	0.009	0.044	0.006	0.037	0.013

In the simulation of waves the LBLmod proved to be more sensitive to the effects of the flows on the waves than in the other way around. Nevertheless, it must be considered that in the shallow areas the effects of both modules are important.

5.3.4 Morphodynamics

In this section the hydrodynamic LBLmod is coupled with the sediment transport module. An analysis of sensitivity is conducted to investigate the effects that a group of parameters might have on the simulated bathymetrical changes in the Luebeck Bay.

Two settings of the model defining the conditions of the four parameters that are considered in this investigation are presented in Table 5-14. Initially, the effects of the hydrodynamics on the morphodynamics are studied. The type of boundary conditions and the inclusion of waves as driving forces in the transport of sediment are the first two aspects to be considered in this analysis. The other two are related to the properties of the sediments, i.e., the sensitivity analysis of the model regarding the porosity and gradation of the sediment.

The first item presented in Table 5-14 is the definition of the boundary conditions. In the morphodynamic module there are two options. The first option (1st setting) corresponds to the assumption that no sediment flux gradients are present at the open boundaries. With the second option it is assumed that no sediment flux gradients for the outgoing direction and no bed level changes in the incoming direction are considered.

In the third column of Table 5-14 the two settings concerning the driving forces in the sediment transport module are compared. In the 1st Setting the waves are included, while in the 2nd Setting the effects of the waves are not taken into account.

The last two parameters in this analysis correspond to the porosity and gradation of the sediment. Two settings for these parameters are defined. The effects of the porosity of the sediment are evaluated considering 0.6 and 0.3 of porosity. As for the gradation 1.3 and 1.4 of gradation are analyzed.

Table 5-14. Setting of the sensitivity analysis of morphodynamic coupled module

	Parameters			
	Boundaries Formulation	Forcing Formulation	Porosity of Sediment	Gradation of Sediment
1st Setting	Boundary 1*	Current-Wave induced	0.6	1.3
2nd Setting	Boundary 2**	No Waves	0.3	1.4

* Zero Sediment Flux gradient
** Zero Sediment Flux gradient for outflow, zero bed changes for inflow

Initially, the bed level changes using the two boundary formulations are compared in Table 5-15. The model indicated that close to the Brodten Cliff-coast, the type of boundary might have some relevance compared to the other locations. The differences in terms of bed level changes at the other four locations have shown minor effects of the choice of boundary formulation on the final results.

Table 5-15. Sensitivity analysis changing boundary formulations

		Statistics of Bed Level Change [m]				
		Aalbeek	Brodten	Kuhl.	Harbor	Timm.
Boundary 2	MAE [m]	0.001	0.003	0.001	0.001	0.001
	ME [m]	0.001	0.003	0.001	0.001	0.001
	StdDev [m]	0.001	0.002	0.001	0.001	0.001

The second step of this analysis consists of determining the relevance of the waves on the morphological evolution in the study area. Table 5-16 shows the differences in terms of bed level changes. The highest differences are observed at the Brodten Cliff-coast location. Although the other four locations are showing moderate values that oscillate between 4 millimeters and half a centimeter, the action of the energy of waves should be considered in the simulations; mostly, in the shallow areas as more sediment is in suspension due to the turbulence and currents that are induced by the waves.

Table 5-16. Sensitivity analysis of LBLmod to the wave action

		Statistics of Bed Level Change [m]				
		Aalbeek	Brodten	Kuhl.	Harbor	Timm.
No waves	MAE [m]	0.004	0.028	0.006	0.013	0.001
	ME [m]	0.004	0.028	0.006	0.013	0.001
	StdDev [m]	0.003	0.024	0.005	0.010	0.001

The sediment porosity effects in the numerical simulation of the bathymetrical changes are shown in Table 5-17. The simulation results of the bathymetrical changes are compared between the two settings of porosities that are shown in the fourth column of Table 5-14. In all locations the statistics reveal an increasing rate of sediment transport with the higher value of sediment porosity (0.6).

Table 5-17. Sensitivity analysis of LBLmod to the sediment porosity

		Statistics of Bed Level Change [m]				
		Aalbeek	Brodten	Kuhl.	Harbor	Timm.
Porosity of sediment 0.3	MAE [m]	0.014	0.015	0.016	0.015	0.004
	ME [m]	-0.014	-0.011	-0.016	-0.009	0.004
	StdDev [m]	0.006	0.015	0.008	0.015	0.003

In Table 5-18 the differences in the simulation results between the two settings of sediment gradation are compared. In general, the effects that were produced by changing the gradation from 1.3 to a higher value (1.4) were quite small (less than 1 cm).

Table 5-18. Sensitivity analysis of LBLmod to the gradation of grain size distribution

		Statistics of Bed Level Change [m]				
		Aalbeek	Brodten	Kuhl.	Harbor	Timm.
Gradation 1.4	MAE [m]	0.007	0.008	0.006	0.012	0.004
	ME [m]	0.007	-0.008	0.006	-0.012	-0.004
	StdDev [m]	0.003	0.005	0.001	0.006	0.002

5.4 Calibration and validation

Measured data and model results of water levels, currents and waves are compared in this section. The locations of the observations are presented in Figure 5-12. Initially, the results of flow simulations were compared with the measurements of water levels and current magnitude. In the calibration and validation of the LBLmod waves are also included.

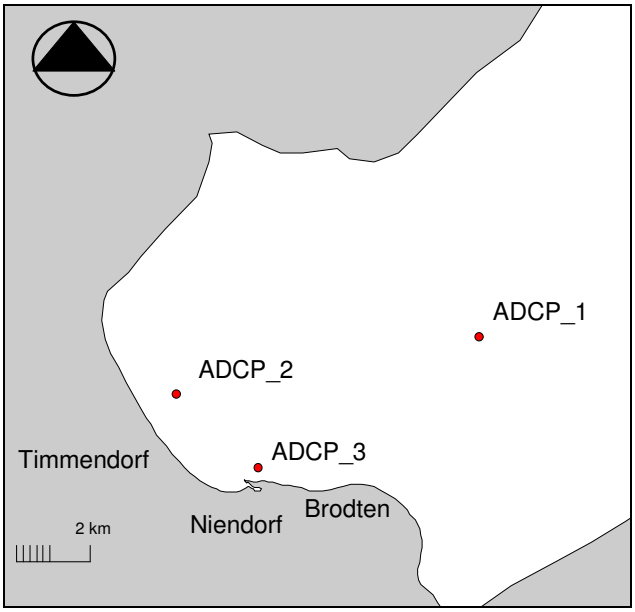

Figure 5-12. ADCP Stations in the Luebeck Bay. ADCP_1: U-boot, ADCP_2:Scharbeutz, ADCP_3: Niendorf

The calibration and validation of the LBLmod were carried out over a period of 8 days in the year 2008. The model was driven with the measured data along its open boundary (see ADCP_1 in Figure 5-12) with water levels, currents and waves. The simulation results are compared with the measurements at Niendorf and Scharbeutz (i.e. see ADCP_2 and ADCP_3 in Figure 5-12). Those data have been provided by CORELAB-FTZ.

Figure 5-13 shows the data of water levels at the observation points close to the coastal areas of Niendorf and Scharbeutz. The model results are in good agreement with the measurements. At the Niendorf station the measurements are slightly higher than the numerical results.

.

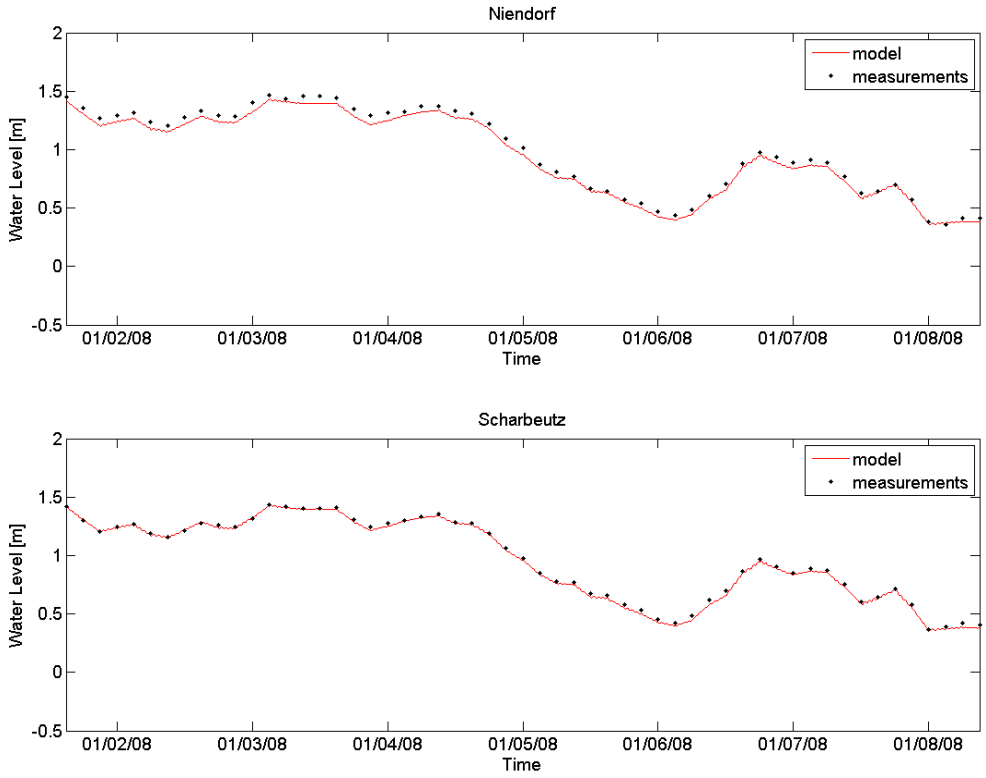

Figure 5-13. Comparison between simulation results and measurements of water levels during calibration of LBLmod

In the second phase of this calibration and validation process the current magnitude is compared at the same two locations that water levels were taken. In Figure 5-14 measurements and results of model simulation of current magnitudes are shown. The values of current velocity were in the range between 0 and 0.15 m/s; in general both, measurements and model results have a similar range of values. The model results using two values of bed roughness are compared. The numerical results were similar as different values of bed roughness were applied. In Table 5-19 the values of the statistics are presented.

Table 5-20 presents the statistics of the calibration of the vertical eddy viscosity of the flow module. In both cases the differences in terms of mean absolute error between measurements and model results were not higher than 0.04 m/s. The ARMAE is 0.01 m/s in the validation based on the current velocities. According to the scale of numerical-model accuracy proposed by Van Rijn (2003) the model is in good agreement with the measurements.

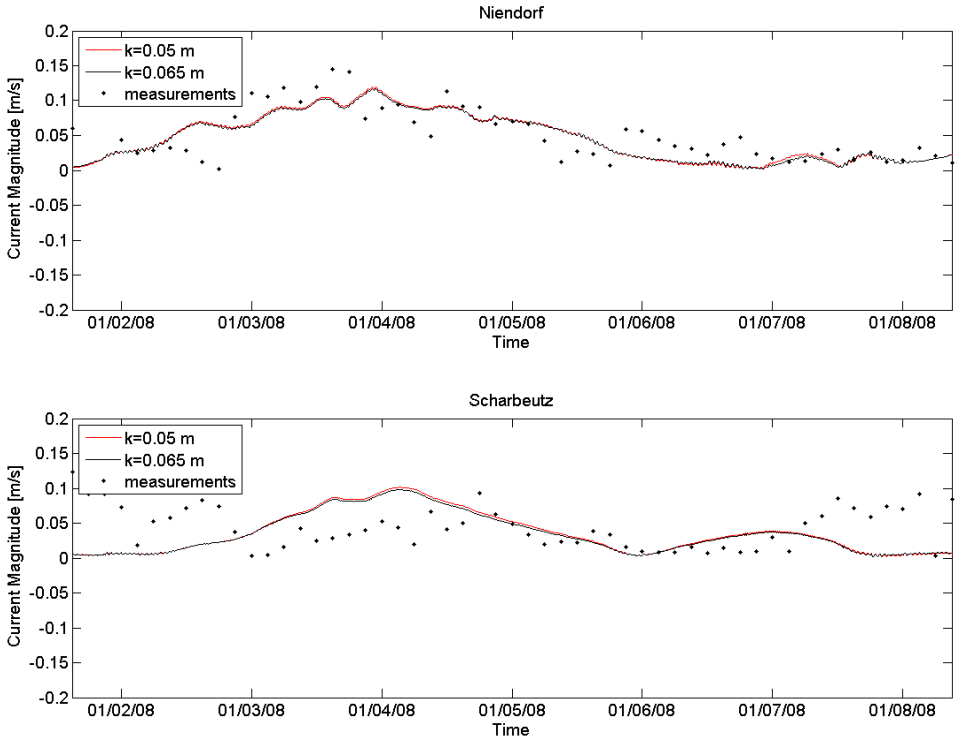

Figure 5-14. Comparison between simulation results and measurements based on magnitude of current velocities using different values of bed roughness

Table 5-19. Statistical analysis comparing measurements and numerical results of currents velocities changing the bed roughness

Bed roughness [m]	Statistics	Statistics of Current Magnitude	
		Niendorf	Scharbeutz
k=0.05	MAE [m/s]	0.04	0.04
	StdDev [m/s]	0.05	0.05
	ARMAE [m/s]	0.01	0.01
k=0.065	MAE [m/s]	0.04	0.04
	StdDev [m/s]	0.05	0.04
	ARMAE [m/s]	0.01	0.01

Table 5-20. Statistical analysis comparing measurements and numerical results of current velocities changing vertical eddy viscosity

Eddy Viscosity (Vertical) [m^2/s]	Statistics	Statistics of Current Magnitude	
		Niendorf	Scharbeutz
Ev=0.002	MAE [m/s]	0.04	0.04
	StdDev [m/s]	0.05	0.05
	ARMAE	0.01	0.01
Ev=0.004	MAE [m/s]	0.04	0.04
	StdDev [m/s]	0.05	0.05
	ARMAE [m/s]	0.01	0.01

In this section of the calibration and validation of the LBLmod, the simulation results of the significant wave height are compared with the measurements at the stations of Niendorf and Scharbeutz. In Figure 5-15 the simulated significant wave height is compared with the measurements considering two values of bed roughness (0.15 mm and 0.25 mm). In both stations the trend observed in the numerical results was consistent with the measurements. The largest differences are seen close to the highest values in the time series.

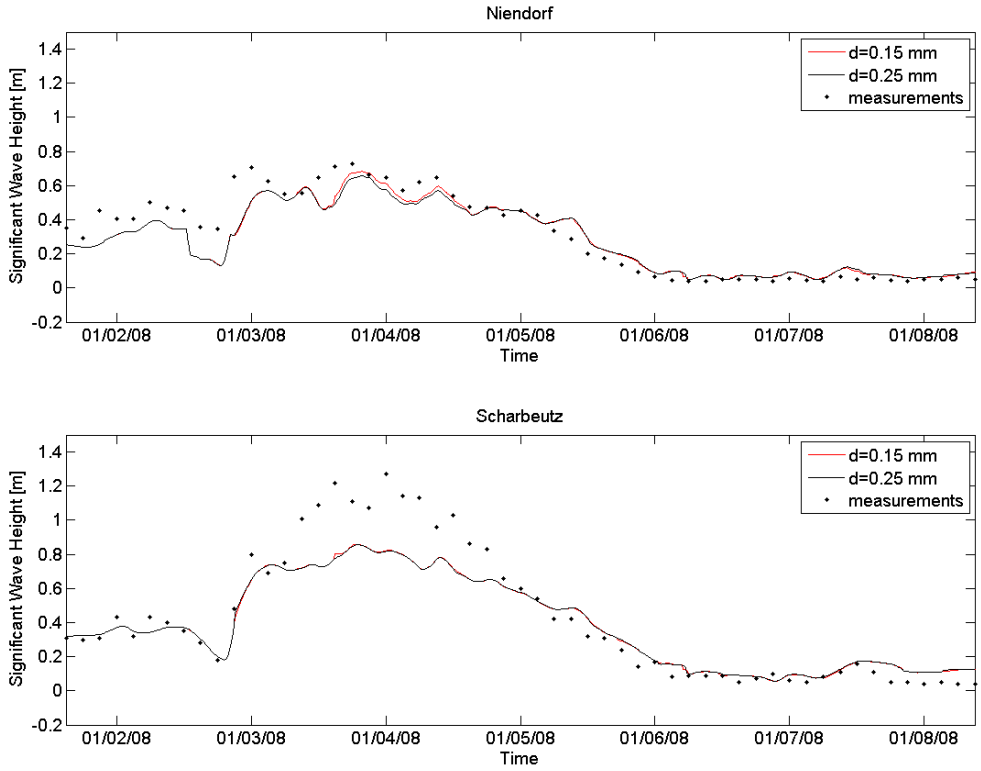

Figure 5-15. Comparison between simulation results and measurements of significant wave height for changing the bed roughness

The statistics shown in Table 5-21 indicates that the discrepancies between simulations and measurements at the two stations are comparatively higher at the Niendorf station. The differences at Scharbeutz are more concentrated at the peak of the time series. The values of the statistics can be considered to be in good agreement with the measurements according to the criteria of accuracy in the scale proposed Van Rijn (2003).

Table 5-21. Statistical analysis comparing measurements and numerical results of significant wave height changing the bed roughness

Bed roughness [mm]	Statistics	Statistics of Significant Wave Height	
		Niendorf	Scharbeutz
0.15	MAE [m]	0.16	0.10
	StdDev [m]	0.21	0.15
	ARMAE [m]	0.23	0.10
0.25	MAE [m]	0.16	0.10
	StdDev [m]	0.22	0.15
	ARMAE [m]	0.24	0.11

By changing the formulation of wave generation, in Table 5-22 the differences between model results and measurements are analyzed. The differences between model results and measurements presented higher discrepancies at the Niendorf station. The range of ARMAE values was observed between 0.25 m and 0.11 m. The numerical results in the significant wave height applying both JONSWAP and SPM73/HBH are comparable; there are no major discrepancies between both options that might indicate an advantage of one of the alternatives over the other. The statistical values were similar to those observed previously in Table 5-21, which indicates that by applying either option, the numerical results obtained can be considered in good agreement with the measurements.

Table 5-22. Statistical analysis comparing measurements and numerical results of significant wave height changing the formulation of the wave generation

Wave-generation scheme	Statistics	Statistics of Significant Wave Height (m)	
		Niendorf	Scharbeutz
JONSWAP	MAE [m]	0.16	0.10
	StdDev [m]	0.22	0.15
	ARMAE [m]	0.24	0.11
SPM73/HBH	MAE [m]	0.16	0.11
	StdDev [m]	0.22	0.16
	ARMAE [m]	0.24	0.12

Chapter 6

Description of the storms and their effects on the morphology of the Luebeck Bay

6.1 Definition of storms in the study area

In marine environments storms are mostly produced by extreme meteorological and hydrodynamic conditions that evolve over short periods of time generating extremely high waves and significant rise of water levels along the coasts (McInnes and Hubbert, 2001). Usually, the magnitude of the wind under storm conditions can be between 17.2 and 20.7 m/s (8, Beuaufort scale). In addition to that, it is mostly seen that in high latitude regions, storms, which are also known as cyclones, are formed due to the low-pressure meteorological conditions. The 'normal' hydrodynamic conditions of mean sea levels, currents and waves are rapidly changed during the storms, producing floods and possible erosion along the coastal areas. Under stormy conditions, it is commonly observed that the landscape of the exposed beaches and the morphology along the seabed in the shallow areas are transformed due to the dissipation of energy produced by strong wind-waves and tides.

In the Luebeck Bay it can be observed that erosion is taken place on areas that are visibly affected by the permanent action of waves (Schrottke, 2001). Whether it is due to the action of isolated storms or the combination of storms and normal conditions over medium-term periods is an issue that still needs to be studied in more detail. It is expected that during calm periods the beaches recover completely and no permanent changes on the morphology occur. In the Luebeck Bay, the changes on the morphology produced by extreme events constitute the topic of this chapter.

The criteria, which may be used to define the occurrence of a storm, are not unique for all coastal regions around the world. The definition of a storm may depend on the local conditions that determine the frequency, duration and intensity of an extreme event. In some cases it would be adequate to define a storm based on wind speeds, which are higher than 17 m/s (Woodroffe, 2002). Extremely large waves (>11 m), on the other hand, are sometimes used as a reference. Time series of water

levels are also used to define the intensity and frequency of storms, for which longer periods of data are usually available.

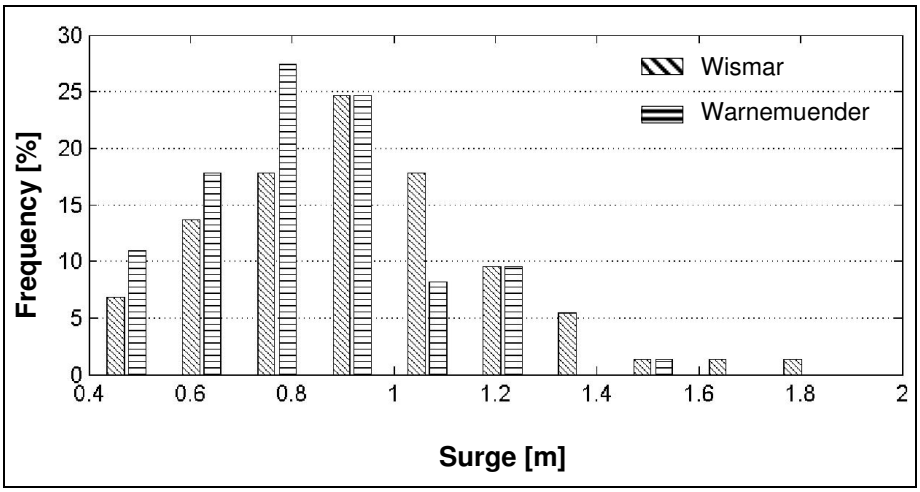

a. Frequency of surges at the locations of Wismar and Warnemuende (within the period from 1976 until 2000)

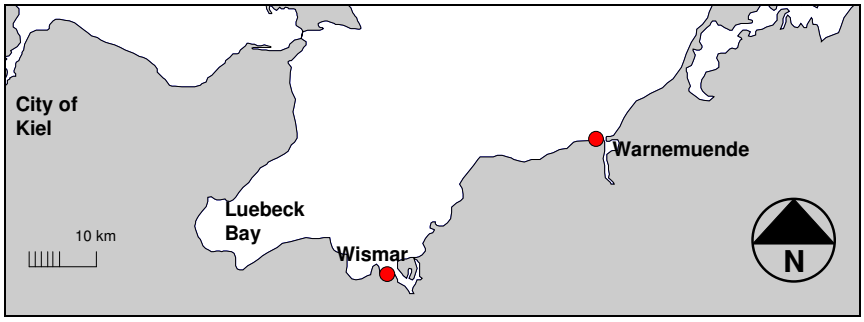

b. Localization of observations of surges

Figure 6-1. Storm surges analysis based on data from 1976 until 2000 (Sztobryn et al., 2005)

In order to give an idea of how intense and frequent the storms in the study area can be, Figure 6-1 presents the frequency and magnitude of the storm surges that occurred along the German Baltic Sea coastline within the period from 1976 until 2000 (Sztobryn et al., 2005). Most of the cases are events that produced water levels along the coast close to 1 m. In that case, the highest frequency of occurrence of storm surges is between 42.5 % and 52 %, which corresponded to the values of water levels between 0.8 m and 0.9 m above MSL. For values of surges higher than 1 m, the frequency is 37 % and 19.2 %. For surges higher than 1.5 m the frequencies decrease to the values of 4.1 % and 1.4 %. The mean of the duration of the storms is 35 hours (1day, 11 hours), with a minimum and maximum duration of about half a day and 5 days, respectively.

In the Baltic Sea, the water levels during the second half of the 20th century have experienced an increasing tendency of extreme values (Sztobryn et al., 2005). The available historical data can confirm that a total number of 13 events during the first decade occurred, while more than 30 events over the last decade of the last century were reported.

6.2 Numerical simulation of storm conditions

The studies of the morphological changes of the coastal areas for medium-term periods require a considerable amount of data consisting of measurements of bathymetries, shorelines and cross-shore profiles. As has been presented in Chapter 2, there are a few studies in which the long-term evolution of the coastal area has been studied with the use of numerical models supported by available measured data. This study contributes to know more about the role of storms on the morphological changes of coastal areas over longer periods.

With the advances of numerical models and the efficient performance of modern computers, numerical model simulations are nowadays fully applied in the research of the morphodynamics in the coastal areas. The possibility of including an unlimited number of conditions is the principal advantage that numerical models have over other techniques, like those of physical models, in the investigation of coastal processes. However, practitioners should bear in mind that measured data are always required for the calibration and validation of the numerical models. Even though the advances on numerical modelling are nowadays significant, for the study and analysis of the morphodynamic coastal process, the most possible information about driving forces and bathymetry should be considered during the setup of the models before the simulations are carried out.

In the following section, the numerical results of the storm scenarios are presented. The analysis of bathymetrical changes during storm scenarios has been included in order to provide information about possible persistent patterns of erosion or deposition under the particular conditions of the storms. In the final sections of this chapter, the analysis of those numerical results is carried out applying the Empirical Orthogonal Functions (EOF) method.

6.2.1 Storm Scenarios

In this investigation a number of scenarios are used to study the morphodynamic effects that storms conditions may have in the area of interest. The storms are driven by meteorological conditions, which are considered physically consistent (Schmitz, 2007, 2009). The meteorological conditions of the scenarios have been created at the European Centre for Medium-Range Weather Forecast (ECMWF, 2001) (see Annex D); the ensemble prediction system (EPS) has been applied to generate them. The wind fields were originally created within the framework of the

MUSTOK-SEBOK-A project (Bruss et al. 2009 and Jimenez et al. 2009). It has been estimated that the probability of occurrence of those scenarios is of 1 in 1347 years (Mudersbach und Jensen, 2009).

Figure 6-2 shows the distribution of the maximum values of water levels and significant wave height of the storm scenarios along the German Baltic Sea coastline. In the coastal areas the variation of the hydrodynamic conditions is evident; the maximum values of waves and water levels present contrasting patterns. The maxima of the water levels are higher in the western Kiel Bay and in the inner Pomeranian Bay with values higher than 3 m. In the local area of the Luebeck Bay the maximum values of the water levels were close to 2.8 meters. The pattern in the spatial distribution of the maximum values of significant wave height is different to the maxima in the water levels. The storms produced higher waves in the Mecklenburg Bay. In the inner Luebeck Bay the significant wave height is already affected by the morphology of the shallow area, which dissipates the energy of the waves.

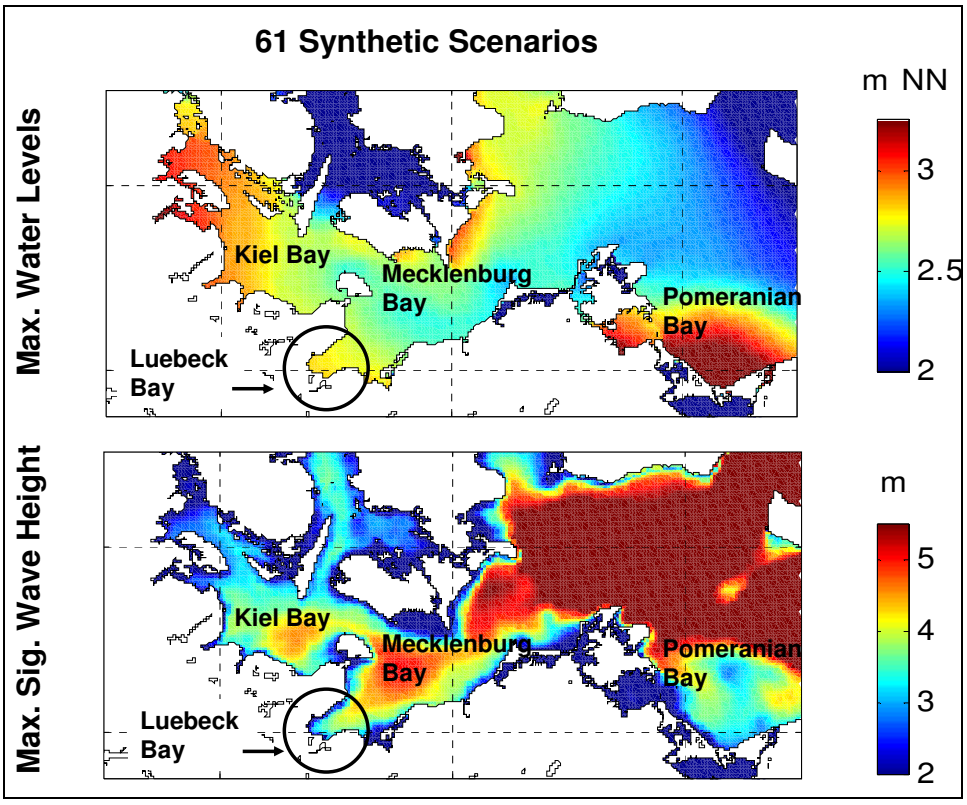

Figure 6-2. Maximum values of water levels and significant wave height based on synthetic storm scenarios in the south-western Baltic Sea (Bruss et al., 2009 and Jimenez et al., 2009)

Figure 6-3 shows the time series of water levels and wave heights in the Luebeck Bay during 4 storm scenarios (S1, S2, S3 and S4). In most cases the peak of water levels does not coincide in time with the peak of the wave heights. Both, water

levels and waves, are affected differently by the action of wind, etc.. The water levels variations during the surge of the storms are caused by lateral variations in barometric pressure, wind-driven surface currents, coastal set-up, and mass transport and setup by the waves. The waves, on the other hand, are primarily produced by the action of the wind on the water surface.

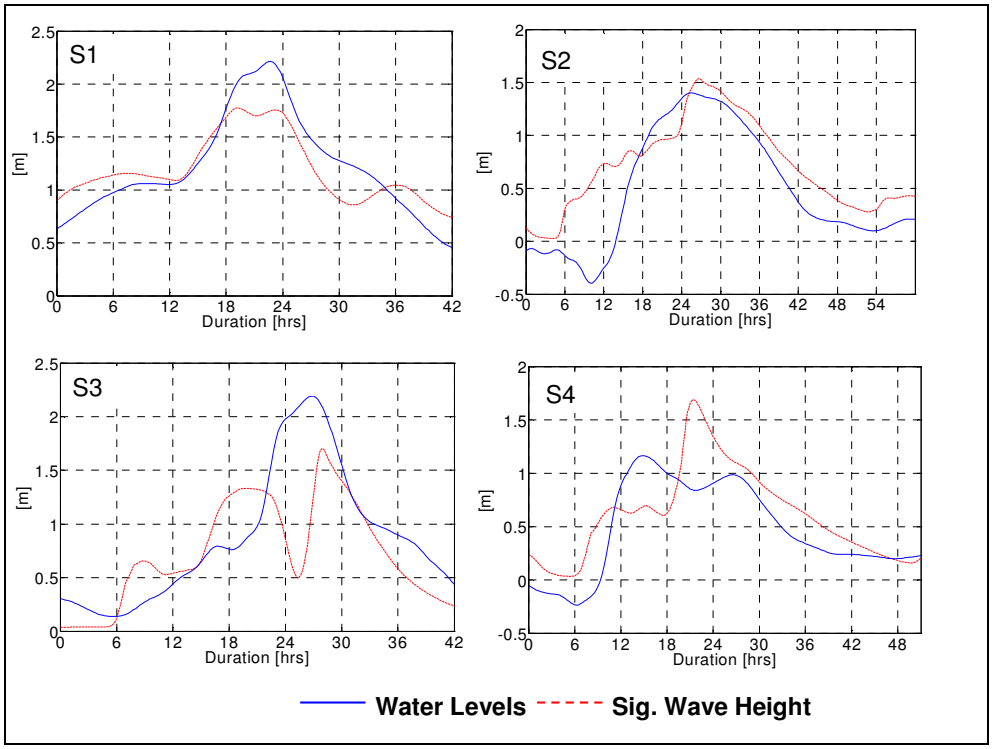

Figure 6-3. Time series of waves and water levels in four storm scenarios

The total number of 16 scenarios is analyzed in the next section. The morphological changes and the hydrodynamics that have been numerically simulated for the storms are studied with the use of EOF.

6.2.2 Morphodynamics in the Luebeck Bay during storm conditions

The analysis of the morphodynamics over periods of storm conditions is especially important to understand the evolution of the coastal areas (Carter and Woodroffe, 1994). The energy that is generated by the winds is transmitted to the seabed by the turbulence and strong currents originated during the winter seasons. Within periods of extreme hydrodynamic conditions offshore currents are generated and sediments from the beaches are transported seawards. This process of beach erosion due to the storms is usually not permanent during longer periods of calm conditions; the beach recovers as onshore currents take the sediment from the deeper areas back to the beaches.

In this section the morphological changes in the Luebeck Bay during storm conditions are analyzed. This study is based on the numerical results of morphodynamic simulations using the local model of the Luebeck Bay (LBLmod). The conditions of the 16 synthetic scenarios used for this analysis are presented in Table 6-1. The scenarios are organized in ascending order based on the maximum value of the water levels generated along the beaches of Timmendorf in the study area.

The wind conditions of the storms are characterized by north-easterly winds with wind speeds within the range from 15 m/s to 20 m/s. The surge of water levels along the coast of the inner Luebeck Bay had maxima between 1.38 m and 2.76 m. The significant wave heights generated by the storms were in the range between 1.0 m and 2.18 m.

Table 6-1. Maximum values during the storm scenarios in the study area (sorted in descending order according to the maximum values of water levels)

Storm No.	Maximum of Water level (m)	Maximum of Significant wave Height (m)	Maximum of Wind Speed (m/s)
S1	2.76	1.78	15.38
S2	2.71	1.82	15.93
S3	2.69	1.71	15.74
S4	2.56	1.58	12.15
S5	2.55	2.18	19.18
S6	2.49	1.74	17.00
S7	2.39	1.46	17.16
S8	2.21	1.77	17.34
S9	2.19	1.69	17.97
S10	2.09	1.74	18.03
S11	2.08	1.98	17.97
S12	2.04	1.59	16.70
S13	1.64	1.00	10.19
S14	1.62	1.68	17.49
S15	1.62	1.30	17.16
S16	1.38	1.46	16.14

The numerical results presented in Figure 6-4 show the depth-average currents during the peak of one scenario of storm conditions. There are several patterns in the circulation of the currents that can be considered relevant during that storm conditions. There is a tendency of the storms to produce regions of recirculation with clockwise movement of water offshore of Timmendorf, Niendorf and Brodten. The flows along the coast are parallel to the coastline with different locations of convergence and divergence of currents. The most notable location of divergence of currents is observed in the eastern side of the study area close to the

Brodten cliff-coast. From that location, the currents are driven westwards until it converges with currents in the opposite direction at several locations along the coast. Under storm conditions significant wave heights of more than 1.5m in the deeper areas are considerably dissipated when approaching the shoreline. Under normal conditions significant wave heights are around 0.3 m.

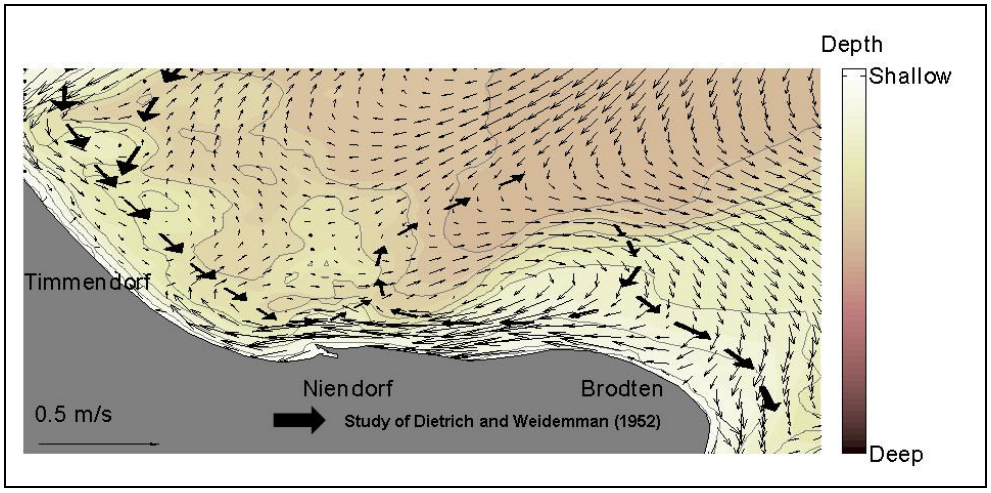

Figure 6-4. Currents in the Luebeck Bay during one storm period

The morphological changes produced by the storm scenarios are illustrated in Figure 6-5, Figure 6-6 and Figure 6-7. Negative values represent erosion, while positive bathymetrical changes indicate areas of deposition of sediment. The changes of the bathymetry reveal the principal areas where the bathymetry is more affected by the action of extreme events.

Close to the Brodten Cliff-Coast (A3), in most of the scenarios, erosion takes place. The ridge in front of the cliffs is under constant erosion. It is most probable that the source of sediment that is transported to the deepest areas, on the west of the ridge, comes from the ridge itself driven by currents in the east-west direction.

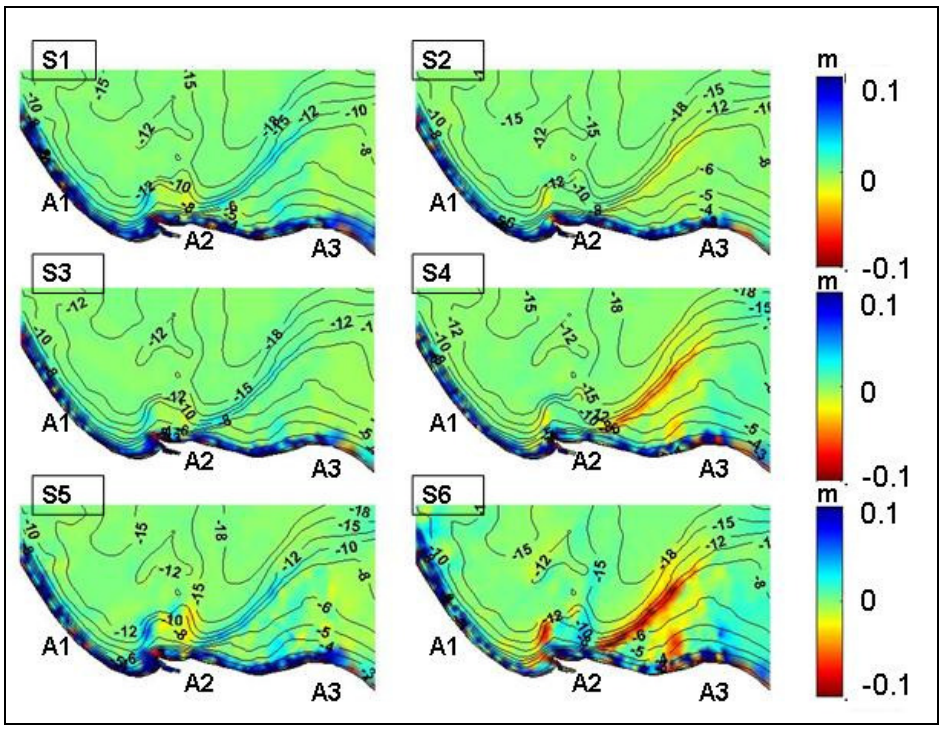

Figure 6-5. Bathymetry isolines and bathymetrical changes (colour contours) produced by synthetic storm scenarios close to Timmendorf (A1), Niendorf (A2) and Brodten (A3) in the inner Luebeck Bay. From scenario S1 to scenario S6

There is one main morphological feature through which the storm scenarios are remarkably different. On the western flank of the ridge in front of A3, in the area between A3 and A2, there are storm scenarios showing erosion process (i.e. S4, S6, S7, S15, and S16). A second group of storms (i.e. S1, S3, S5, S8, S9, S10, S11 and S14) presents more deposition of sediment in that particular area. A third group of cases (i.e. S2, S12 and S13) is composed of those scenarios in which it is not that clear to define whether it is under a process of erosion or deposition of sediment in that specific area.

There are other results of morphological changes in the Luebeck Bay from the numerical simulation of the storm scenarios that are worth mentioning. For instance, in the offshore area of Niendorf (A2) the patterns of erosion and/or sediment deposition are not that clear. The bathymetrical changes in the deeper areas offshore Timmendorf revealed low activity of sediment transport. In contrast, along the shoreline, the bathymetrical changes appeared to be very important, which is most likely due to cross-shore sediment transport produced by wave-induced currents combined with the action of longshore drift.

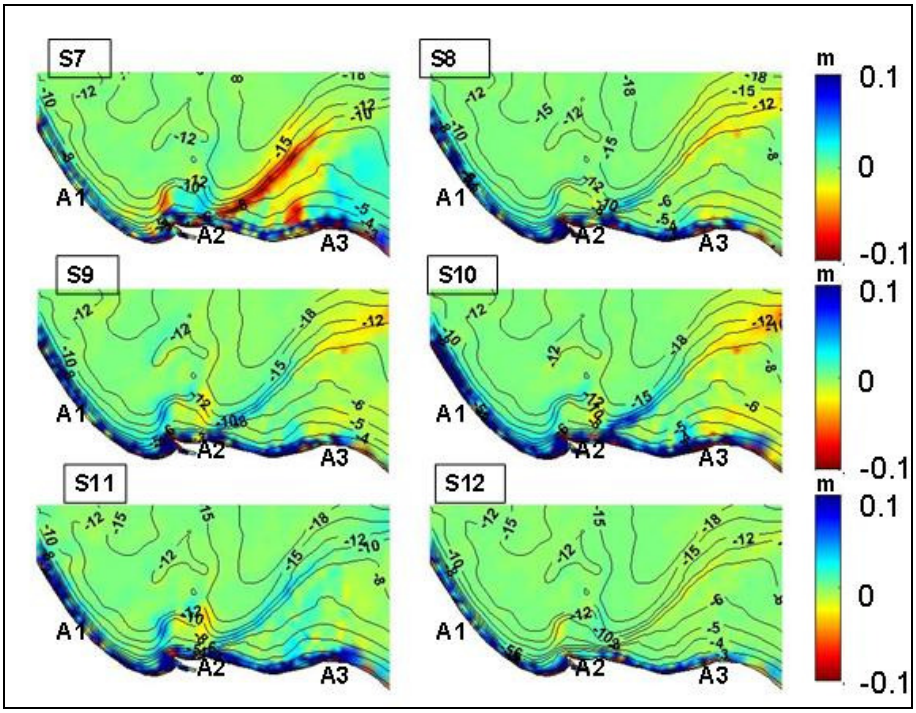

Figure 6-6. Bathymetry isolines and bathymetrical changes (colour contours) produced by synthetic storm scenarios close to Timmendorf (A1), Niendorf (A2) and Brodten (A3) in the inner Luebeck Bay. From scenario S7 to scenario S12

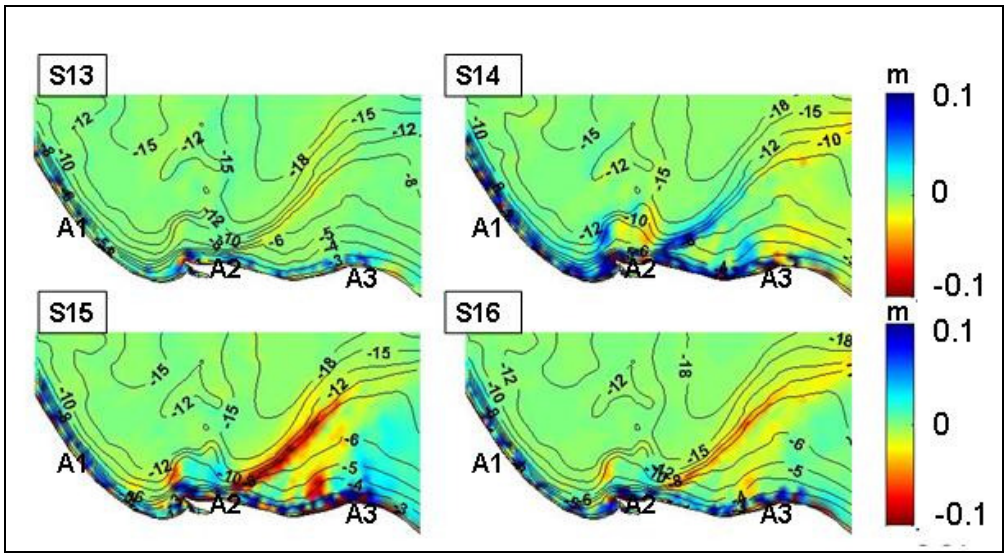

Figure 6-7. Bathymetry isolines and bathymetrical changes (colour contours) produced by synthetic scenarios close to Timmendorf (A1), Niendorf (A2) and Brodten (A3) in the inner Luebeck Bay. From scenario S13 to scenario S16

In the following, the interaction between morphological changes and hydrodynamics under storm conditions is analyzed based on two cases out of the 16 synthetic storms (see Figure 6-8 and Figure 6-9). Storm S6 and storm S14 represent two contrasting cases in terms of morphological changes. In the first case, the most relevant morphological features indicate that erosion can happen in the area between A3 and A2 (see red-colour contour in Figure 6-8). In the second case, the morphological changes contrast with those presented in storm S6. At the end of the simulations applying storm S14, the deposition of sediment is present in that particular area, which is in contrast with the observations at the end of the simulation of storm S6.

In Figure 6-8 the dominant hydrodynamic conditions in the period of time close to the peak of storm S6 are compared with the total changes of the bathymetry. The erosion in the offshore areas close to Brodten (A3) and Niendorf (A2) is produced due to the currents in the eastward direction. The combination of flow velocities and the gradients in the bathymetry contributes to the erosion of the western berms that surround the platform in front of the Brodten Cliff-coast (A3) and the shallow area in front of the Niendorf Harbour (A2). The most significant changes along the coastline consist of progradation in the western and central sectors in front of the Timmendorf beaches (A1) and Niendorf (A2), respectively, and erosion in the eastern coastline in front of the cliff-coast (A3). The incident waves are almost perpendicular to the coast in all the sectors along the coastline. A dominant cross-shore sediment movement is expected due to the waves breaking and mass balance in the shallow nearshore areas.

In Figure 6-9 the patterns of currents during storm S14 are illustrated. In contrast with the uniform pattern of currents shown in the first case (storm S6), in this second scenario, more complex patterns of eddies and convergent/divergent currents can be observed. Under those particular conditions the bathymetrical changes are affected in another direction; the deposition of sediment offshore Brodten (A3) is taking place due to the transport of sediment from the shallow platform to the deeper areas. The wave conditions that are present in Storm S14 are similar to those in Storm S6; the incident waves are normal to the coastline everywhere in the domain generating cross-shore sediment transport.

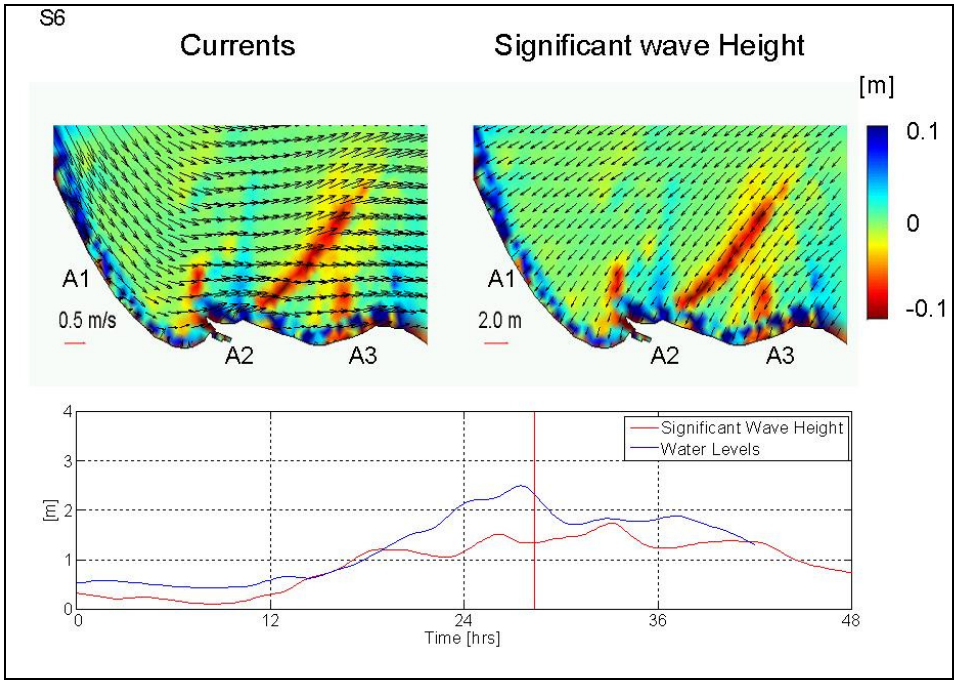

Figure 6-8. Bathymetrical changes and current-flow vectors (upper left), bathymetrical changes and significant-waves-heights vectors (magnitude and direction) (upper right), and time series of waves and water level during storm number S6

The simulation results of the bathymetrical changes of the storm scenarios show a complex relation between the morphodynamics and the particular conditions of each extreme event. In that regard, a unique spatial distribution of morphological changes corresponding to a combination of all storms is improbable. In the analysis of the spatial distribution of the morphological changes statistics can be applied in the computation of their representative patterns. In the following section, the use of the Empirical-Orthogonal-Functions method (EOF) is proposed as an alternative to be used in the definition of relevant bathymetrical change of the Luebeck Bay due to the effects of the storms.

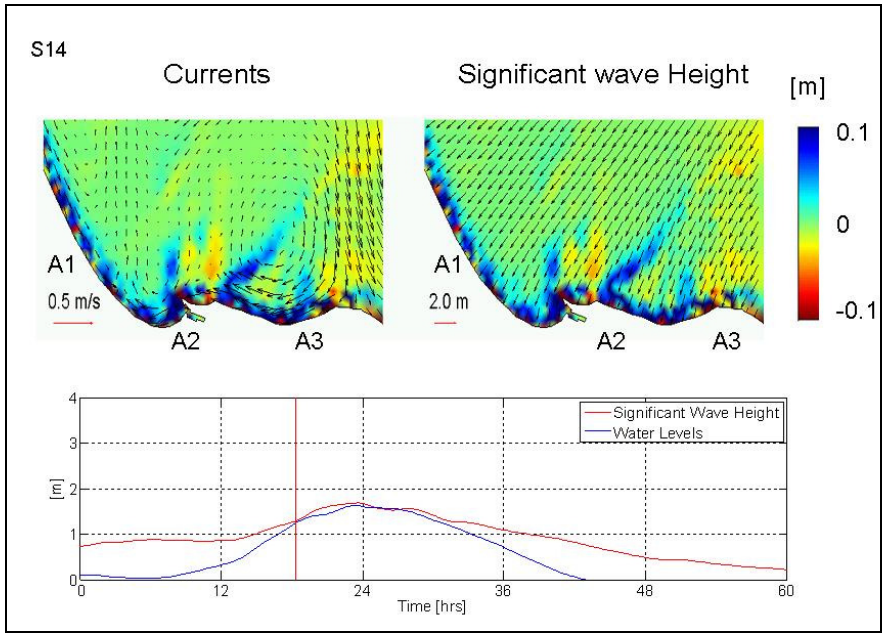

Figure 6-9. Bathymetrical changes and current-flow vectors (upper left), bathymetrical changes and significant-waves-heights vectors (magnitude and direction) (upper right), and time series of waves and water level during storm number 14 (S14)

6.2.3 Application of statistical analysis of the spatial distribution of the morphological changes driven by the 16 storms in Table 6-1 (EOFs analysis)

With the use of Empirical-Orthogonal-Functions the bathymetrical changes close to the coastal area are studied. The spatial distribution of morphological changes over the Luebeck Bay is the variable used for this analysis. For such analysis the EOF method is proposed to find the most relevant bathymetrical changes that are produced by the storm scenarios. The numerical results of bathymetrical changes presented in Figure 6-5, Figure 6-6 and Figure 6-7 are used for the EOF analysis. All the numerical results are organized in the matrix of samples in the order indicated in Figure 2-6 of Chapter 2.

Figure 6-10 shows the plot of eigenvalues with the corresponding number of modes. The 90% of the information of the bathymetrical changes is found within the first two modes. The first mode contains more than 50% of the information, while in the second mode, 40% of the information is accounted for.

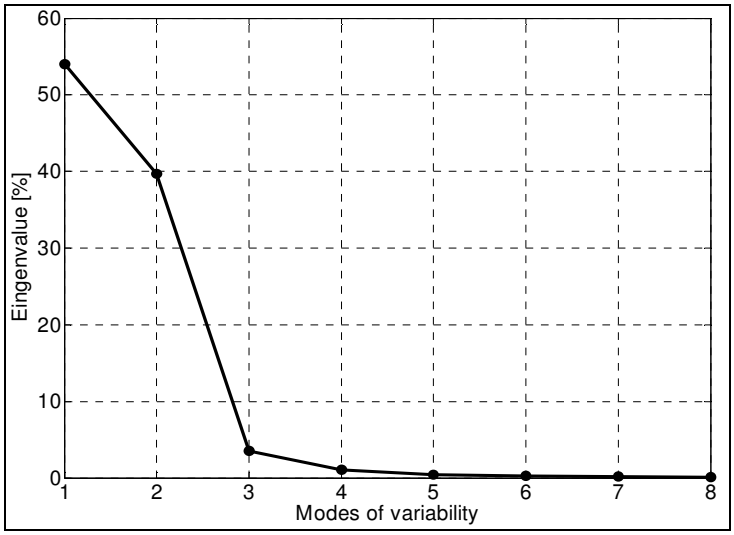

Figure 6-10. Eigenvalues of EOF analysis with the corresponding number of modes

As shown in Figure 6-10, not much of the information is expected to be taken into account in the remaining less-than 10 % that corresponds to the modes higher than 2. Modes 1 and 2 capture the characteristic bathymetrical changes to draw conclusions about the trends in the morphological changes of the Luebeck Bay under storm conditions. Below, Figure 6-11 shows the representative morphological changes based on mode 1 and the cumulative mode 2. In addition to that, the two contrasting storms (S6 and S14) are presented to contrast with the information provided by the EOF analysis.

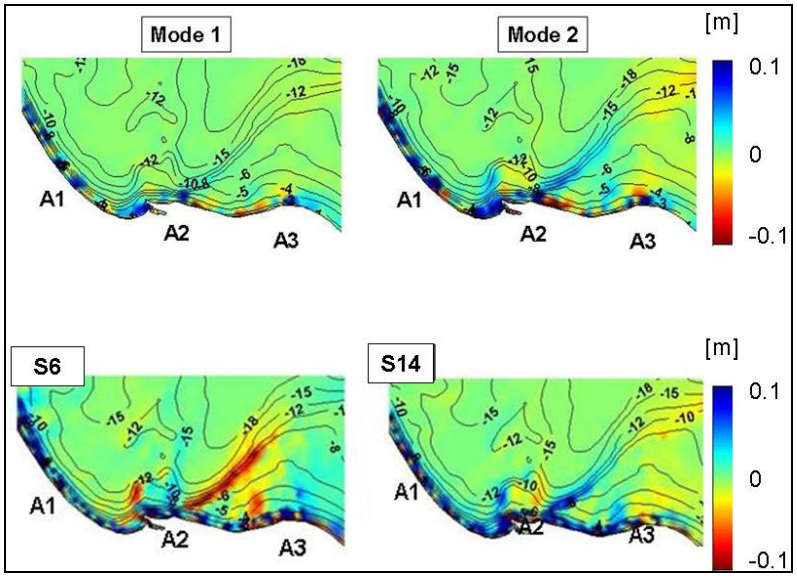

Figure 6-11. Reconstruction of bathymetrical changes produced by the 16 storm scenarios in Table 6-1 (first mode and cumulative second mode of the EOF analysis). Two contrasting storms out of the 16 storm scenarios (S6 and S14)

The statistical analysis based on the EOF method indicates that more than 50 % of the information can be accounted for in the map of bathymetrical changes applying mode 1 (left-upper side of Figure 6-11). According to the results applying the first mode, erosion is one relevant feature of morphological changes on some locations of the coastal areas on the east side between A2 and A3. The erosion in front of A3 (on top of the ridge of the cliff-coast) is also an important feature of bathymetrical changes under the effects of the storms. The effects of storm conditions can also be reflected on the western sector of the study area. The deposition of sediment along the coast is more evident along the sector between A2 and A3. In that section of the coastline there are also locations in which erosion and deposition of sediment appear one after the other.

By including the second mode to the first mode, an additional 40% of the information about the morphological changes is summed up to the first mode. The total of that information accumulated can reach more than 90% (see Figure 6-10). According to that, it is assumed that the relevant features of morphological changes produced by the storms in the study area can be represented by the first and second mode of the EOFs. That information is graphically presented in Figure 6-11 on the right-upper panel. In fact, the second mode appears to increase the features already indicated by mode one. On the eastern sectors, the erosion appears stronger on top of the ridge in front of A3 and along the coast between A3 and A2. Offshore A2, along the western flank of the ridge, the accumulation of sediment is more evident. From A2 to A1, the deposition of sediment appears along the coast in that section of western Luebeck Bay. Within that section of the coast, in the western side of the study area, the located erosion in the southeast of A1 outstands in the midst of a sector where deposition of sediment dominates.

In this section the results provided by the EOF are compared with two individual cases that have been included in the 16 storms scenarios. Note that not all features from these particular cases coincide with the results from the EOF analysis. The storm S6, for example, differs significantly in the morphological changes close to the mid-eastern region between A2 and A3. In that particular storm erosion takes place along the eastern flank of the ridge in front of the Brodten Cliff-coast (see Figure 6-11). Meanwhile, the principal patterns of morphological changes computed through the use of EOF analysis, indicates that deposition of sediment is most probable to occur in that same location (see Figure 6-11). On the other hand, in Figure 6-11, storm S14 shows one individual case in which, in contrast with storm S6, a significant resemblance to the results presented in the morphological changes computed through the EOF analysis is evident. That comparison indicates that through the used of EOF, instead of finding the definite bathymetrical changes produced by storms, it can give a general picture of the principal effects of storms on the morphological changes of the study area.

In this section the EOFs method has been used with the support of numerical modeling to find out the principal morphological changes produced in the Luebeck Bay by the effects of storms. The possibility of using statistical tools combined with numerical models can be an alternative in those cases where the measured

data (i.e. bathymetries, profiles) are not enough to determine the relevant morphological changes in a specific area.

Chapter 7

The medium-term morphological process in the Luebeck Bay during storms and calm periods

The objective of morphodynamic studies is to know about the morphological evolution of the coastal areas. For those studies it is necessary to analyze the variables that play a role in the development of the morphology. The particular conditions of the meteorology, hydrodynamics and sedimentology are studied together within a single defined spatial and temporal scale. The definition of the temporal and spatial scales is closely related to the objectives that researchers and stakeholders determine in advance. In this study the main objectives are principally the identification of important morphological changes that can occur under both storm and normal conditions in the Luebeck Bay. In this investigation it is expected to know more about the areas that are persistently under erosion and/or sedimentation in the Luebeck Bay within periods that include both normal and extreme-event conditions.

In this chapter, the evolution of the morphology in the Luebeck Bay is analyzed with the use of numerical simulations. The storm and normal conditions are executed sequentially; firstly a period of storm and then one of normal conditions are run one after the other in order to compute the total changes of the bathymetry at the end of the whole term of simulations.

7.1 Computation of the morphodynamics along the coastline of the Luebeck Bay

In this section it is intended to present the studies of the coastal areas of the Luebeck Bay based on morphodynamic simulations with the use of a high-resolution local model. The methodology proposed including the effects of storms and calm conditions is explained in detail below.

7.1.1 Methodology

The methodology is composed of two basic steps. Firstly, a storm period of regular intensity is simulated. Secondly, a representative calm period is used after the storm period. In the simulations of calm conditions a representative period of one month is considered. Subsequently, a morfac of 12 has to be applied to consider a total period of calm conditions for one year. The results of this analysis are intended to give insight into the evolution of the morphology in the study area.

7.1.1.1 Storm period

The simulation of the morphological changes is investigated along three transects in the study area. Figure 7-1 shows the position of each transect. Transect 1 corresponds to the cross section normal to the beaches of Timmendorf (see Figure 7-2). Low gradients of the bathymetry along that profile are observed. In a distance longer than 1 km the depths increase gently from 0 m to 15 m towards the deeper areas.

The position of transect 2 is in the center of the Luebeck Bay close to Niendorf (see Figure 7-2). In that section two submerged berms are observed 100 m and 800 m offshore Niendorf. At 900 m, the depths are close to 15 m just after the second berm. Transect 3 shows the cross-section normal to the Brodten Cliff-coast (see Figure 7-2). Along transect 3 the characteristics of a typical profile of Cliff-coastal areas are observed. In that section a platform with low gradients extends more than 1400 m offshore the Brodten Cliff-coast.

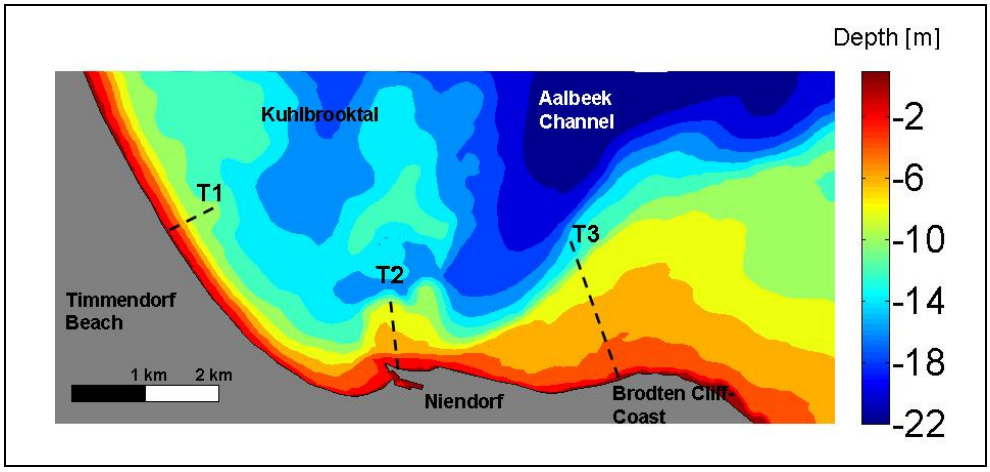

Figure 7-1. Locations of transects (T1, T2 and T3) for the analysis of morphological changes based on numerical simulations

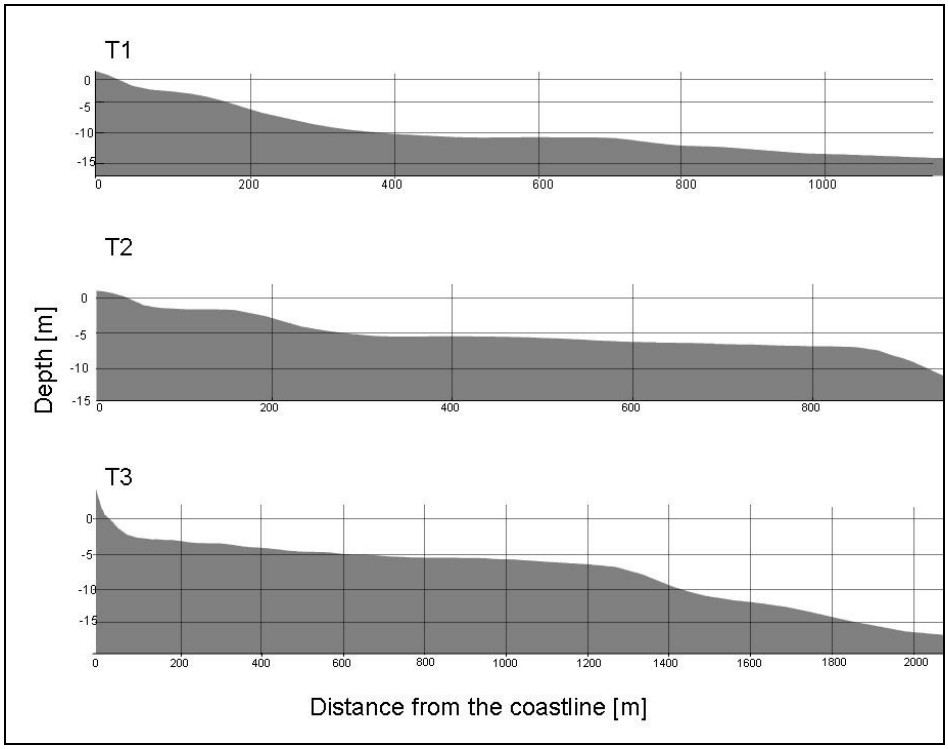

Figure 7-2. Profiles of transects

Several assumptions in this methodology have to be made. It is assumed that the effects of the initial bathymetry, i.e. before the storms, are not relevant. It is also considered that one storm can be representative over medium-term periods. In the next section the first assumption is investigated based on the analysis of sensitivity to modifications on the initial bathymetry (e.g. building-up of new bars). In section 7.1.1.1.2, the second assumption is evaluated based on the results of medium-term simulations of two cases; each case is setup with two distinct storm scenarios.

7.1.1.1.1 Assessment of sensitivity to changes on the initial bathymetry

A 2-meters-high longitudinal bar along the coastline is added to the original bathymetry. Figure 7-3 shows the position of the bar along the coast. In this investigation the distance of the artificial bar to the coastline is defined following the 5-m isobath. In this way the hydraulic conditions are comparable between the three transects. The cross sections presented in Figure 7-4 shows the position of the artificial bar on each of the three profiles. The distances of the bar to the coastline are not uniform in all the three transects as indicated in Figure 7-4. Along Transect 1 the bar is found 200 meter offshore the coastline within the 5 m and 8 m isoline. In the middle transect of the study area, the bar is localized 350 m offshore the coastline within the 5 m and 7 m isoline. In the third transect the distance of the bar to the coastline is the farthest between all the three profiles. The depths along Transect 3 can vary between 5 m and 6 m.

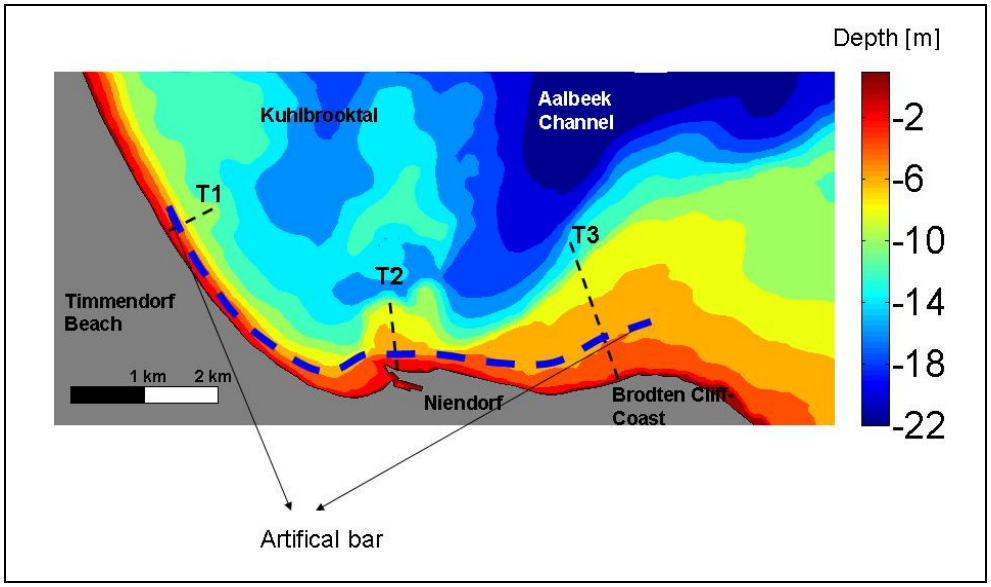

Figure 7-3. Location of artificial bar in planview

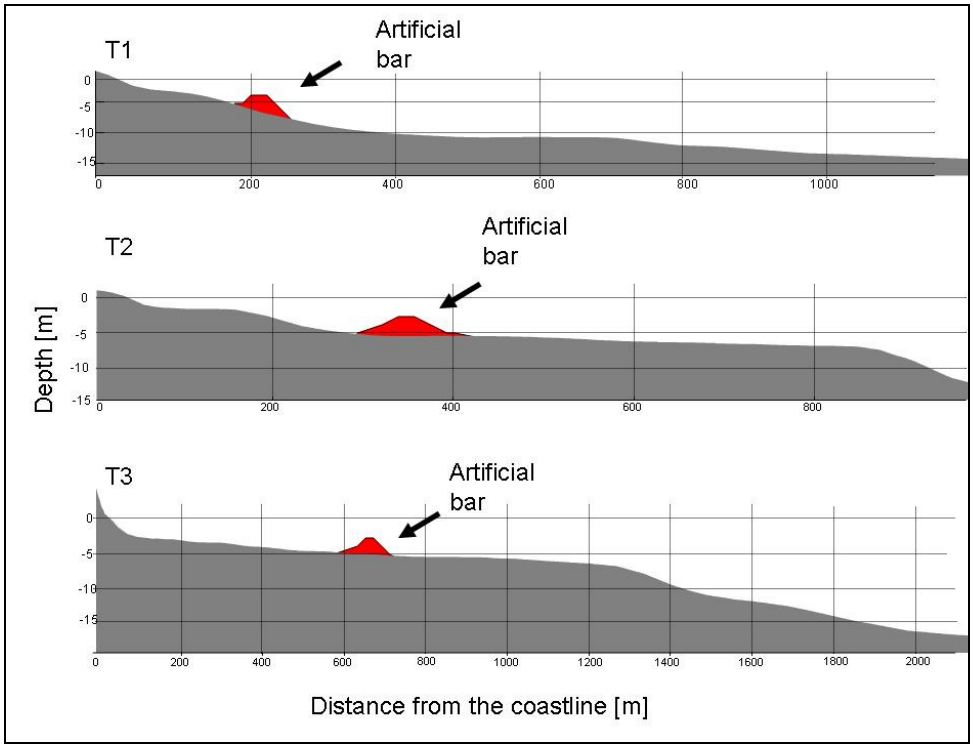

Figure 7-4. Location of artificial in cross-section

Figure 7-5, Figure 7-6 and Figure 7-7 show the transects and the resulting bathymetrical changes applying the modifications on the bathymetry. In this analysis storm S14 from Table 6-1 is the scenario used to investigate the effects of the initial bathymetry on the final morphological changes.

In Figure 7-5 the bathymetrical changes are presented along the first transect. The bathymetrical changes show both sedimentation and erosion processes in that particular location. The positive values of the upper panel indicate sediment deposition whereas the negative ones show the erosion. In both cases, i.e. with out bar (red) and with bar (blue), the numerical results are comparable. Inland, on the left side of Figure 7-5, the morphological changes shows erosion with very low values. From that point on, the changes in the bathymetry continue as deposition of sediment and then, once again, erosion appears just before the artificial bar begins. The largest differences in terms of bathymetrical changes are found within the region where the bar is localized. The effects of the artificial bar on the sediment-transport activity are locally represented by larger quantities of erosion on top of the bar. After the end of the bar, the bathymetrical changes are similar in both cases of the simulation, which extends farther offshore along the entire transect.

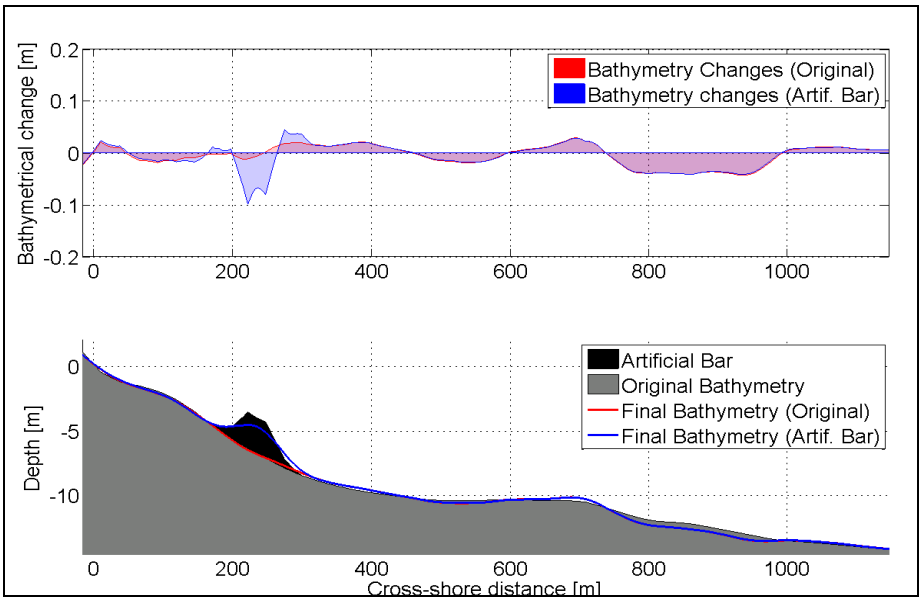

Figure 7-5. Bottom: cross-section along transect 1 of initial original bathymetry (gray area), initial modified bathymetry (black area), final bathymetry after storm applying the original bathymetry (red solid line) and modified bathymetry (blue solid line). Top: Bathymetrical changes along cross-section considering original bathymetry as initial (red area), and modified bathymetry as initial (blue area)

Figure 7-6 shows the bathymetrical changes of numerical simulations along the second transect in the study area. It can be seen that also for that transect the main

differences of bathymetrical changes occur at the position where the artificial bar is localized. The erosion presented at that location applying the original bathymetry is contrasted with the combination of erosion and deposition presented in the other cases where the artificial bar has been built up.

Figure 7-7 presents the results along the third transect in this part of the investigation. In this case the larger differences between both conditions of initial bathymetries are seen just at the position where the artificial bar is placed. The morphological change applying the artificial bar suggests that the effects of the bar are mainly the displacement of the material of the bar in the offshore direction. The material on the lee side of the bar is moved and deposited just farther offshore at the end of the artificial beach.

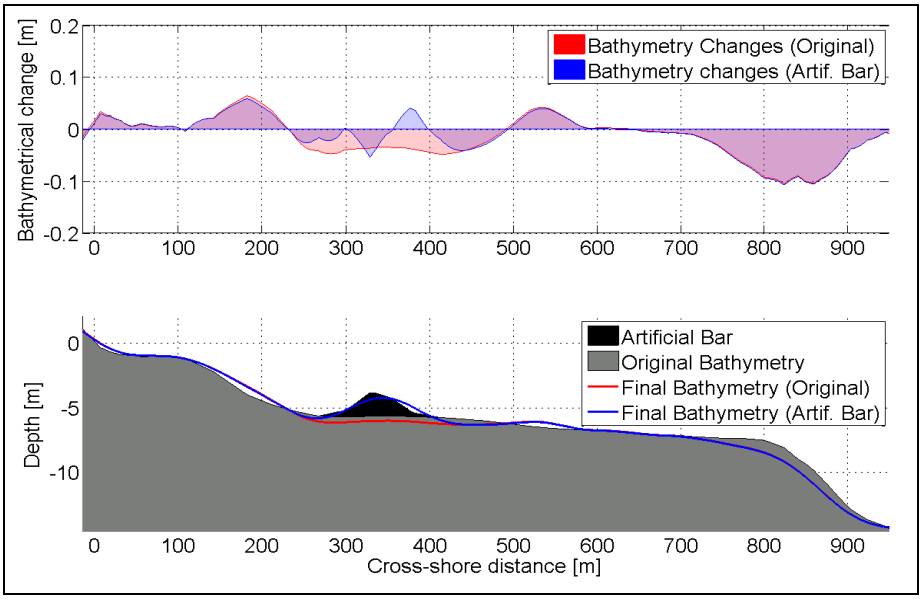

Figure 7-6. Bottom: cross-section along transect 2 of initial original bathymetry (gray area), initial modified bathymetry (black area), final bathymetry after storm applying the original bathymetry (red solid line) and modified bathymetry (blue solid line). Top: Bathymetrical changes along cross-section considering original bathymetry as initial (red area), and modified bathymetry as initial (blue area)

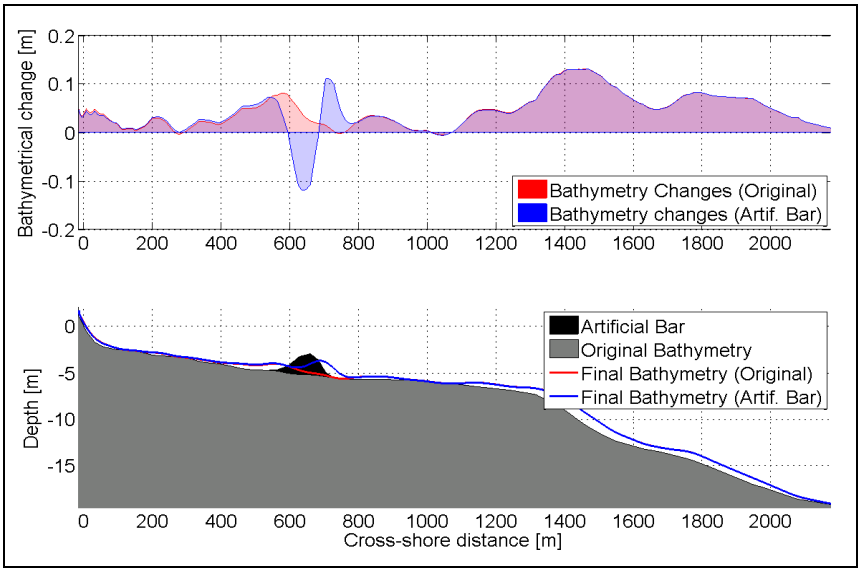

Figure 7-7. Bottom: cross-section along transect 3 of initial original bathymetry (gray area), initial modified bathymetry (black area), final bathymetry after storm applying the original bathymetry (red solid line) and modified bathymetry (blue solid line). Top: Bathymetrical changes along cross-section considering original bathymetry as initial (red area), and modified bathymetry as initial (blue area)

7.1.1.1.2 Assessment of bathymetrical changes for two contrasting storm scenarios (S6 vs. S14)

From the group of synthetic storms in Table 6-1 two storms (S6 and S14) are considered in this analysis. As it has been previously shown in Figure 6-5 and Figure 6-6, respectively, the bathymetrical changes produced by those storms are significantly different; the regions of erosion and deposition in those two scenarios did not show a similar pattern. In this investigation, the two cases are run separately in order to compare the effects on the medium term bathymetrical changes. The first scenario selected from Table 6-1 is S6. In that case the water levels were significantly high (2.49 m), the maximum significant wave height was among the highest of all the scenarios (1.74 m), and the wind velocity was in the order of 17 m/s. In the second case (S14), although the water levels were not as high as that of the first scenarios, the significant wave height reached values comparable with that of S6 (1.68 m), the wind magnitude was also comparable with that of the first scenario (17.49 m/s).

Figure 7-8, Figure 7-9 and Figure 7-10 show the results of simulations of bathymetrical changes along the transect 1, transect 2 and transect 3, in which the morphological changes produced by storms S6 and S14 are compared.

Along transect 1 in Figure 7-8 the results of the two scenarios are similar in the first ~80 meters from the shoreline; in both cases it is observed that the sediment is

moving in the offshore direction. Discrepancies between the two morphological results can also be observed. Within a distance not longer than 300 m offshore, the storm S14 tends to accumulate sediment while in the other case, storm S6 shows erosion. In the sector between 450 m and 250 m offshore, the bathymetrical changes in both scenarios are comparable. From that point on, in the 10 m depth isoline, storm S6 is clearly different from S14. The quantity of deposition along the profile did not exceeded 250 mm. Maximum values of erosion close to 400 mm are observed 800 m offshore.

Along the entire transect 2 in Figure 7-9 the morphological changes produced by both scenarios are similar. In a distance of 100 m and 800 m there are patterns of erosion that may indicate the transport of sediment from the berms situated at those locations. In between, sedimentation and erosion alternate one after the other indicating that sediment transport may be taking place in the cross-shore direction. Maximum values of erosion are close to 10 cm, 800 m offshore, while deposition of sediment is as high as 7 cm, 200 m offshore, along that transect.

Along transect 3 similar morphological changes are observed in a distance not longer than 1 km from the shoreline. Deposition of sediment is taking place close to the shoreline and along the platform until 1 km of distance. By comparing both scenarios, it can be seen that in a distance farther than 1 km the deposition of sediment presented by S14 contrast with that of erosion observed during storm S6. The values of deposition of sediment reach a maximum of 14 cm, while erosion did not exceed 300 mm.

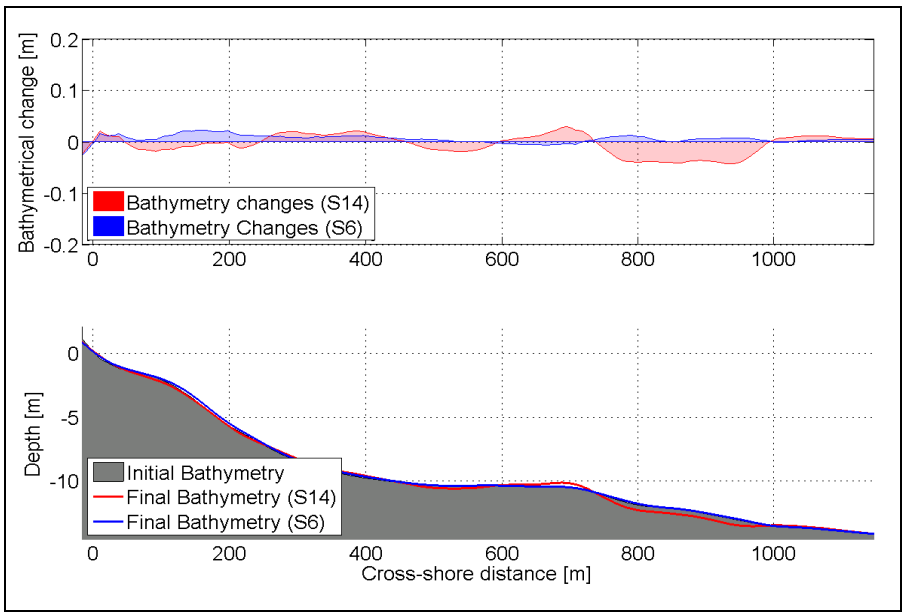

Figure 7-8. Bottom: cross-section along transect 1; initial (gray area) and final bathymetry after storm S6 (red solid line) and storm S14 (blue solid line). Top: bathymetrical changes after storm S6 (red area) and storm S14 (blue area)

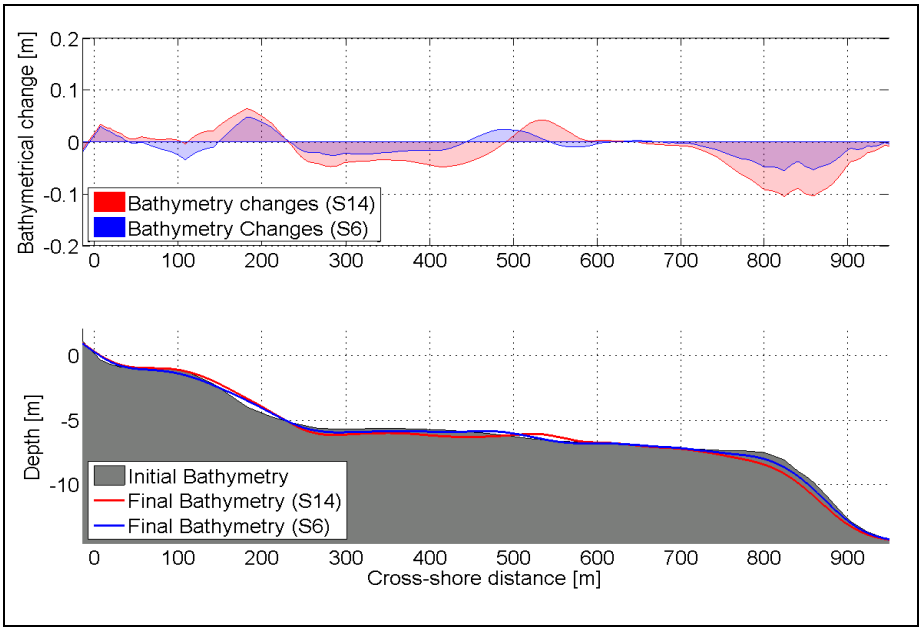

Figure 7-9. Bottom: cross-section along transect 2; initial (gray area) and final bathymetry after storm S6 (red solid line) and storm S14 (blue solid line). Top: bathymetrical changes after storm S6 (red area) and storm S14 (blue area)

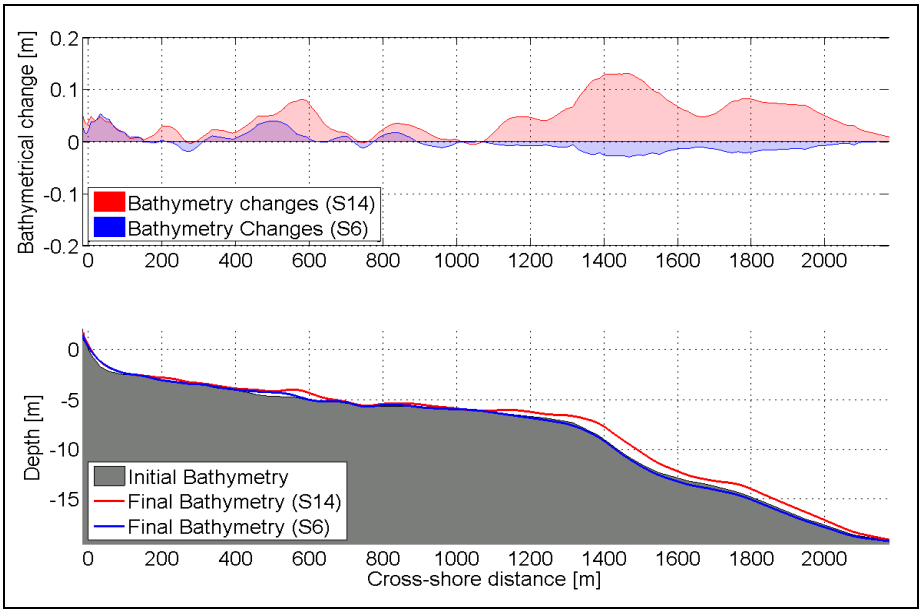

Figure 7-10. Bottom: cross-section along transect 3; initial (gray area) and final bathymetry after storm S6 (red solid line) and storm S14 (blue solid line). Top: bathymetrical changes after storm S6 (red area) and storm S14 (blue area)

7.1.1.2 Medium Term Period (storms and normal-conditions period combination)

7.1.1.2.1 Definition of representative period

Normally the morphodynamic model simulations are extremely time-consuming when predictions on the medium term have to be carried out. In this study the medium term simulations of one year are accelerated through the method based on morphological factors – morfac (cf. Chapter 2). In the application of that method the definition of a representative period of normal conditions is necessary. In this study the selection of the representative period of normal conditions of one month of duration is considered. The technique used to find that representative period is known as the cost-function method (cf. Chapter 2).

In this investigation the data of wind components are used to find the representative period of normal conditions during one year of measurements. The wind components are applied in the equations 1, 2 and 3 in section 2.4.1.

Figure 7-11 shows the values of cost functions. A minimum value in the three functions indicates the definition in time of the representative period. The three cost functions have a minimum value during the period of one-month between November 21 and December 21. In case that one year of simulations have to be carried out, one-month period of representative conditions would correspond to a morfac equal to 12. It is assumed that the selected period covers the average weather conditions which can be considered normal in the study area. Outliers such as storms and other relevant variations with respect to the mean should not be present. This can be seen by a comparison of the cost function C3 for the selected period with the measured water level variation in the same period (see Figure 7-12). Notice that during the period in question the increases in water level do not exceed 0.5m, which is well below the 1m threshold assumed in the selection of the storms.

7.1.1.2.2 Simulation results of medium term periods

In the following section of this thesis, the numerical results of medium-term simulations combining storms and normal conditions, is presented. In Figure 7-13, the scheme of the numerical simulations is illustrated. Firstly, the Luebeck Bay Local model (LBLmod) is setup to run one period of storm conditions. Subsequently, the period of normal conditions is simulated taking into account the morphological changes that have been already calculated through the simulations of storm conditions.

Initially, the driving forces in terms of wind fields, water levels and waves during one storm scenario are prepared for the morphological model. The initial bathymetry is the one used in the morphological simulations in previous sections in this thesis work. Once the simulations of storm conditions are finished, the

bathymetry and driving forces for the subsequent numerical simulations under normal conditions are prepared.

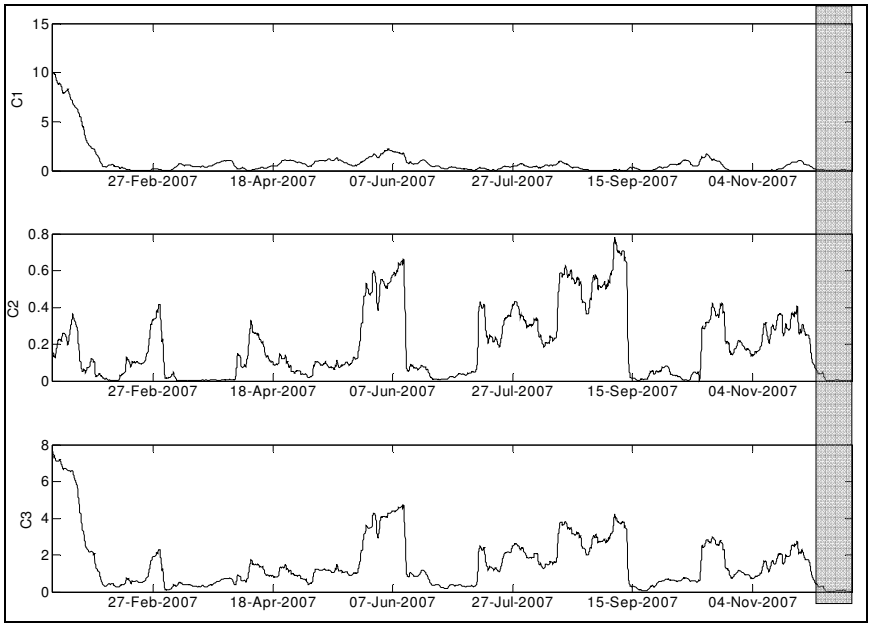

Figure 7-11. Coast functions for period January to December 2007 (stripe shows the selected period

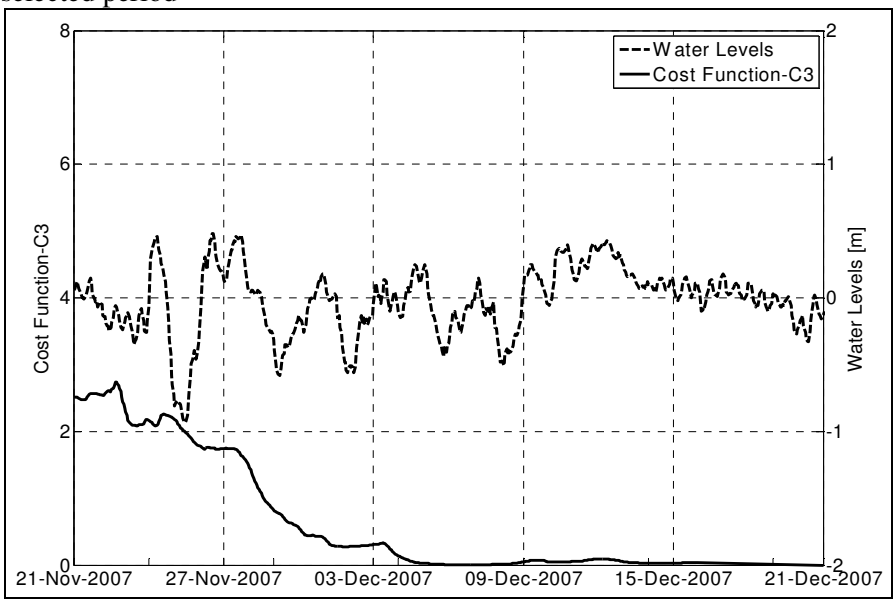

Figure 7-12. Coast function C3 and water levels during the representative period of normal conditions

The numerical results are presented as planview and, in more detail, in cross-sections profiles of morphological changes. The same three sections presented in the previous section are here analyzed. The plan view is presented as contour lines of bathymetrical changes in combination with the updated bathymetry (isobaths).

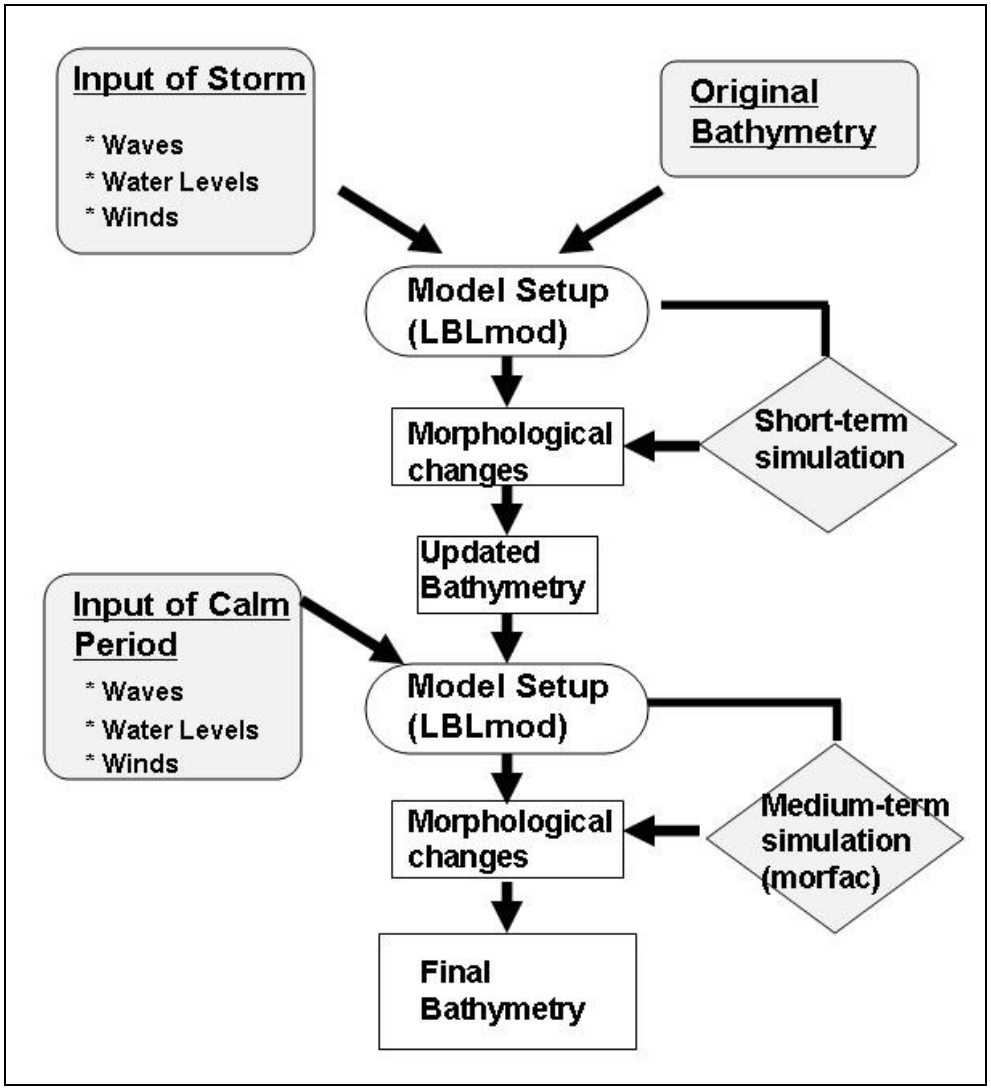

Figure 7-13. Scheme of the process to simulate storms and calm period

Figure 7-14 presents the plan view of the numerical results of morphological changes in the Luebeck Bay. As explained before, the simulations of morphological changes are carried out in two phases (i.e. first storm, then calm period). On the upper section of Figure 7-14 the results during the first phase –i.e. storm period- are presented. The results of bathymetrical changes combining the first and second phase (i.e. storms and normal conditions) are presented in the lower section of Figure 7-14. Additionally, the plan views are complemented by the computation of relative volumetric-changes (i.e. Volumetric change i / Total

Volumetric changes in three areas), which is computed for each area marked with A1, A2, and A3. The relative volumetric changes are presented in diagrams as percentage bars on the left side of each planview.

The simulation results after the storm in Figure 7-14 (upper panel) shows the most relevant morphological changes in the study area. Deposition of sediment is seen at the western bank of the ridge in front of the Brodten Cliff-coast. In front of the harbor in Niendorf a mixed region of deposition of sediment and erosion appears. The sediment deposition takes place in front of the harbor and the erosion is observed on the eastern side of the harbor. In the east of Brodten as well as in the western sector of the study area in front of Timmendorf, lower morphological changer occurred. The diagram of bars on the left side confirms the above mentioned observations on the numerical results. The lowest values of relative volumetric changes have been obtained on the areas A1 and A3, corresponding to the extreme western and eastern regions of the study area. In the middle region (A2) the change in volume is higher than in the other two sectors (A1 and A3).

The numerical results during the period of normal (calm) conditions, which are presented in the lower panel of Figure 7-14, show a different pattern to that of the storm period. In the middle zone, the deposition of sediment in front of the harbor and the erosion in the east are proportionally increased. The sedimentation on the western bank of the ridge in front of the Brodten Cliff-Coast is overweighed by increased erosion. Farther eastwards, in A3, it is observed that the region at that location tends to accumulate sediment. In the western region, in front of Timmendorf, the sediment is accumulated in its north-western sub-region, while in the south-east the erosion is increased. In the corresponding diagram of bars, on the left side of Figure 7-14, the relative volumetric-changes indicates that in the medium term period, the western and eastern (A1 and A3) sides of the study area tend to produce erosion and deposition of sediment, respectively.

Figure 7-15, Figure 7-16 and Figure 7-17 show the numerical results along the three transects of Figure 7-1. Below, the bathymetrical changes that were shown in the planviews are presented in more detail along those transects.

Some morphological processes can be observed in the medium term period. For example, along transect 1 a recovery process generated by the onshore movement of sediment at the end of the calm period, indicates that in the medium-term period most of the sediment that is eroded in the surf zone ends up close to the shoreline. In the sectors deeper than 5 meters, the profile stays close to the conditions initially presented after the storm period.

Figure 7-16 shows along transect 2 low changes along the coastline in the medium term. The bar observed 100 m offshore is eroded and the sediment in the mid section is redistributed. The berm is eroded during the storm, while, in the post-storm period the berm remains stable.

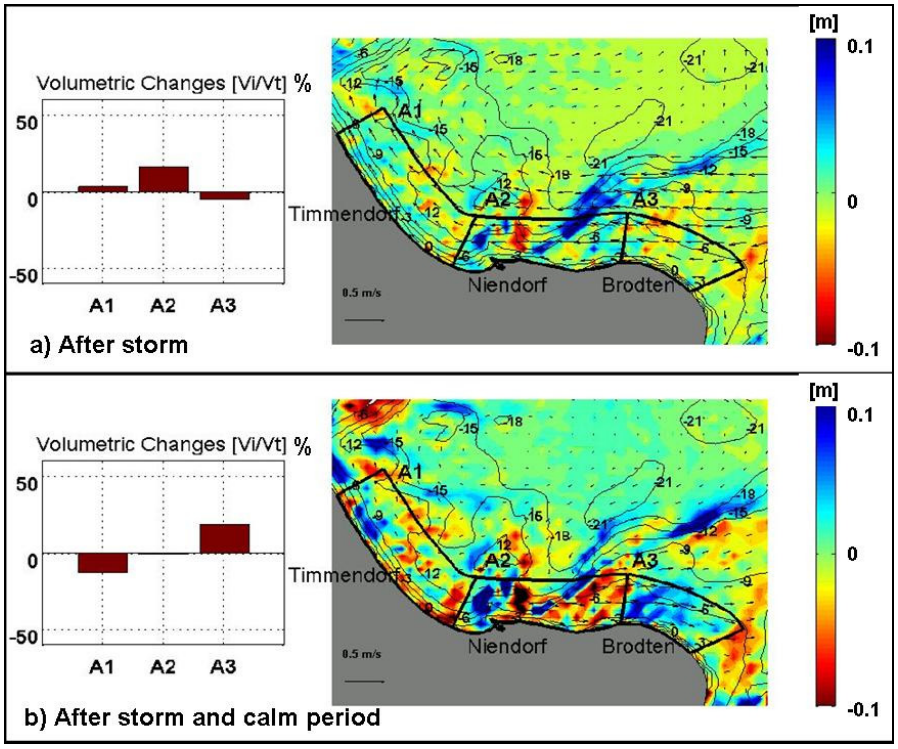

Figure 7-14.Results of morphological changes after storms and calm periods. Vi/Vt: relative volumetric-changes (Volume i / Total Volume)

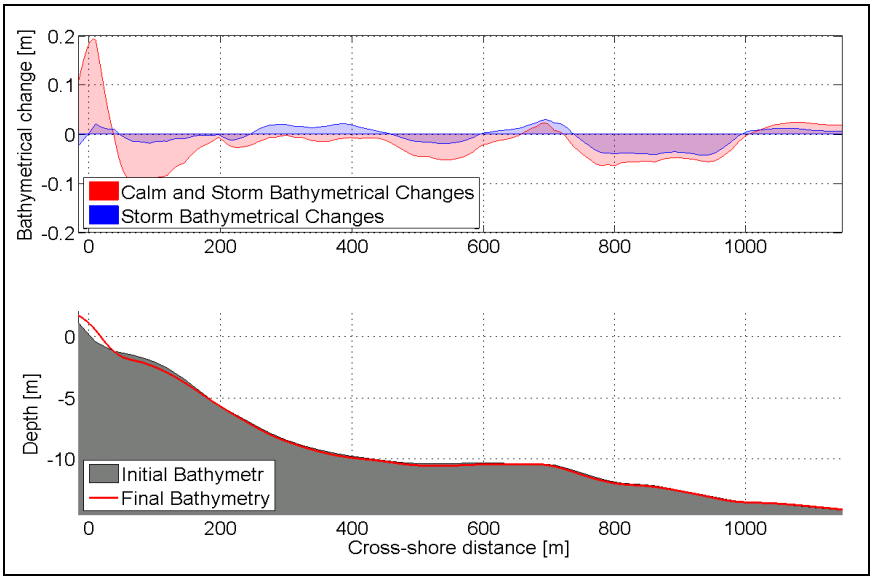

Figure 7-15. Bottom: bathymetrical profile along transect 1 (initial and final bathymetry). Top: bathymetrical changes (after storm S14 –blue area- and after storm and calm period together –red area)

The tendency along transect 3 is characterized by sediment deposition close to the coastline. During the storm period the sediment is accumulated close to the shoreline, and, on top of that, more material is deposited during the calm period. In the submerged areas deeper than 4 meters, the accumulation of sediment during the storms is counteracted by the erosion processes along the platform, and less deposition of sediment on the berm (1400 meters offshore).

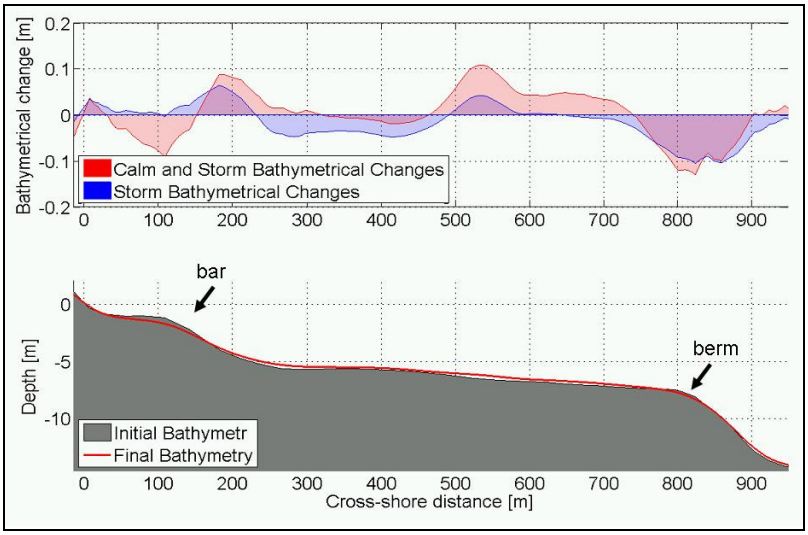

Figure 7-16. Bottom: bathymetrical profile along transect 2 (initial and final bathymetry). Top: bathymetrical changes (after storm S14 –blue area- and after storm and calm period together –red area)

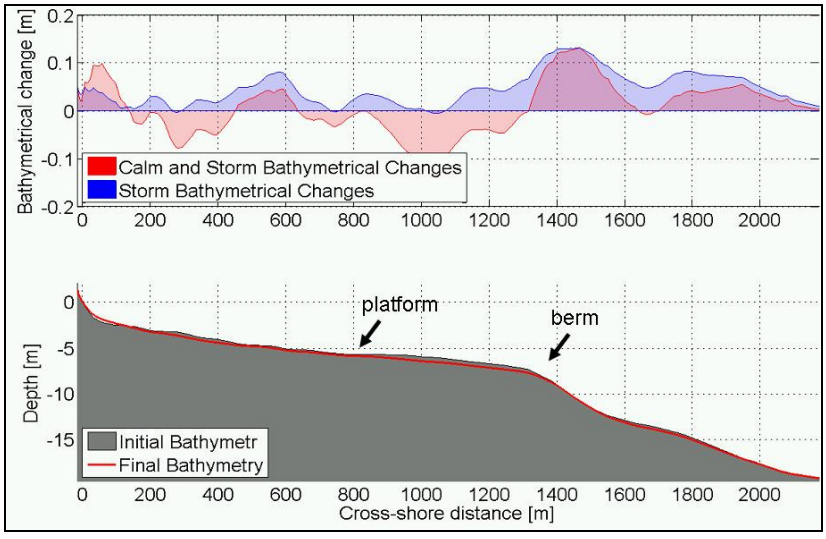

Figure 7-17. Bottom: bathymetrical profile along transect 3 (initial and final bathymetry). Top: bathymetrical changes (after storm S14 –blue area- and after storm and calm period together –red area)

Chapter 8

Conclusions and Recommendations

- The assessment of the morphological changes in the Luebeck Bay, including conditions under storm and calm periods, has been carried out based on numerical results of two models. The first model (Baltic Sea Regional model-BSRmod) is used for generating and transmitting all hydrodynamic forcings from the deep ocean to the local areas in the German Baltic Sea coasts. The domain in the regional model contains the whole area of the Baltic Sea. In the second model (Luebeck Bay Local model-LBLmod) a nesting procedure between both, BSRmod and LBLmod, makes possible the exchange of the hydrodynamic conditions that are generated in the Baltic Sea region. In order to simulate the bathymetrical changes in the Luebeck Bay, the morphological module is also included in LBLmod.

- The sensitivity analysis of both models is studied in this thesis. In the south-western Baltic Sea the wind is a relevant factor in the setup of the waves and flow modules. The effects of the winds on the flow module of LBLmod, is less important that those observed in BSRmod. Other physical parameters of the models proved to be important as well, for example, the configuration of the breaking of waves in the wave module and the bed roughness in the flow module. The sensitivity analysis in both models was also extended to the study of the online-coupling of waves and flows. The effects of the flows on the computation of wave heights are more important than what the wave heights do represent in the simulation of flows and water levels.

- The flow and wave modules of both models have been calibrated and validated. The model results of flows were in good agreement with the measurements. According to the scale of accuracy proposed by Van Rijn, et al., (2003), the performance of the wave module is good.

- The hydrodynamic simulations in the study area revealed differences in the circulation of currents between calm and storm conditions. During the

storms, the flows generate circulation patterns near to the coast of Niendorf. The circulation patterns of the currents in the Luebeck Bay under storm conditions were consistent with former investigations in the area. Several locations of convergence and divergence of currents were observed along the shoreline in front of Niendorf and Timmendorf.

- The morphological changes produced by the storms have been studied based on numerical simulation. It was observed that the spatial distribution of the bathymetrical changes is different depending on each case of storm. Nonetheless, it was possible to identify certain patterns. In general, the coastline of the Luebeck Bay is stable and only small changes in the bathymetry due to the storms are expected.

- The use of statistical methods combined with numerical models is proposed as an alternative to study patterns of morphological changes under extreme conditions. For example, in this investigation, the empirical orthogonal functions analysis has been applied for the bathymetrical changes produced by storms with the use of numerical models. It has been identified that under the effects of the storms, on the east (Brodten) more erosion is taking place when compared with the western regions (Timmendorf) of the Luebeck Bay. In the coastal area of Timmendorf accumulation of sediment occurs; while, offshore the eastern cliff-coast erosion takes place under extreme events.

- Morphodynamic numerical simulations have been carried out including one storm period and one period of normal conditions. The morphological changes in the Luebeck Bay after the storm and after normal conditions showed differences. Based on the relative volumetric changes it has been found that after the storm period the central region of the Luebeck Bay is more affected than the western and eastern regions of the study area. In contrast, the normal conditions period, at the end, presented more changes in the bathymetry in the western and eastern regions that during the storm period.

- Over the medium term period the beaches of Timmendorf experienced deposition of sediment in the northern region. A stable coastline is found in the eastern sectors close to Niendorf and Brodten. Erosion takes place on the submerged platform of the cliff-coast in Brodten and, on the outer berm and bars offshore Niendorf.

- Even though the morphological model has not been validated, the numerical results are consistent with the expected changes during the transformation of the coastal zones. The preliminary results of simulations of offshore transport of sediment during extreme conditions, and the recovery of the beach with onshore movement of sediment during the calm period, indicates that in the Timmendorf a cross-shore transport of sediment is dominant. On the other hand, in the east, long-shore sediment

transport prevail over the cross-shore direction, by which sediment is transported to the central area offshore Niendorf.

- In the Luebeck Bay no major transformation of the coastal zone is expected. After the storms, bathymetrical changes close to the coastline do not exceed 10 cm. Erosion in that region of the coast is less than 1 cm. The changes in the bathymetry during the storms are much lower than those produced after medium-term periods. The parts of beaches subjected to erosion recover quickly after storm periods, indicating that the region is stable.

- A more detail investigation in several sectors along the coast of the Luebeck Bay is necessary. For example, in this study, in the Cliff-coast sector, the erosion of the cliff has not been considered in the numerical simulations. Erosion is expected from that area, which might contribute to an increase of load of sediment being transported alongshore to the east and west of the Cliff-coast.

- The results in this investigation constitute a preliminary analysis of the short and medium term morphodynamic process in the Luebeck Bay. The numerical results have to be validated with measurements of bathymetrical changes taken before an after the storms.

References

Anderson, T.R., Frazer, L.N., Fletscher, C.H., 2010. Transient and persistent shoreline change from a storm. Geophys. Res. Lett., 37, L08401, doi:10.1029/2009GL042252.

Bayerl, K.-A., Schwarzer, K., Luebecker-Hammann, U., 1992, Das Kuestenholozaen an der inneren Luebecker Bucht, Meyniana, 44, 97-110, in German.

Bochev-van der Burgh, L.M., Wijnberg, K.M., Hulscher, S.J.M.H., Mulder, J.P.M., 2008, Long-term dune behavior and coastal safety, Proc. of the 31st International Conference on Coastal Engineering, ICCE 2008, Hamburg, Germany.

Boon, J., Kerkamp, H., Dardengo, L., 2002, Alternative dumping sites in the Ems-dollar estuary.

Bruss, G., 2006, Set-up, calibration and validation of a three-dimensional numerical model of the Mecklenburg Bight, MSc. Thesis, University of Kiel, Germany.

Bruss, G., Jimenez, N.,Eiben, H., Mayerle, R., 2009, Entwicklung von Methoden zur Bestimmung maßgebliche Bemessungsparameter fuer Kuestenschutzanlagen an der deutschen Ostseekueste, Abschlussbericht 2.2 zum KFKI-Verbundprojeckt Modellgestuetzte Untersuchungen zu extremen Sturmflutereignissen and er Deutsche Ostseekueste (MUSTOK), Kiel, in German.

Carter, R.W.G. and Woodroffe, C.D., 1994, Coastal evolution: Late quaternary shoreline morphodynamics. Cambridge University Press, Cambridge,United Kingdom.

Costas, S., Alejo, I., Vila-Concejo, A., Nombela, M.A., 2005. Persistence of storm-induced morphology on a model low-energy beach: A case study from NW-Iberian Peninsula. Mar. Geol. 224, 43-56.

Cowell, P.J. and Thom, B.G., 1997, Morphodynamics of coastal evolution. In: R.W.G. Carter and C.D. Woodroffe, Coastal evolution, Late Quaternary shoreline morphodynamics, Cambridge University Press, 33-86.

Dastgheib, A., Roelvink, J.A., Wang, Z.B., 2008, Long-term process based morphological modeling of the Marsdiep Tidal Basin, Marine Geology, 256, 90-100.

De Vriend H.J., Capobianco, M., Chester, T., De Swart, H.E., Latteux, B., Stive, M.J.F., 1993, Approaches to long-term modeling of coastal morphology: a review, Coastal Engineering, Volume 21, 225-269.

Dietrich, G. and Weidemann, H., 1952, Stroemungsverhaeltnisse in der Luebecker Bucht, Die Kueste, Heft 1, in German.

DHI-GROUP, URL: http://www.dhigroup.com.

Duphron, K., Kliewe, H., Niedermayer, R.-O, Janke, U., Werner, F., 1995, Die Deutsche Ostseekueste. -Samml. Geol. Frueher, 88,281 p., in German.

ECMWF, 2001, The 80-km High-Resolution ECMWF EPS. European Centre for Medium-Range Weather Forecasts, Newsletter No. 90.

ECMWF. Era-40, 2004, Ecmwf 45-year reanalysis of the global atmosphere and surface conditions 1957-2002.European Centre for Medium-Range Weather Forecasts, Newsletter No. 101.

Engelund, F. and Fredsøe, J., 1976, A sediment transport model for straight alluvial channels, Nordic Hydrology, 293-306.

Engelund, F. and Hansen, E., 1967, A monograph on sediment transport in alluvial streams, Teknisk Forlag, Danish Technological University, Copenhagen, Denmark.

Etri, T., 2007, Effects of storms on short and medium-term morphodynamics of a tide-dominated coastal region, Ph.D. thesis, University of Kiel, Germany.

Fischer, M., 2005, Development, calibration and validation of a three-dimensional numerical model for the Kiel Bight., MSc. Thesis, University of Kiel, Germany.

Fredsøe, J. and Deigaard, R., 1992, Mechanics of coastal sediment transport, World Scientific, Singapore 369 p.

Grasmeijer, B.T., 2002, Process-based cross-shore modeling of barred beaches, Ph.D. thesis, University of Utrecht, 251p.

Holthuijsen, L.H., Booij, N., Herbers, T.H.C., 1989, A prediction model for stationary, short-crested waves in shallow water with ambient currents, Coastal Engineering, Volume 13, 23-54.

Houser, C., Greenwood, B., 2005, Profile response of a lacrustine multiple barred nearshore to a sequence of storm events, Geomorphology, 69, 118-137.

Houser, C., Hapke, C., Hamilton, S., 2008, Controls on coastal dune morphology, shoreline erosion and barrier island response to extreme storms, Geomorphology, 100:223-240.

Hupfer, P., Harff, J., Sterr, H., Stigge, H.-J., 2003, Die Wasserstaende an der Ostsee, Entwicklungen- Sturmfluten – Klimawandel, Die Kueste, Heft 66, in German.

Jawahar, P. and Kamath, H., 2000, A high-resolution procedure for Euler and Navier Stokes computations on unstructured girds, Journal Comp. Physics, 164, 165-203.

Jimenez, N., Bruss, G., Eiben, H., Mayerle, R., 2009. Seegangsmodellierung der Ostsee für Extremereignisse und Rekonstruktion des Sturmes von 1872, die Küste, 75, 191-205 (in German).

Kannenberg, G.E., 1952, Das Luebecker Lokal-Schrifttum ueber das Brodtener Ufer, Die Kueste, Heft 1, in German.

Kroon, A., Larson, M., Möller, I., Yokoki, H., Rozynski G., Cox, J., Larroude, Philippe, 2008, Statistical analysis of coastal morphological data sets over seasonal to decadal time scales, Coastal Engineering, 55, 581-600.

Lane, A., 2004, Bathymetric evolution of the Mersey Estuary, UK, 1906-1997: causes and effects, Estuarine Coastal and Shelf Science, 59, 249-263.

Lesser, G.R. and Roelvink, J.A., van Kester, J.A.T.M., Stelling, G.S., 2004, Development and validation of a three-dimensional morphological model, Coastal Engineering 51 (8-9), 883-915.

Margar, V., Evans, P., Jones, O. and William, N.W.H., 2009, Damage from Waves, Surges and Overtopping at Vertical Seawalls, Coasts, Marine Structures and Breakwaters 2009, Institution of Civil Engineers, Edinburgh, UK.

Martin, J.L. and McCutcheon, S.C., 1998, Hydrodynamics and transport for water quality modeling: Lewis Publishers, New York.

Maspataud, A., Ruz, M-H, Hequette, A., 2009, Spatial variability in post-storm beach recovery along a macrotidal barred beach, Southern North Sea, J. of Coastal Research, 56, 88-92.

McInnes, K.L. and Hubbert, G.D.,2001. The impact of eastern Australian cutoff lows on coastal sea levels. Meteorological Applications, 8,229-243.

Mudersbach, C. und Jensen, J., Statistische Extremweteranalyse von Wasserständen an der Deutschen Ostseeküste. Abschlussbericht 1.4 zum KFKI-Verbundprojekt Modelgeschützte Untersuchungen zu extremen Strumflutereignissen an der Detuschen Ostseeküste (MUSTOK), Universität Siegen, 2009.

Ojeda, E., Guillen, J., and Ribas, F., 2010. The morphodynamic responses of artificial embayed beaches to storm events. Adv. Geosciences, 26, 99-103.

Preisendorfer, R.W., 1988, Principal component analyses in meteorology and oceanography, Elsevier.

Ojeda, E., Guillén, J., Ribas, F., 2010, The morphodynamic responses of artificial embayed beaches to storm events, Adv. in Geosciences, 26, 99-103.

Rahka, K.A., 1998, A quasi-3D phase-resolving hydrodynamic and sediment transport model, Coastal Engineering, Vol. 34, 277-312.

Reeve, D. Chadwick, A., Fleming, C., 2004, Coastal engineering-processes, theory and design practice: Spon Press, New York.

Reeve, D.E., Horrillo, J.M., Magar, V., 2009, Statistical analysis and forecast of long-term sandbank evolution at Great Yarmouth, UK, Estuarine, Coastal and Shelf Science, 79, 387-399.

Roelvink, J.A., 2006, Coastal morphodynamic evolution techniques, Coastal Engineering, Volume 53, 277-287.

Ruck, K.-W, 1952, Seegrundkartierung der Luebecker Bucht, Die Kueste, Heft 1, in German.

Ruggiero, P., Gelfenbaum, G., Sherwood, C.R., Lacy, J., Buijsman, C., 2003, Linking the neashore process and morphology measurements to understand large scale coastal change. Coastal Sediments ‘03.

Ruggiero, P., Kaminsky, G.M., Gelfenbaum, G., and Voigt, B., 2005. Seasonal to interannual morphodynamics along a high-energy dissipative littoral cell. Journal of Coastal Research, 21(3), 553–578. West Palm Beach (Florida), ISSN 0749-0208.

Schmager, G., 1984, Ein Beitrag zur Dynamik der aperiodischen Wasserstandsschwankungen und ihrer Vorhersage im Uebergangsgebiet zwischen Nordsee und Ostsee. Dissertation an der Universitaet HU Berlin, 176p, in German.

Schmitz, R., 2007, Vorhersage von historisch aufgetretenen Stuermen ueber der Ostsee mithilfe des Ensemble Prediction System und COSMO, in German.

Schmitz, R., 2009. Modellierung von historisch aufgetretenen Stuermereignissen ueber der Ostsee mithilfe von Vorhersagen eines Ensemblesystems und eines Regionalmodells. Die Kueste, Heft 75, in German.

ECMWF, 2001. The new 80-km High-Resolution ECMWF EPS. European Centre for Medium-Range Weather Forecasts, Newsletter No. 90.

Schrottke, K., 2001, Rueckgangsdynamik schleswig-holsteinischer Steilkuesten unter besonderer Betrachtung submariner Abrasion und Restsedimentmobilitaet. Report, Geosciences Research Institute, University of Kiel, 16, 168p, in German.

Schwarzer, K., 1995, Die Dynamik der Kueste, Rheinhemer, G., Meereskunde der Ostsee, 25-33, Berlin, in German.

Schwarzer, K., Schrottke, K., Stoffers, P., Kohlhase, S., Froehle, P., Fittschen, P., Mohr, K., Riemer, J., Weinhold, H., 2000, Einfluss von Steiluferabbruechen an der Ostsee auf die Prozessdynamik angrenzender Flachwasserbereiche, in German.

Schwarzer, K. und Krause, R., 2008, Untersuchung zur Morpho- und Sedimentdynamik im Hinblick auf eine Kuestensicherungs- und Hochwasserschutzmaßnahme im Bereich Timmendorf Stand, University of Kiel, in German.

Seifert, G., Der Aufbau und geologische Entwicklung des Brodtener Ufers und der angrenzenden Niederungen, 1952, Die Kueste, Heft 1, in German.

Sleigh, P.A., Gaskell, P.H., Bersins, M., Wright, N.G., 1998, An structure finite volume algorithm for predicting flow in rivers and estuaries, Computers & Fluids, Vol. 27, No. 4, 479-508.

Steijn, R.C. and Hartsuiker, G., 1992, Morphodynamic response of a tidal inlet after a reduction in basin area, Delft Hydraulics, Coastal Genesis Rept. H840.00, 75p.

Sterr, H., Schwarzer, K., Kliewe, H., 1998, Holocene evolution and morphodynamics of the German Baltic Sea Coast- recent research advances. In: Kalletat, D. (Editor), German Geographical Coastal Research, The last decade, Institute of Scientific Co-operation, pp 107-134.

Sztobryn, M., Stigge, H-J., Wielbinska, D., Weidig, B., Stanislawczyk, I., Kanska, A., Krzysztofik, K., Kowalska, b., Letkiewicz, B., Mykita, M., 2005, Storm Surges in the Southern Baltic Sea (Western and Central Parts). Bundesamt für Seeschifffahrt und Hydrogrphie-BSH.

Van Rijn, L.C., Walstra, D.J.R., Grasmeijer, B., Sutherland, J., Pan, S., Sierra, J.P., 2003, The predictability of cross-shore bed evolution of sandy beaches at the time scale of storms and seasons using process-based Profile models, Coastal Engineering, Volume 47, 295-327.

Von Storch, H. and Navarra, A., editors 1995, Analyses of climate variability applications of statistical techniques, Springer.

Wijnberg, K.M., Terwindt, J.H.J., 1995, Extracting decadal morphological behaviour from high-resolution, long-term bathymetric surveys along the Holland coast using eigenfunction analysis. Marine Geology, 123, 301-330.

Wilkens, J., 2004, Medium scale morphodynamics of the central Dithmarschen Bight, Ph.D. thesis, University of Kiel, Germany.

Wilkens, J. and Mayerle, R., 2005, Morphodynamic response to natural and anthropogenic influences in the German Bight, Die Kueste, Heft 69, 311-337.

Williams, W.W., 1960, Coastal Changes, Routledge & Kegan Paul, London, 220 pp.

Winant, C.D., Inman, D.L., Nordstrom, C.E., 1975, Description of seasonal beach changes using empirical eigenfunctions. Journal of Geophysical Research 80 (15), 1979-1986.

Woodroffe, C.D.,2002, Coasts: form, process and evolution: Cambridge University Press, Cambridge, 623pp.

Zhang, K., Douglas, B. C., and Leatherman, S. P., 2002, Do Storms Cause Long-Term Beach Erosion along the U.S. East Barrier Coast? J. Geology 110, 493–502.

Zhao, D.H., Shen, H.W., Tabios, G.Q., Tan, W.Y., Lai, J.S., 1994, Finite-volume two dimensional unsteady-flow model for river basins, Journal of Hydrodynamic Engineering, ASCE, 120, No. 7, 863-833.

Zyserman, J.A. and Fredsøe, J., 1994. Data analysis of bed concentration of suspended sediment, Journal of Hydraulic Engineering, ASCE, Vol. 120, No. 9, 1021-1042.

Erklärung

Hiermit erkläre ich, dass die Abhandlung -abgesehen von der Beratung durch meine akademischen Lehrer, nach Inhalt und Form meine eigene Arbeit ist. Diese Arbeit hat an Keiner anderen Stelle im Rahmen eines Prüfungsverfahrens vorgelegen. Außerdem erkläre ich, dass diese mein erster Promotionsversuch ist.

Kiel, den 16 Januar 2012

Néstor Jaime Jiménez Echeverri

About the Author

Néstor Jiménez was born in Colombia on the 7th of February, 1972. He started his bachelor degree in 1991 at the University of Medellin in the civil engineering faculty. At the end of the five-year undergraduate program he was granted the title of civil engineer. From 1996 until 2000 he participated in several contracts of construction involving both, design and execution of engineering projects.

In 2001 he started his graduate studies at the National University of Colombia in the Master of Science program. In the following three years his graduate studies were focused on the implementation of numerical models to simulate the hydrodynamics of lakes and reservoirs. The author has developed an innovative technique to design networks of monitoring based on genetic algorithms and advanced methods of interpolation. Being granted the title of Master of Science, in 2004, he participated in a project dedicated to the set up of the hydrologic numerical models and measuring campaigns to investigate the main river in the city of Medellin, Colombia.

In April 2005 the author came to Germany to do his doctorate program at the University of Kiel. Under the supervision of Dr. Prof. Roberto Mayerle he was part of the coastal research team at the FTZ-CORELAB institute. Since the beginning of his PhD program acquired expertise in the implementation of numerical models covering all issues related to the simulation of hydrodynamics and morphodynamics in several areas along the German Coasts.

Currently, the author is focused on the development of engineering projects, including planning, construction and the design of methods to apply efficient energy.

ANNEX A: Mike 21/3 FM model system

A.1. Hydrodynamics

Over the simulations of the bathymetrical changes in the Luebeck Bay a hydrodynamic model implementing depth-average currents and waves has been coupled with a wave-induced turbulence empirical formulation in order to calculate mean flow and wave motion effects on the sediment transport.

Water level variations and depth average flows are calculated in the spatial-temporal formulations of conservation of mass and momentum integrated over the vertical as presented below in equation (A-1) and equations (A-2a) and (A-2b).

Conservation of Mass

$$\frac{\partial \zeta}{\partial t} + \frac{\partial p}{\partial x} + \frac{\partial q}{\partial y} = \frac{\partial d}{\partial t} \tag{A-1}$$

Momentum integrated over the vertical

x-direction

$$\begin{aligned} &\frac{\partial p}{\partial t} + \frac{\partial}{\partial x}\left(\frac{p^2}{h}\right) + \frac{\partial}{\partial y}\left(\frac{pq}{h}\right) + gh\frac{\partial \zeta}{\partial x} \\ &+ \frac{gp\sqrt{p^2+q^2}}{C^2 \cdot h^2} - \frac{1}{\rho_w}\left[\frac{\partial}{\partial x}\left(h\tau_{xx}\right) + \frac{\partial}{\partial y}\left(h\tau_{xy}\right)\right] - \Omega_q \\ &- fVV_x + \frac{h}{\rho_w}\frac{\partial}{\partial x}\left(p_a\right) = 0 \end{aligned} \tag{A-2a}$$

y-direction

$$\frac{\partial q}{\partial t}+\frac{\partial}{\partial y}\left(\frac{q^2}{h}\right)+\frac{\partial}{\partial x}\left(\frac{pq}{h}\right)+gh\frac{\partial \zeta}{\partial y}$$
$$+\frac{gq\sqrt{p^2+q^2}}{C^2\cdot h^2}-\frac{1}{\rho_w}\left[\frac{\partial}{\partial y}\left(h\tau_{yy}\right)+\frac{\partial}{\partial x}\left(h\tau_{xy}\right)\right]-\Omega_p \qquad \text{(A-2b)}$$
$$-fVV_y+\frac{h}{\rho_w}\frac{\partial}{\partial y}\left(p_a\right)=0$$

d(x,y,t) is time varying water depth (m), ζ(x,y,t) is surface elevation, p,q(x,y,t) is flux densities in x- and y- directions ($m^3/s/m$)=(uh, vh); u,v=depth average velocities in x- and y-directions, h(x,y,t) is water depth (m)= ζ-d, C(x,y) represents Chezy resistance ($m^{1/2}/s$), g denotes the acceleration due to gravity (m/s^2), f(V) is the wind friction factor, $V,V_x,V_y(x,y,t)$ is the wind speed and components in x- and y-directions (m/s), Ω(x,y) represents the Coriolis parameter, Pa(x,y,t) is the atmospheric pressure (kg/m^3), ρ_w is the density of water (kg/m^3), t is time (s), τ_{xx}, τ_{xy} and τ_{yy} correspond to the components of effective shear stress, and x,y are the space coordinates.

Apart form the general transport-diffusion equation for the calculation of salinity and temperature, the above equations also include the scalar terms. The turbulence is taken into consideration by the eddy viscosity theory. Additionally, bottom and wind stress, ice coverage, tidal potential, and heat exchange are included as well. In equation (A-2) the effects of breaking-short-period waves can be included through the radiation stress terms given by the spectral wave model.

A finite volume scheme has been implemented to solve the governing equation for both, flows and waves model. The horizontal spatial discretization follows the unstructured-mesh distribution implementing triangular elements. The time integration in the flow model (MIKE 21 HD) has been executed by a first order explicit Euler method (see Jawahar et al., 2000). At the open boundaries discharges and water levels can be added as input. Along the close boundaries (land boundaries) the movement of the shoreline is represented by flooding-drying cells defining depth threshold-values (for more details see Zhao et al, 1994 and Sleigh et al, 1998).

In addition to the currents effects, the integrated modelling system gives the possibility to simulate simultaneously, and through dynamic coupling, the basic processes that wind-generated waves and swell induce to the sediment transport model. The conservation equation for wave action represents the physical processes of growth, decay, and transformation of waves which has to be considered in the spectral wave model of MIKE SW (see eq. (3)). The time discretization of the spectral wave model can be either instationary or quasi-stationary. For the actual investigation both approaches are used; the former

corresponds to the regional model, and the later to the local model. Further explanations about this issue in particular are found in chapters 4 and 5.

Conservation equation for wave action

$$\frac{\partial N}{\partial t} + \nabla \cdot \left(\overline{v} N \right) = \frac{S}{\sigma} \tag{A-3}$$

$N\left(\vec{x}, \sigma, \theta, t\right)$, *is the action density,* t *is the time,* $\vec{x} = \left(x, y\right)$ *is the Cartesian co-ordinates,* $\vec{v} = \left(c_x, c_y, c_\sigma, c_\theta\right)$ *is the propagation velocity of a group in the four-dimensional phase space and* S *is the source term for energy balance equation.*

In the wave action equation (equation A-3) the density of wave action *N*, the propagation velocity of the waves group $\vec{v}$ and the source terms in the energy balance equation are solved in the spatial, directional and spectral dimensions. In the Luebeck Bay, a directional decoupled parametric formulation (see Holthuijsen et al., 1989) is applied to solve equation (A-3).

The source energy term in equation (A-3) contains the energy components that are used to include the effects due to the winds, bathymetry and wave-wave interaction. On the one hand, the growth of the waves is induced by frictional forces that the wind produces on the water surface. Non-linear wave-wave interaction is also considered in the generation of waves in the source terms equation. The factors that absorb energy, i.e. whitecapping, bottom friction and depth-induced wave breaking are included in the energy balance equation as well (see equation (A-4) below).

Source terms balance equation

$$S = S_{in} + S_{nl} + S_{ds} + S_{bot} + S_{surf} \tag{A-4}$$

S *is the total energy balance due to sources and sinks,* S_{in} *wind-energy wave generation,* S_{nl} *nonlinear wave energy transfer,* S_{ds} *energy dissipation due to white capping,* S_{bot} *energy dissipation due to the bottom friction, and* S_{surf} *is energy dissipation due to depth-induced wave breaking.*

The boundary conditions in the spectral wave model are fully absorbed along the land. The incoming fluxes are represented by the spectral description of the waves along the open boundaries.

A.2. Sediment transport

Sediment transport models are the integration of three types of sediment discharges: i) bed load, ii) suspended load and iii) wash load (Engelund and Hansen, 1976). By using MIKE 21/3 FM, a quasi three-dimensional sediment transport model (STPQ3D) has been integrated to the hydrodynamic modules into one whole system of morphodynamic simulation-package. The simulation of transport of very fine material (d50<0.06 mm) by STPQ3D is not advisable. The formulations and assumptions implemented in the sediment transport model are restricted to the bed load and suspended load transport simulation. Overestimations may be expected for those areas where the grain-size corresponds to the wash-load sediment group or mud.

The sediment transport formulations solve the problem of the force balance across the water column. According to equation (A-5) the sediment transport is the combination of bed load discharge and the discharge of sediment in suspension; these are constituents of the total instantaneous sediment discharge that are affected by the distribution of forces along the vertical (equation (A-6)). The concentration of sediment constitutes is an essential part in the aforementioned equations every time the balance of forces induces the sediment to move.

Sediment transport balance equations

$$q_t = q_b + q_s \tag{A-5}$$

q_t is the total sediment transport, q_b is the bed load transport, and q_s is the load of transport in suspension

Forces balance across the water column

$$\tau = \rho v_t \left| \frac{\partial \bar{U}}{\partial z} \right| \tag{A-6}$$

τ is the shear stress, ρ is the water density, v_t is the kinematic viscosity, $\bar{U}$ is the flow velocity and z is the bed level.

To each component in equation (A-5) corresponds one equation to calculate the sediment discharges. The computation of the morphodynamics including both, bed- and suspended-load transport rate, is based on the sediment transport model proposed by Engelund and Fredsøe (1976). Through equation (A-7) and equation (A-8) the bed load and suspended load are computed. The reference concentration is computed based on the empirical formulation developed by Zyserman and Fredsøe (1994).

Bed load transport rate

$$S_{bl} = 5p \cdot \left(\sqrt{\theta'} - 0.7\sqrt{\theta_c}\right)\sqrt{(s-1)\,g d_{50}^3} \tag{A-7}$$

S_{bl} is the bed load transport rate, p is probability of a moving sediment grain, θ' denotes the skin shear stress, θ_c is the critical shear stress, s refers to the relative density of the sediment, g is the acceleration due to the gravity, d_{50} is the mean grain size.

Suspended load transport rate

$$S_{sl} = c_b Vh \cdot \int_{\eta o}^{1} u(\eta) \cdot c(\eta)\, d\eta \tag{A-8}$$

S_{sl} is the suspended load rate, c_b corresponds to the reference concentration near the bed, V is the velocity, h is the total depth, $u(\eta)$ velocity along the vertical, $c(\eta)$ is the concentration along the vertical.

A.3. Morphology

The morphological changes are computed on basis of the sediment continuity equation as follows:

$$-(1-n)\frac{\partial z}{\partial t} = \frac{\partial S_x}{\partial x} + \frac{\partial S_y}{\partial y} - \Delta S \tag{A-9}$$

n is the bed porosity, z is the bed level, t is the time, S_x is the bed load or total transport in the x direction, S_y is the bed load or total transport in the x direction and ΔS is the sediment sink or source rate.

The differential equation (A-9) is solved applying a forward-in-time difference scheme. The morphodynamics are integrated in such a way that the feedback of the bathymetrical changes affects the hydrodynamic conditions. Thus, flows, and waves are permanently adjusted to the new bathymetrical conditions.

ANNEX B: An Introduction to Empirical Orthogonal Functions (EOF)

The method based on Empirical Orthogonal Functions is an application used in the analysis of spatial and temporal variability of geophysical fields. This method is also known as Principal Component Analysis (PCA). This is a useful tool to study the relevant patterns of a single-field variable. During the analysis of the data using EOF it is strongly recommended to have a well founded background of the variable; in this way, the modes can be related with the real physics of the data that is analyzed.

In the following the essential matrix operations are described. The data is illustrated in the general approach used in EOF analysis, i.e. maps of a variable spatially distributed (along rows) for different time steps (along columns). Remember that the way the scheme of the data presented in §2.3.2.1 had a variation of the matrix mentioned above; in this investigation the different extreme scenarios have been taken the position of the time steps in the matrix.

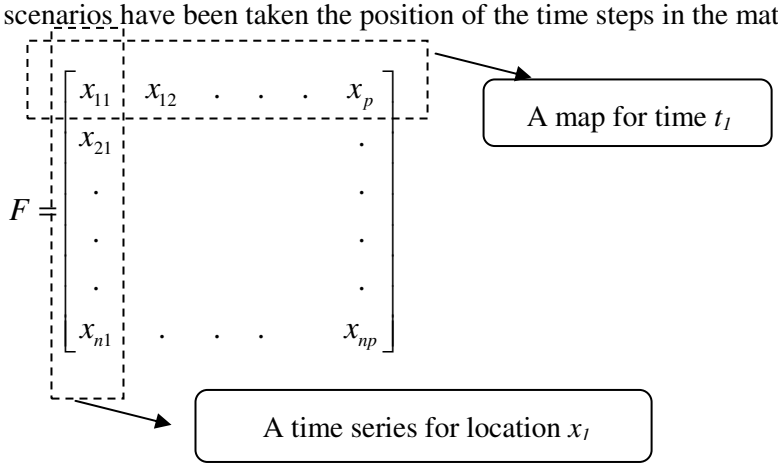

Figure B-1. Matrix of data containing times series (along columns) for a variable at the given locations (along rows).

Figure B-1 shows the set of data taken at times t_1, t_2,…t_n. For each time t_j (j=1,…n) there is one map x_i (i=1,…p) to define the locations where the values of the variable are taken. Finally, the matrix F is constituted with n maps each being p points long. In this way the size of the matrix F becomes n by p.

Initially, the covariance matrix of F is calculated $R = F^t F$ and then the eigenvalue problem is solved as follows:

$$RC = C\Lambda \tag{B-1}$$

Λ is a diagonal matrix that contains the eigenvalues of λ and R. The c_i column vectors of C are the eigenvectors of R, which in turn are the eigenvalues λ_i. The size of the matrices Λ and C is p by p.

To each eingenvalue λ_i corresponds one eigenverctor c_i. Each eigenvector is also named as one EOF. In this way, EOF1 is the eigenvector that is associated with the highest eigenvalue, and the second highest eigenvalue corresponds to EOF2, and so on. Each eigenvalue λ_i is proportional to the importance that each EOF may represent in the total variance R.

Matrix C has the property that $C^t C = C C^t = I$ (where I is the identity matrix). Therefore, the EOFs are uncorrelated over space or, in other words, the eigenvectors are orthogonal to each other.

The EOF plotted as a map represents a standing oscillation. The evolution of the patterns in time can be observed though the equation below:

$$\vec{a}_1 = F\vec{c}_1 \tag{B-2}$$

The projections of the maps in F on EOF1 are the components n of the vector $\vec{a}_1$. The vector is the time series for the evolution of EOF1. Subsequently, for each calculated EOFj a corresponding $\vec{a}_j$ could be found. The later are the *principal component time series* (PC's) of the *expansion coefficients* of EOFs. As the EOFs are uncorrelated in space the expansion coefficients are uncorrelated in time.

The most useful application of the EOFs method is the reconstruction of the data in a 'cleaner' version by truncating the sum of the eigenvectors at some $j = N << p$. In this way, the most relevant patterns of the variable can be captured by considering the first modes of the EOFs. Equation (B-3) below shows the way to reconstruct the data using the desired number of modes in the computations.

$$F = \sum_{j=1}^{p} \vec{a}_j (EOF_j) \tag{B-3}$$

ANNEX C: ADCP Measurements

This annex contains the basic information about the ADCP measurements conducted in the Luebeck Bay. As indicated in §5.4, at the Research and Technology Centre (in German: Forschungs- und Technologyzentrum Westkueste-FTZ) three ADCP units in the Luebeck Bay area were deployed. Under the direction of Dr. Klaus Ricklefs, the information regarding water levels, current velocity and wave parameters (wave height, period and direction) have been provided since 2006. The specifications of that equipment are presented below in Table C-1.

Table C-1. Specification of ADCP units in the Luebeck Bay.

Specification	U-boot	Niendorf	Scharbeutz
Transducer offset	0.5 m	0.5 m	0.5 m
Magnetic Variation	0	0	0
Frequency	600 kHz	600-1200 kHz	600-1200 kHz
Streambed	Muddy	Medium Sand	Medium Sand

At RD Instruments, Inc., the Wave View Application has been developed for the post-processing of the measured data. Below in Figure C-1 an example of the out put of ADCP measurements illustrates the available information regarding water levels, flows and waves. Figure C-1 shows the different panels in which time series of the aforementioned variables is presented (upper panel). The height and directional spectra is also given for a specific time step (middle-left and right panels, respectively), and finally, the time series of the 2D spectrum is plotted on the lower panel. All the time series is provided have a temporal resolution of 3 hours.

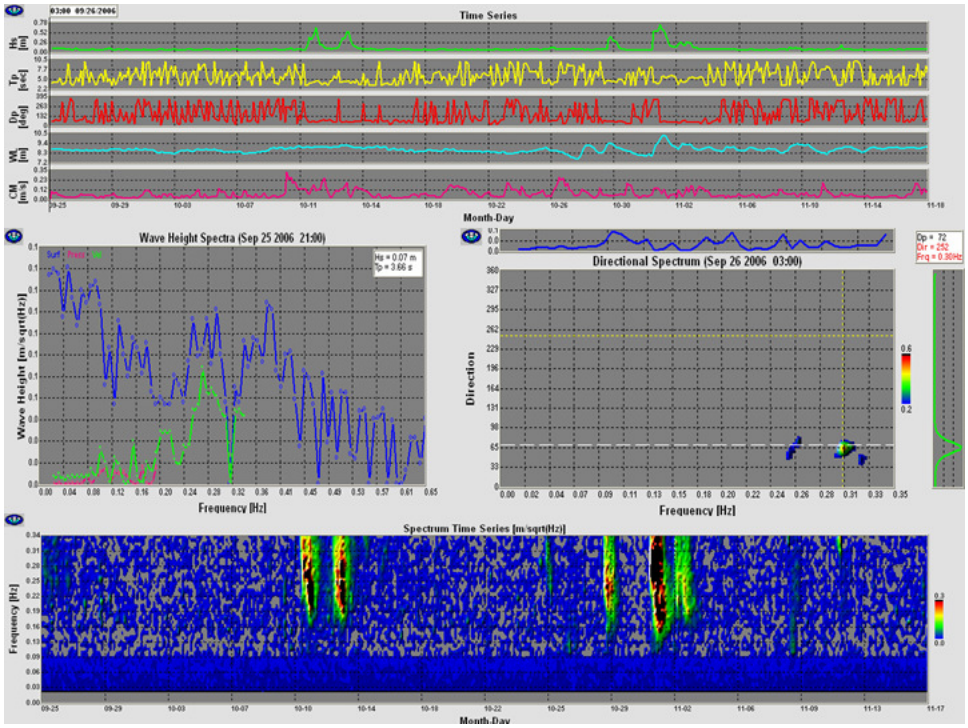

Figure C-1.Post-processing of measured data with ADCPs in the Luebeck Bay.

ANNEX D: Extreme Synthetic Scenarios

The primary objective of the MUSTOK project was the generation of extreme scenarios that could produce the conditions of historic extreme events. The extreme hydrodynamic conditions close to the German Baltic-Sea coast were analyzed by the implementation of numerical hydrodynamic models. In the aforementioned project, the German Weather Service (in German: Deutscher Wetterdienst) contributed in the generation of physically consistent atmospheric data, through which the highest water levels along the German Baltic-Sea coast were produced. In the generation of extreme atmospheric scenarios the Ensemble Prediction System (EPS) was used. This computational tool was created at the European Centre for Medium-Range Weather Forecast (ECMWF).

EPS consists of fifty weather predictions, also known as members of one ensemble. Initial conditions of the EPS are provided by ERA40 (European reanalysis project) from 1958 until 2002 or through the analysis operational system starting in year 2003. The target storms are predicted combining members and different initial dates of the storms. Figure D-1 shows the scheme implemented in MUSTOK to generate the 60 extreme events applying EPS.

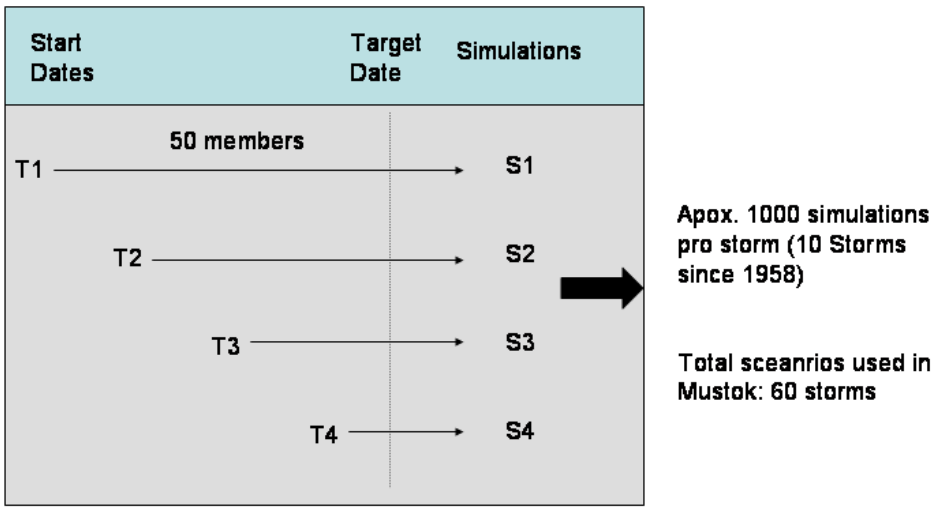

Figure D-1. Schematization of storms prediction using the Ensemble Prediction System.